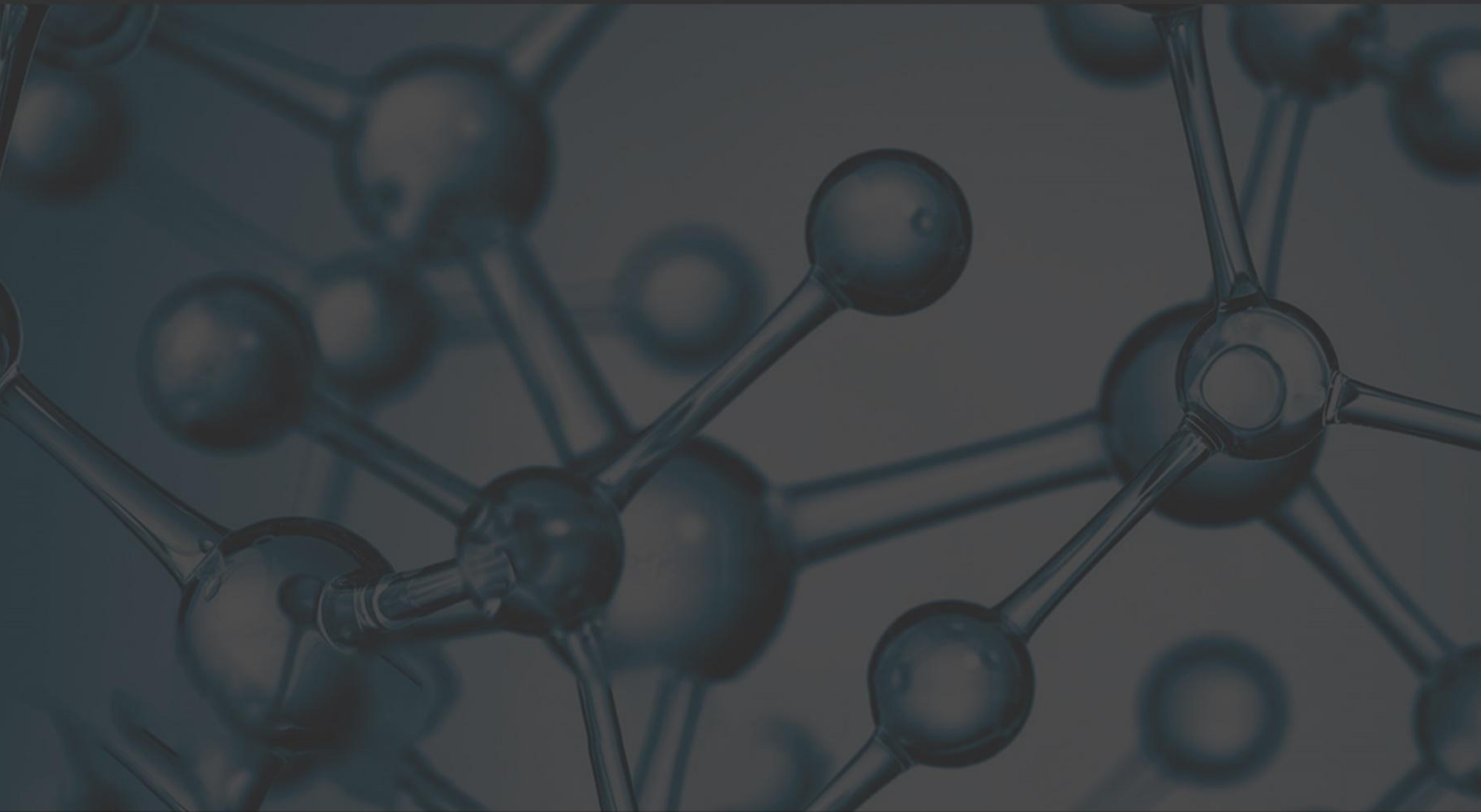


ARID

International Journal for Science and Technology
مَجَلَّةُ أَرِيدَ الدَّوْلِيَّةُ لِلْعُلُومِ وَالتَّكْنُولُوجِيَا

VOL. 6 NO. 11 JUNE 2023

ISSN : 2662-009X



ARID PUBLICATIONS

ARID.MY/J/AIJST

ARAB RESEARCHER ID

ARID International Journal for Science and Technology (AIJST)

Published by Arabic Researcher ID (ARID)

Editorial Board	هيئة التحرير
Prof. Salwan K. J. Al-Ani, Ph.D. State of Qatar, Editor –in- Chief Arid.my/0001-1999	أ.د سلوان كمال جميل العاني ، قطر رئيس التحرير
Prof. Dr. Bassim H. Hameed Qatar University, Qatar	أ.د باسم حامد حميد العاني ، قطر
Prof. Karim El-Din El-Adham, Ph.D., Nuclear and Radiological Regulatory Authority, Egypt Arid.my/0001-5271	أ.د كريم الدين الأدهم ، مصر
Prof. Sabah Jassim, Ph.D. Windsor University and, CEO Applied BioResearch, Canada. Arid.my/002-0784	أ.د صباح جاسم ، كندا
Prof. Mahmoud Abdel-Aty, Ph.D. Sohag University & Zewail University– Egypt Arid.my/0001-8321	أ.د محمود عبدالعاطي ، مصر
Prof. Yousuf Pyar Ali Hassan, Ph.D. Jazan University, KSA. Arid.my/0002-0829	أ.د يوسف بيار علي حسن ، السعودية
Prof. Dr. Adel Sharif, Surrey University, Surrey, Guildford, UK	أ.د عادل شريف ، المملكة المتحدة
Prof. Razzak H. Yousif University of Baghdad-IRAQ arid.my/0002-6656	أ.د رزاق حميد يوسف - العراق
Prof. Mazin Aunay Mahdi, Ph.D. University of Basrah- Iraq. Arid.my/0001-3615	أ.د مازن عونى مهدي ، العراق
Prof. Alaauldeen S. M. Al-Sallami Kufa University- Iraq, Arid.my/0001-6394	أ.د علاء الدين صبحي محسن السلامي ، العراق
Prof. Kasim Mousa Alwan Al-aubidy Philadelphnia University, Jordan	أ.د قاسم موسى علوان العبيدي - الاردن

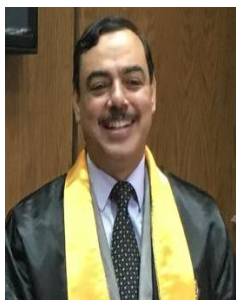
Prof. Ali A. Alraouf HBK University Doha, Qatar	أ.د علي عبد الرؤوف جامعة حمد بن خليفة الدوحة، قطر
Assist. Prof. Abdulsalam Almuhamady, Ph.D. Cairo- Egypt. Arid.my/0001-4059	أ.م.د. عبد السلام المحمدي ، مصر
Assistant Professor Fatih Alemdar, Ph. D. Yildiz Technical University -Turkey arid.my/0004-0654	أ.م.د فاتح علم دار ، تركيا
Dr.Mohamad A. Alrshah University Putra Malaysia(UPM) Arid.my/0001-0002	أ.م.د محمد الهادي الرشاح، ماليزيا
Assistance Prof. Ahmed Rushdi Abdullah Ph.D. Immunology, Aliraqia University, Baghdad-Iraq. Arid.my/0004-6626	أ.م.د احمد رشدي عبد الله، العراق
Assist. Prof.Abdullah Taher Qaed Naji University of Science and Technology-Yemen arid.my/0002-3088	أ. م.د عبدالله طاهر - اليمن
Dr.Ahmed Zaini, Ph.D. Rheinische Friedrich Wilhelms Universität Bonn – Germany arid.my/0004-1767	د. احمد زيني الياسري ، ألمانيا
Dr. Daoud Salman, Ph.D. International School E.I.B of Paris. Arid.my/0001-3561	د. داوود سلمان ، فرنسا
Dr.Saif Alsewaidi, Ph.D. UM University – Malaysia. Arid.my/0001-0001	د.سيف السويدي ، ماليزيا
Dr. Maryam Qays Oleiwi, Ph.D. UKM University, Malaysia. arid.my/0001-1034	د.مريم قيس عليوي ، ماليزيا
Dr. Hani Jassim Kbashi Aston University, United Kingdom. Arid.my/0003-8746	د. هاني جاسم كباشي –المملكة المتحدة

International Scientific Advisory Committee	الهيئة الاستشارية العلمية الدولية
Prof. Ali Sayigh - UK	أ.د علي الصايغ- المملكة المتحدة
Prof. Mariam Ali S A Al-Maadeed- Qatar	أ.د مريم العلي المعاضيد – قطر
Prof. NABIL YOUSEF - Jordan	أ.د نبيل يوسف ايوب – الاردن
Prof.Mohamed Ashoor Alkathiri - Yemen	أ.د محمد عاشور الكثيري – اليمن
Dr. Kai-Henrik Barth - USA	د. كاي هنريك بارث – الولايات المتحدة الامريكية
Prof. Saad Mekhilef - Malaysia	أ.د سعد مخيلف – ماليزيا
Prof.Mohamed Abdula'al A. Al- Nuiami- Jordan	أ.د محمد عبد العال أمين النعيمي - الاردن

Language Review & Translation Committee	لجنة المراجعة اللغوية والترجمة
Dr. Muna A.Al-Shawi, Qatar	د. منى أحمد عبد الغني الشاوي، قطر
Dr. Bader-Eddine Ezziti, Morocco	د. بدر الدين العربي الزيتي، المغرب
Ms. Maha Sharaf, Syria	أ.مها محمد علي شرف، سوريا

Journal details	معلومات عن المجلة
Semi-annual	نصف سنوية
Free publication fees	رسوم النشر في المجلة / مجاناً
Printing, formatting and typesetting fees: \$100	أجور طباعة وتنسيق : 100 دولار
All researches are open access	جميع البحوث العلمية مفتوحة الوصول
All scientific research should be sent for publication through	ترسل البحوث العلمية الى المجلة عبر التفاصيل أدناه
<p>ARID.MY/J/AIJST</p> <p>AIJST@ARID.MY</p>	

مجلس الامناء The Board of Trustees



أ.د. عبدالرازق مختار محمود
Prof. Dr. Abdel Razek Mokhtar

arid.my/0001-2264



أ.د. سلوان كمال جميل العاني
Prof. Dr. Salwan K.J. Al-Ani

arid.my/0001-1999



أ.د. محمود عبد العاطي ابو حسوب
Prof. Dr. Mahmoud Abdel-Aty

arid.my/0001-8321



أ.د. رحاب يوسف
Prof. Dr. Rehab Yousif

arid.my/0003-9655



أ.د. صالح احمد العلي
Prof. Dr. Salaeh al ali
arid.my/0003-6525



أ.د. سعد سلمان عبد الله المشهداني
Prof. Dr. Saad Salman Abdallah

arid.my/0001-6136



د. سيف السويدي
Dr. Saif Al-Sewaidi

arid.my/0001-0001



أ.م.د. ناصر محمود احمد الراوي
Assoc. Prof. Dr. Naser Mahmoud

arid.my/0002-0775



أ.م.د. مصطفى عبدالله السويدي
Assoc. Prof. Dr. Mustafa Abdullah

arid.my/0001-7762

Index | فهرس المجلة

ص	اسم الباحث / الباحثين	البحث
6	Salwan K.J.Al-Ani سلوان كمال جميل العاني	Editor's Letter رسالة المحرر
10	Ahmad Khalaf Alkhawaldeh أحمد خلف الخوالدة	A platinum nanostructur electrode with an iodine coating to measure the bio-electrochemical behavior of arctigenin using cyclic voltammetry استخدام قطب جسيمات نانوية بلاتينيوم مع طلاء اليود لقياس السلوك الكهروكيميائي للأركتيجينين باستخدام فولتامتري الموجة المربعة
25	Rezan Hassan Mahammad ريزان حسن محمد	The Impact of Environmental Pollution on Congenital Anomalies of New Birth in Kirkuk City - Iraq أثر التلوث البيئي على التشوهات الخلقية للمواليد الجدد في محافظة كركوك - العراق
43	Aseel Fadhil Kareem Amal Talib Al Sa'ady أسيل فاضل كريم أمل طالب السعدي	Preparation and analysis of heterocyclic rings made from (Thioxanthone) derivatives Methods of biological activity, thermal analysis تحضير وتحليل الحلقات الهيدروكسيلية المصنوعة من مشتقات (ثايوكزانثون) وطرق النشاط البيولوجي والتحليل الحراري
63	Sami Mohammed Salih Ahmed AmrajaAbdulrraziq Sameer Salih Mohammed سامي محمد صالح أحمد امراجع عبد الرازق سمير صالح محمد	Effect of seawater irrigation on germination and growth of Bauhinia variegata seedlings and seed treatment with gibberellins تأثير الري بمياه البحر على إنبات ونمو شتلات أشجارخف الجمل <i>Bauhinia variegata</i> ومعالجة البذور بالجبرلين
76	Maryam Qays Oleiwi Mohd Khairul Azhar Mat Sulaiman Mohd Farid Mohamed مريم قيس خيرول الازهر مت سليمان محمد فريد محمد	Passive Cooling Strategies in the hot-humid climate: a review study استراتيجيات التبريد السلبي للمباني في المناخ الحار الرطب: دراسة مرجعية
107	Abdullah Al-Numan Salwan K. J. Al-Ani عبدالله النعمان سلوان كمال جميل العاني	Investigation of the effect of Disorder on the Tauc Edge of Hydrogenated Amorphous Silicon using Dunstan's Bandgap Fluctuations Model استقصاء تأثير اللاانتظام على حافة تاوس للسليكون العشوائي المهدرج باستخدام نموذج دونستان لفجوة الطاقة المتعاقبة



ARID Journals

ARID International Journal for Science and Technology (AIJST)

ISSN: 2662-009X

Journal home page: <http://arid.my/j/aijst>

ARID

International Journal for Science and Technology

مجلة أريد الدولية للعلوم والتكنولوجيا

VOL. 6 NO. 11 JUNE 2023

ISSN: 2662-009X

ARID
ARID PUBLICATIONS
ARID.MY/JST

مجلة أريد الدولية للعلوم والتكنولوجيا

المجلد 6 ، العدد 11 ، حزيران 2022 م

رسالة المحرر

اعتادت مجلة أريد الدولية للعلوم والتكنولوجيا على تقديم في مقدمة كل عدد رسالة رئيس التحرير لتتحدث عن مجالات بحثية جديدة أو تجارب تقنية عالمية غاية في الصعوبة أو التطرق للمجالات الحديثة في تعليم العلوم، وستكون رسالتنا في هذا العدد عن تجربة تسخير الضوء بسرعه العاليه لمعالجة البيانات في الكمبيوتر الكمي لكي يتمكن من عمل محاكاة لأصعب حدث ممكن في ثواني معدودة على سبيل المثال ما يحصل في الثقوب السوداء أو لحظة الانفجار العظيم أو في التفاعلات الكيميائية وفي مجالات الطب وغيرها.

والتجربة هي عبارة عن مشروع بحثي في جامعة دارمشتات للعلوم التطبيقية (DUAS) في ألمانيا حيث تمكن علماء الفيزياء من التحكم بطبيعة الضوء وإيقاف سرعته في المواد الصلبة النادرة لمدة دقيقة، واستخدامها في صناعة حاسوب كمي.

كما هو معروف يتم نقل المعلومات التقليدية من خلال اسلاك موصلة معدنية أو أشباه موصلات أو غيرها من الأدوات المستخدمة في نقل المعلومات، وبعد أبحاث ودراسات ظهرت الألياف الضوئية كأحد أفضل الحلول في معالجة البيانات، والذي عمل طفرة بالاتصالات وفي نقل البيانات؛ لأن الضوء يسير بسرعة 300 ألف كم/الثانية، وهذا جعل علماء الفيزياء يفكرون بتشغيل أجهزة الحاسوب المستقبلية بالضوء حتى تحقق سرعات معالجات خيالية تواكب عمليات المحاكاة المعقدة الخاصة بدراسات الكون التي يتم العمل عليها حالياً وتعطي نتائج بمنتهى السرعة والدقة، ولكن التكنولوجيا الضوئية تعتمد حالياً على شبكات الاتصال الضوئية التقليدية ويتم نقل المعلومات بواسطة الألياف الضوئية ولكن في نهاية الألياف ستتحول المعلومات إلى

إشارات كهربائية عادية التي تستخدم في أجهزة الحاسوب التقليدية لمعالجة البيانات، وهذا ما جعل العلماء يفكرون في استخدام أجهزة الحاسوب الكمومية الضوئية لمعالجة المعلومات باستخدام الضوء .

وأول خطوة لتنفيذ الفكرة هي القدرة على تخزين البيانات الضوئية في داخل أنظمة الكم .

يشير العالم توماس هالفمان / رئيس الفريق البحثي بوجود حاجة إلى وسيط لتخزين الضوء وهو ما يسمى بالذاكرة الضوئية أو الكمومية أو يكون هناك سيادة وسيطرة على حركة الضوء ونستطيع الاحتفاظ به داخل حيز معين بالحاسبات، وهي التي تتم باستخدام ذاكرة ضوئية بنظام كمي لتخزين الضوء لمدة من الزمن .

وباستخدام شعاع ليزر فائق السرعة إذ تعد السرعة من الأمور الجوهرية التي لا يمكن التغلب بها استطاع الفريق البحثي من نقل الإلكترونات بسرعات دون الفيمتو ثانية، أي أقل من ربع المليون جزء من الثانية، حيث تمكن هذا الفريق من إبطاء سرعة الضوء إلى 17 كم/ثانية في العام 1999م، ويعتبر هذا رقماً قياسياً آنذاك، وفي عام 2003، تمكن نفس الفريق من إيقاف سرعة الضوء بصورة كاملة لمدة أجزاء من الثانية، وفي عام 2013، استطاع إيقاف سرعته لمدة 16 ثانية، والآن تمكنوا من إيقاف سرعته لمدة 60 ثانية باستخدام بلورة مبردة.

واستطاع الفريق عمل ذلك من خلال استخدام أشعة ليزر ومن خلالها يمكن التحكم بسرعة الضوء داخل بلورة وهذه البلورة تحتوي على تركيز منخفض من الايونات في ذرات مشحونة كهربائياً من عنصر البراسيدينيوم، وعند حصول تلامس من مصدر الضوء مع البلورة كان يحصل تباطؤ في سرعة الضوء بشكل كبير، وفي هذه اللحظة يفصل العلماء تشغيل شعاع الليزر ويوقفوا الضوء تماماً، ولكن الذي حصل أن الضوء لم يتوقف إنما تحول إلى وسط ذري أي تحولت نبضة الضوء إلى شكل آخر يسمى المذبذب الذري .

بكلام آخر، نقل الطاقة من مذبذب واحد (مجال الضوء) ووضعه داخل مذبذب ثاني هي الذرة وهنا يمكن استعادة الضوء بسهولة، وبالفعل استطاع الفريق البحثي تخزين الصورة بهذه الطريقة واستطاعوا طباعة الصورة المكونة من ثلاثة خطوط على نبضة الضوء وهو دليل على تخزين الصورة داخل البلورة لمدة دقيقة، وبعدها أعادوا عرضها مرة أخرى واستطاعوا تحطيم سجل تخزين الصور السابق الذي كان أقل من 10 مايكروثانية فقط، وأصبح حقيقة تخزين الصورة أمر مهم في مستقبل تطور الحاسبات أو الكومبيوترات الكمية الضوئية فبدلاً من احتواء الحواسيب في حساباتها على نبضة ضوئية واحدة داخلها أي بت واحد (Bit) من البيانات فالصورة الحالية ستخزن كمية من البيانات أعلى بكثير من الحالية .

إضافة لذلك يمكن تخزين أي صورة لأي غرض ما، ويمكن أن يكون التخزين من غير الصور، وعلى الرغم من أن أوقات تخزين الضوء تكون عادة قصيرة جداً وهو عائق بالتجربة لأن البيانات المضطربة تعطل التذبذب لكن استطاع الفريق العلمي من تحقيق وقت تخزين قياسي من خلال حماية المذبذب بالمجالات المغناطيسية ونبضات عالية التردد من خلال استخدام خوارزميات معقدة لتحسين أشعة الليزر والمجالات المغناطيسية والنبضات عالية التردد لأطول فترة ممكنة داخل البلورة. وفيما يخص الوقت لحفظ البيانات داخل البلورة فلن يكون محدداً بدقة وإنما سيمتد من ساعات إلى أسبوع كامل.

ومن تطبيقات التجربة أجهزة الحاسبات التي تستخدم الضوء في المستقبل وتمهد الطريق للاتصالات والحاسبات الكمية وتجعل الكمبيوترات الكمومية أقوى بكثير، وتحل المشكلات المعقدة خارج نطاق الحاسبات التقليدية ذلك لأن هذه الحاسبات تستخدم الأرقام الثنائية (0،1) أو البت (Bits) أما أجهزة الكمبيوتر الكمومية سوف تخزن المعلومات في Qubits (0،1) باستخدام الفوتونات أو الذرات التي تعطيها القدرة الجبارة على معالجة البيانات بمقدار 1000 مرة عن الحاسبات التقليدية، ومن المتوقع استخدام هذه التقنية خلال فترة 5-10 سنوات حتى تكون جاهزة للاستخدام. ويُخطط مستقبلاً في زيادة مدة بقاء الفوتونات داخل البلورة دون التلاعب بالمعلومات التي تحملها ووضعها الكمي، وحسب قولهم أنه في المستقبل القريب سيسمح هذا الإكتشاف بصنع الكمبيوتر الكمي، ومن المحتمل أيضاً أنه سيتم قريباً تصنيع أجهزة بإمكانها اجتياز حدود سرعة الضوء.

ومن مميزات الكمبيوترات الكمومية اختصار الزمن التي تجريها الحاسبات التقليدية التي تأخذ سنين طويلة إلى ثواني فقط، كما تستخدم لمحاكاة البيانات بدقة عالية وبذلك يمكن التنبؤ بالطقس وعمل محاكاة للتفاعلات الكيميائية المعقدة ومعرفة ماذا يحدث داخل الثقوب السوداء وما الذي حصل منذ بداية الكون وحتى نهايته.

بالإضافة لذلك الثورة في مجال الطب لاكتشاف الأمراض والأدوية وسهولة تشخيص الأمراض، وفي مجالات حماية البيانات التي تقدمها هذه الكمبيوترات والتشفير العالي، وعدم نسخها وحمايتها من السرقة أو التجسس على البيانات.

ومع ظهور هذا الاختراع ظهر أيضاً الإنترنت الكمومي الذي يعمل عن طريق توليد معادلات ومفاتيح رقمية ولكن باستخدام فوتونات الضوء. وهكذا لن تكون هناك حدود لقدرات العقل البشري في تسخير الضوء وهو أسرع شيء بالكون ليكون جزء من وسائل الاتصال وتداول البيانات، والذي يفتح آفاق جديدة في تسخير العلوم والتكنولوجيا في خدمة الإنسان وتنقله في الكون بسرعة عالية وخلال ثواني فقط .

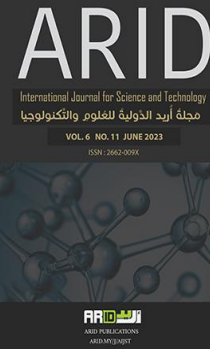
ونتمنى أن تستخدم الإنسانية التطور التكنولوجي الهائل لخدمتها فقط وليس للأسلحة والذكاء الصناعي الذي قد يصبح خطراً في المستقبل عندما يستقل بذكاءه.



ARID Journals

ARID International Journal for Science and Technology (AIJST)

ISSN: 2662-009X

Journal home page: <http://arid.my/j/aijst>

مجلة أريد الدولية للعلوم والتكنولوجيا

المجلد 6 ، العدد 11 ، حزيران 2023 م

A Platinum Nanostructur Electrode with an Iodine Coating to Measure the Bio-Electrochemical Behavior of Arctigenin Using Cyclic Voltammetry

Ahmad Khalaf Alkhawaldeh

Department of Allied medical sciences, Zarqa University College, Al-Balqa Applied University, Jordan.

استخدام قطب جسيمات نانوية بلاتينيوم مع طلاء اليود لقياس السلوك الكهروكيميائي للأركتيجينين باستخدام فولتامتري الموجة المربعة

أحمد خلف الخوالدة - قسم العلوم الطبية المساندة، كلية الزرقاء الجامعية، جامعة البلقاء التطبيقية، الأردن.

ahmad.khawaldeh@bau.edu.jo
arid.my/0003-8855
<https://doi.org/10.36772/arid.aijst.2023.6111>

ARTICLE INFO

Article history:

Received 20/08/2022

Received in revised form 13/02/2023

Accepted 03/03/2023

Available online 15/06/2023

<https://doi.org/10.36772/arid.aijst.2023.6111>

ABSTRACT

The cyclic voltammetric method was utilized to build an iodine-modified platinum nanoparticle electrode for measuring arctigenin electrochemically. The findings of the experiments showed that this modified electrode had a considerable voltammetric response to arctigenin, which was due to the electrocatalysis properties of iodide and the strong conductivity and large specific surface area of the platinum nanostructure electrode. The proposed approach demonstrated a broad linear range, good sensitivity, low detection limit and high selectivity. The examination of the scan rate change revealed that the electrode process is adsorption-controlled. The oxidation of arctigenin was demonstrated to involve both protons and electrons. Finally, this method can be used to develop a sensitive arctigenin detection sensor.

Keywords: Volumetric sensor, Iodine-coated, Nanoparticle, Arctigenin, Platinum electrode, Iodide, Electrocatalytic ability.

الملخص

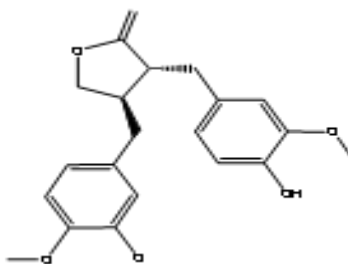
تم استخدام طريقة قياس الفولتامترية الحلقية لبناء قطب جسيم نانوي باليود معدّل باليود لقياس الاركتيجينين كهربائياً. أظهرت نتائج التجارب أن هذا القطب المعدل له استجابة فولتامترية كبيرة للأركتيجينين، والتي كانت بسبب خصائص التحفيز الكهربائي لليوديد والموصلية القوية ومساحة السطح المحددة الكبيرة لقطب البلاتين النانوي. أظهرت الطريقة المقترحة نطاقاً خطياً واسعاً وحساسية جيدة وحداً منخفضاً للكشف وانتقائية عالية. كشف فحص تغيير معدل المسح أن عملية القطب الكهربائي يتم التحكم فيها عن طريق الامتصاص. تم إثبات أن أكسدة الاركتيجينين تشمل كل من البروتونات والإلكترونات. أخيراً، يمكن استخدام هذه الطريقة لتطوير مستشعر حساس للكشف عن الاركتيجينين.

الكلمات الرئيسية: مستشعر حجمي، مغلف باليود، جسيمات نانوية، الاركتيجينين، قطب بلاتينيوم، يوديد، قدرة التحفيز الكهربائي.

1. Introduction

Arctigenin is extracted from the seeds of the traditional Chinese herb *Fructus Arctii* [1]. Arctigenin has been shown to have a variety of pharmacological effects, including anti-cancer, anti-asthmatic, anti-influenza, anti-austeric, anti-HIV, and anti-inflammatory activities [2-5]. Arctigenin has a wide range of pharmacological effects; hence quantifying it is crucial [6]. However, there are only a few analytical methods now available for arctigenin, including HPLC, LC-MS/MS, fluorescence, UPLC-ESI-MS/MS, and HPLC-UV [7-11]. Arctigenin electrochemical studies and electroanalytical methods have a large linear range, great sensitivity, and simplicity [12]. As a result, developing a sensitive and reliable electrochemical sensor for measurement and mechanism investigation of arctigenin remains an exciting prospect [13]. Among the numerous various ways for modifying electrode surfaces, the production of iodine on metallic electrode surfaces has attracted a lot of interest [14]. It is for reasons such as environmental friendliness, chemical stability, technological suitability on the electrode surface and low cost [15]. The ligand's significant surface activity on common solid-metal electrodes changes the redox chemistry of the iodine in the surface-bound state [16]. This is where the chemisorption species come in. Iodine adlayer modified electrodes have been widely used in various metallic electrodes [17], and the fabrication of nanoparticles is rich in anticipated properties [18]. Platinum nanoparticles electrode has a long history of application as electrode-modified materials [19-21]. Iodine adlayer modified electrodes have been widely used in various metallic electrodes [22-23], particularly in self-assembly electrodes [24] and the synthesis of nanoparticles rich in expected properties [25]. Only one article on iodine modified glassy carbon electrode (GCE) has been found so far [26]. By electrochemically depositing KI ($10^{-3} \text{ mol.L}^{-1}$ in H_2SO_4 solution, pH 1.5), an iodine modified GCE was created. The deposition was carried out

using a cyclic scan potential between -0.75 V and 1.2 V for 30 cycles [26]. The proposed iodide modified electrode demonstrated the highest electrocatalytic activities in different buffer solutions for As (III) oxidation, CrO_4^{2-} , and IO_3^- reduction. Nonetheless, the conductivity of iodide-modified GCE is poor. As a result, the iodide modified GCE with improved conductivity is worth investigating [27]. The electrochemical determination of arctigenin was reported for the first time in this work using a biosensor Iodide/platinum nanostructure electrode.



Scheme(1): Chemical structure of arctigenin.

2. Experimental

2.1 Reagents, Apparatus and Instrumental

For the electrochemical procedures, a Model CHI650 electrochemical system (Chenhua Instrument Company, Shanghai, China) used Ag/AgCl reference electrode, a platinum auxiliary electrode, and a bare or modified platinum nanostructure as a working electrode employed in a typical three-electrode setup (diameter 3 mm). The remaining chemicals were all of the analytical quality and were utilized without further purification. Aladdin Co. Ltd. provided the KI powder and the arctigenin analytical standard (Shanghai, China). Arctigenin stock solution (1×10^{-4} M) was produced in methanol and stored in a refrigerator at 5 °C. When utilized, it was diluted to an appropriate concentration. 0.2 M phosphate buffer solution (PBS) was made by combining 0.15 M Na_2HPO_4 . For the experiments, double-distilled water was employed. X-ray

powder diffraction (EDX) and scanning electron microscopy (SEM) (Inspect F50 Company, Netherlands) were used.

2.2 Fabrication of Iodide/Pt nanostructure electrode

The platinum electrode (3 mm diameter) was polished to a mirror-like surface with 0.05 μ m alumina slurry. The Pt (nano) was then cleaned in ethanol and water for 5 minutes using an ultrasonic treatment before drying at room temperature. The I-Pt (nano) electrode was created by sprinkling 1 L of iodine solution onto pre-cleaned Pt (nano) and drying it at room temperature. The Pt nanostructure surface was then electro-deposited with iodide by cyclic scanning between -0.2 V and 1.3 V with 100 mV/s for ten cycles in pH 7.5 PBS containing 1.0×10^{-4} M of KI.

The genuine sample arctigenin was used to assess the performance of the suggested voltammetric sensor in terms of practical application. Arctigenin powder was disseminated in 25 mL of methanol and super sonicated for 180 minutes. Finally, the filtrates were mixed and evaporated until just 10 ml of solution remained. As a detection sample, the solution was employed.

3. Results and Discussion

3.1 Morphological analysis of an I-Pt (nano) electrode

The SEM analysis was performed to identify and describe I-Pt (nano) electrode's precise microstructure. The SEM micrograph of the I-Pt (nano) surface may be seen in Figure 1. They could observe that iodide had effectively electrodeposited onto the platinum electrode. Another effective method for testing the interfacial characteristics of surface-modified electrodes is scanning electron microscopy (SEM). That is, for modified electrodes, the charge transfer rate at the electrode/electrolyte interface is kinetically fast.

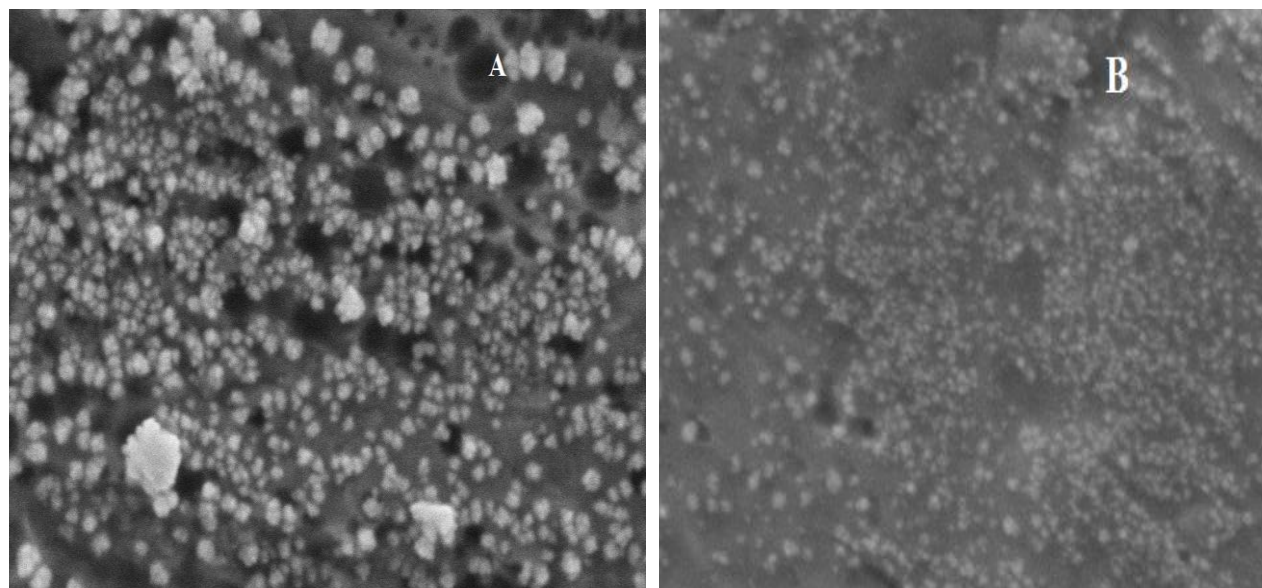


Figure (1): (A) SEM micrograph of platinum nanostructured electrode unmodified, (B) SEM micrograph of Iodine-modified platinum nanostructured electrode.

The identity of the deposited particles was confirmed by energy-dispersive X-spectroscopy. The EDX spectra in Figure 2 indisputably confirm the identity of the deposited platinum nanostructures. Thus, SEM, EDX spectra on the one hand, and cyclic voltammetry on the other, show that for the formation of pt (nano).

Spectrum: Acquisition 6372

El	AN	Series	unn. C [wt.%]	norm. C [wt.%]	Atom. C [at.%]	Error [%]
I	53	L-series	9.49	11.82	17.08	0.7
Pt	78	M-series	70.80	88.18	82.92	2.9
Total:			80.29	100.00	100.00	

Figure (2): EDX spectra of I-Pt (nano) electrode.

3.2 Electrochemical character of platinum nanostructure electrode modified by iodine

Using cyclic voltammetry at a scan rate of 100 mV/s, the electrochemical behavior of a Pt nanoparticle electrode modified by iodine was investigated. Figure 3 depicts the iodine coated

platinum nanoparticles electrode representative voltammograms recorded in 0.5 M H_2SO_4 (dashed line) superposed to the bare platinum electrode nanoparticles process voltammograms (solid line). The lack of redox (oxidation/reduction) activity, specifically oxygen and hydrogen adsorption, suggests a near total surface suppression between the hydrogen production limits (around -0.2 V) and surface iodine suppression levels (around 0.95 V). When the potential of the electrode with iodine-coated scans exceeds 0.95 V, the iodine is partially desorbed.

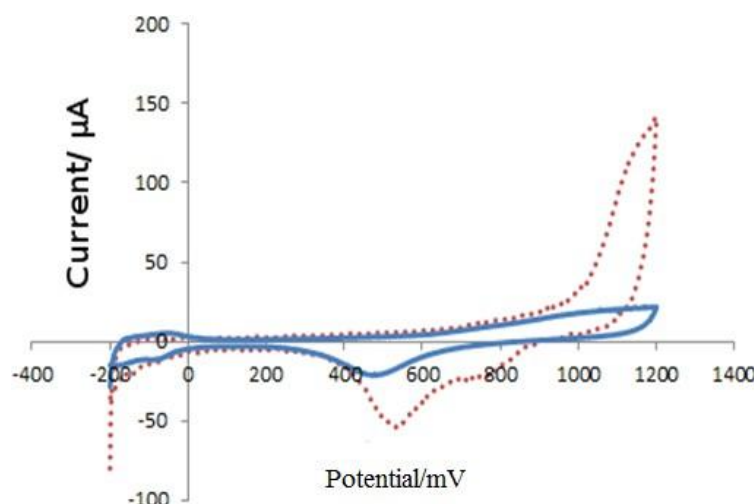


Figure (3): Voltammograms of platinum nanoparticle electrode (solid line) and iodine-coated platinum nanoparticle electrode (dashed line). At a scanning rate of 100 mV/s.

In the first cycle, anodic peaks at 0.510 V and cathodic peaks at -0.4585 V were found (Figure 4). At the platinum nanostructure electrode modified by iodine, a pair of reversible redox peaks with $i_{pa} = 15.6$ A and $i_{pc} = 12.8$ A was discovered. In succeeding cycles, the anodic peaks at 0.481 V moved negatively, peak currents increased first then fell, and all other peaks grew. The results showed that the electroactive area was enlarged with the use of platinum nanostructure electrodes and Iodide modified electrode surfaces, which would increase electrochemical activity and enhance electrochemical sensing.

Figure 4 shows cyclic voltammograms for an iodine-Pt (nano) electrode and a Pt (nano) electrode with a variable surface area generated under the same experimental conditions. The identity of the nanostructured electrode is demonstrated by the striking similarity of the two electrodes' cyclic voltammograms and the appearance of the well-known typical voltammetric characteristics of platinum electrodes.

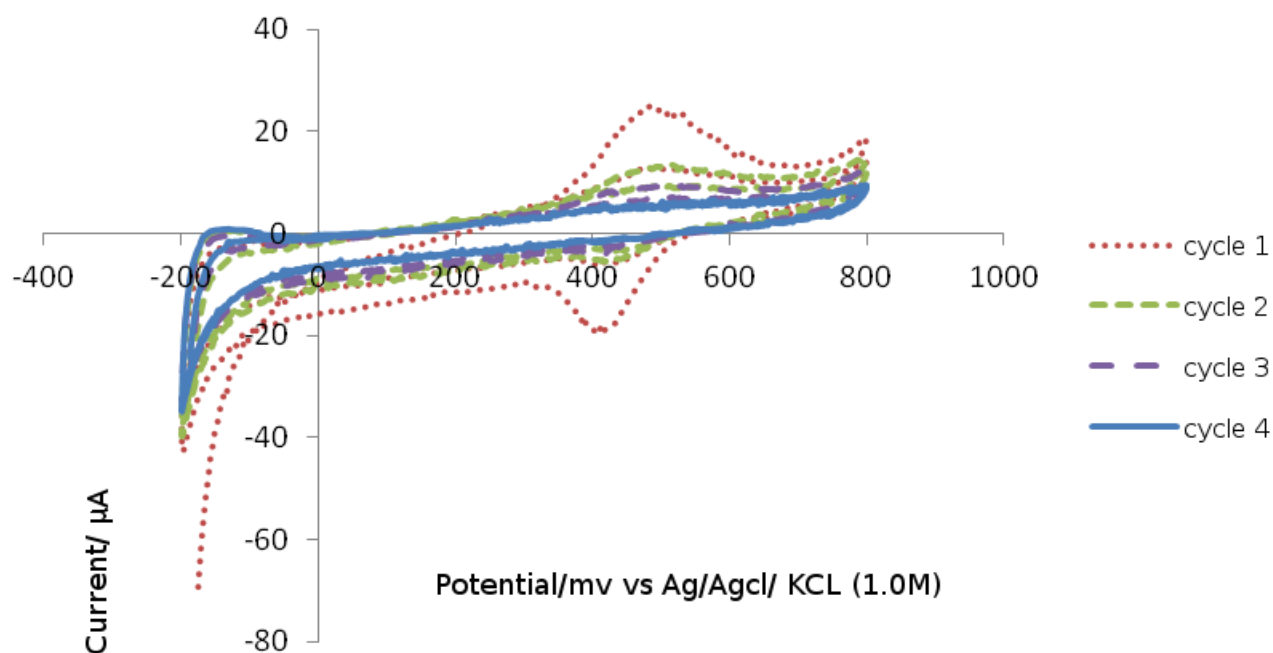


Figure (4): Cyclic voltammograms for the iodine-Pt (nano) electrode at different scan times.

They used an electrochemical probe to examine the properties of the many changing layers by CV. These were the charging currents: an unmodified platinum electrode with a platinum nanostructure electrode with iodine alteration. Furthermore, the considerable increase of these peaks indicates the sequential building of the iodide monolayer on the surface of the platinum nanostructure.

3.3 Voltammetric behavior of arctigenin at Iodide- Pt (nano) electrode

Cyclic voltammograms for an iodine-coated Pt (nano) electrode 1×10^{-4} M of arctigenin in 0.1 M PBS buffer solution were investigated at a scan rate of 100 mV/s is shown in Figure 5. The voltammograms show anodic arctigenin oxidation peaks from 0.6 to 1.1 V. As a result, its behavior is irrevocable. A small fluctuation in peak potentials for varying concentrations is to be expected for the various electrochemical processes. The iodine monolayer did not decay during the studies, although due to the ease of production of the iodine-coated electrode, the surface was re-coated frequently.

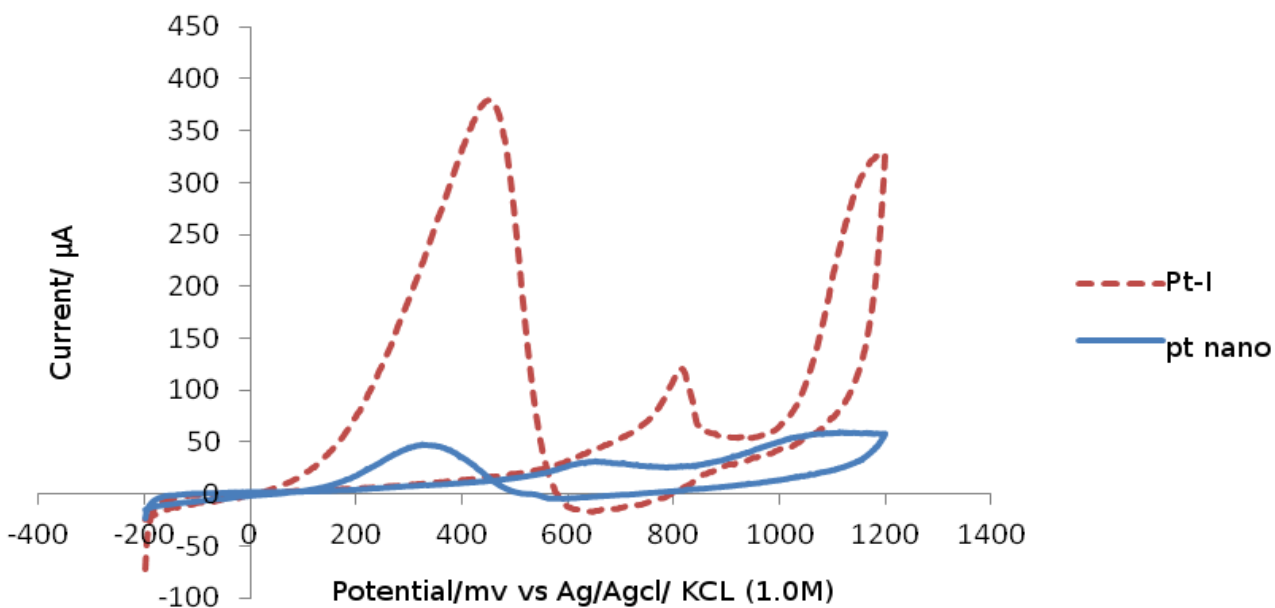


Figure (5): Cyclic voltammogram of iodine-Pt (nano) electrode with 1×10^{-4} M of arctigenin.

It lowered resistance to the bare Pt (nano) electrode significantly at Iodide-Pt (nano) electrode, attributing to the function of nanostructure and iodide working together. These findings agreed with the debate in cyclic voltammetry. The voltammograms contour matched the current peak order of arctigenin. Arctigenin showed one oxidation peak around 0.8 V and one reduction peak at -0.6 V during the first cyclic scan. The potential window was varied to better understand the

electrochemical behavior of arctigenin at the Iodide-Pt(nano) electrode. There were no redox peaks identified when the potential window was set between 0.1 V and 0.55 V for the cyclic scan.

In the complex electrochemical reaction process of arctigenin at the Iodide-Pt (nano) electrode, triple potential step chronoamperometry was used to measure the diffusion coefficient and adsorption capacity. Experiments were carried out in an arctigenin solution (1×10^{-4} M) and blank PBS. The sensor was immersed in the solution for 5 minutes before the potential step to obtain saturation adsorption.

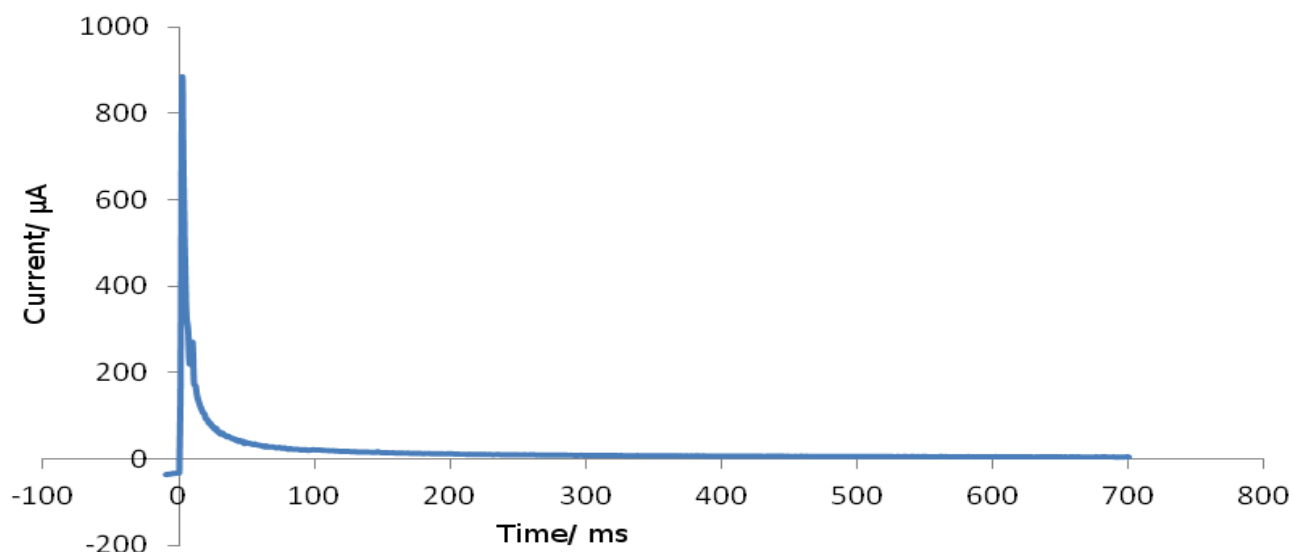


Figure (6): Chronoamperometric of iodine-Pt (nano) electrode with 1×10^{-4} M of arctigenin.

Figure 6 depicts the charge together with the time curve. The potentials were stepped from 0.6 V to 1.1 V, matching the arctigenin oxidation peak, implying that arctigenin oxidation is controlled by adsorption. According to Anson's CC theory (equation 1) [21].

$$Q = nFA\Gamma^* \quad (1)$$

Where D is the diffusion coefficient, Q is the double-layer charge, Γ^* is the adsorption capacity, A is current, and F is the Faradaic charge owing to arctigenin oxidation.

The saturating adsorption capacity was predicted to be $3.21 \times 10^{-9} \text{ mol.cm}^{-2}$ of oxidation peak.

4. Conclusion

A volumetric sensor based on electrochemical iodide deposition and simple dipping-drying of platinum nanostructure electrode was successfully developed and employed for high-sensitivity arctigenin detection. The proposed approach demonstrated outstanding effectiveness against arctigenin, which was attributed to iodide's electrocatalytic capacity, large specific surface area, and platinum nanostructure electrode's excellent electric conductivity. It performed particularly well for arctigenin detection, with a wide linear range, low detection limit, high sensitivity, selectivity, and good stability. Finally, the current approach was applied to real-world samples with positive results.

List of Abbreviations and Symbols

A	Current
CV	Cyclic voltammograms
D	Diffusion coefficient
EDX	X-ray powder diffraction
F	Faradaic charge owing
GCE	Glassy carbon electrode
Nano	Nanoparticle
PBS	Phosphate buffer solution
Q	Double-layer charges
SEM	Scanning electron microscopy
Γ^*	Adsorption capacity

References

- [1] L. Yang, E. Cai, J. HanZhang, W. Zhao, Y. Chen, Q. Guo, M. He, "Novel method of preparation and activity research on arctigenin from fructus arctii", *Pharmacognosy Magazine*, 14(53) (2018) 87.
- [2] J. C. Qin, B. Y. Li, Y. F. Shen, T. Wang, G. X. Wang, "In vitro and in vivo inhibition of a novel arctigenin derivative on Aquatic Rhabdovirus". *Virus Research*, 316, (2022), 198798.
- [3] X. Y. XU, D. Y. WANG, C.F. KU, Y. ZHAO, H. CHENG, K. L. LIU, L. J. RONG, H. J. ZHANG, "Anti-HIV lignans from Justicia procumbens". *Chinese Journal of Natural Medicines*, 17(12), (2019), 945–952.
- [4] J. Huh, C.M. Lee, S. Lee, S. Kim, N. Cho, Y. C. Cho, "Comprehensive characterization of Lignans from Forsythia viridissima by UHPLC-ESI-QTOF-MS, and their no inhibitory effects on Raw 264.7 cells". *Molecules*, 24(14), (2019), 2649. <https://doi.org/10.3390/molecules24142649>
- [5] S. Smith, S. Holland, J. Slade, M. Hallam, D. Heal, "Progressive ratio (PR) intravenous self-administration testing in rats to assess the relative reinforcing effects of a wide range of substances of abuse". *Journal of Pharmacological and Toxicological Methods*, 99, (2019), 106595. <https://doi.org/10.1016/j.vascn.2019.05.007>
- [6] L. Ge, F. Liu, Y. Hu, X. Zhou, "Qualitative and quantitative analysis of arctiin and arctigenin in Arctium tomentosum mill by high-performance thin-layer chromatography". *JPC – Journal of Planar Chromatography – Modern TLC*, 33(1), (2020), 19–26. <https://doi.org/10.1007/s00764-019-00005-z>
- [7] K. Susmitha, M. Menaka, "LC-ESI-MS/MS method for the fosamprenavir quantification bioanalytical method development and validation for the quantification fosamprenavir in human plasma by LC-ESI-MS/MS". *Indian Journal of Pharmaceutical Education and Research*, 56(3s) (2022). <https://doi.org/10.5530/ijper.56.3s.168>
- [8] Z. Cai, C. Wang, C. Chen, L. Zou, C. Chai, J. Chen, M. Tan, X. Liu, "Quality Evaluation of Ionicerae japonicae flos and Ionicerae flos based on simultaneous determination of multiple bioactive constituents combined with multivariate statistical analysis". *Phytochemical Analysis*, 32(2), (2019), 129–140. <https://doi.org/10.1002/pca.2882>
- [9] H. leu, "Growth, yield and phytochemical constituents of Arctium Lappa L. in response to phosphorous and potassium fertilizers application". *SETWM-20, ACBES-20, EEHSS-20 Nov.* (2020), 16-17. <https://doi.org/10.17758/eaes10.eap1120122>
- [10] H. Son, W. Kang, "Quantitative determination of Bilobetin in rat plasma by HPLC–ms/MS and its application to a pharmacokinetic study". *Biomedical Chromatography*, 34(4) (2020), <https://doi.org/10.1002/bmc.4784>
- [11] E. M. Rabie, A. A. Shamroukh, M. Khodari, "A novel electrochemical sensor based on modified carbon paste electrode with zno nanorods for the Voltammetric determination of indole-3-acetic acid in plant seed extracts". *Electroanalysis*, 34(5), (2022). 883–891. <https://doi.org/10.1002/elan.202100420>
- [12] G. İskifoğlu, "A proposal for developing culture sensitive, reliable and valid measurement tools of constructs". *INTED-Proceedings* (2019). <https://doi.org/10.21125/inted.2019.0229>
- [13] M. Seo, "Methods for investigating electro-chemo-mechanical properties of solid electrode surfaces". *Electro-Chemo-Mechanical Properties of Solid Electrode Surfaces*, (2020). 39–66. https://doi.org/10.1007/978-981-15-7277-7_2

- [14] A. G. Kvashnin, P. V. Avramov, S. Sakai, Y. S. Nechaev, P. B. Sorokin, "Estimation of graphene surface stability against the adsorption of environmental and technological chemical agents". *Physica Status Solidi (b)*, 254(6), (2017). 1600702. <https://doi.org/10.1002/pssb.201600702>
- [15] H. Xu, H. Shang, C. Wang, Y. Du, "Surface and interface engineering of noble-metal-free electrocatalysts for efficient overall water splitting". *Coordination Chemistry Reviews*, 418, (2020). 213374. <https://doi.org/10.1016/j.ccr.2020.213374>
- [16] A. K. Alkhawaldeh, "Electrochemical reduction from carbon dioxide to urea through the application of a polycrystalline palladium electrode potential Square Wave Regime". *J. Indian Chem. Soc.*, Vol. 97, No. 11a, (2020): pp. 2321-2328. DOI: [10.5281/zenodo.5654279](https://doi.org/10.5281/zenodo.5654279).
- [17] A. K. Alkhawaldeh, "Biochemistry properties of Platinum nanoparticles and Adatoms". *Journal of Pharmaceutical Negative Results*, 14 (3) (2023): 1159-1164. <https://doi.org/10.47750/pnr.2023.14.03.153>
- [18] A. K. Alkhawaldeh, "Electrocatalytic activities of a platinum nanostructured electrode modified by gold adatom toward methanol and glycerol electrooxidation in acid and alkaline media". *Journal of Oleo Science*, 72 (3) (2023): 347-356, doi: [10.5650/jos.ess22376](https://doi.org/10.5650/jos.ess22376).
- [19] A. K. Alkhawaldeh, "Platinum nanoparticle electrode electro-chemical lead (ii) determination with square-wave voltammetry modified with iodine". *AIP Conference Proceedings*, (2021), <https://doi.org/10.1063/5.0045328>
- [20] A. Alkhawaldeh, "Photocatalytic degradation of platinum nanostructure in tantalum electrode". *Journal of Pharmaceutical Negative Results*, Vol 13, Special Issue 9, (2022), 6264–6272.
- [21] T. Manny, R. Miah, F. Islam, D. Sen, R. Mahmud, "Enhanced oxidation of uric acid at thiourea-modified gold electrode in Alkaline Media". *Russian Journal of Electrochemistry*, 56(7), (2020), 570–577. <https://doi.org/10.1134/s1023193520070046>
- [22] C. Shruthi, Y. Venkataramanappa, G. Suresh, "Reduced mwcnts/palladium nanotubes hybrid fabricated on graphite electrode for simultaneous detection of ascorbic acid, dopamine and uric acid". *Journal of the Electrochemical Society*, 165(10) (2018). <https://doi.org/10.1149/2.1161810jes>
- [23] H. Ueda, K. Nishimori, T. Hisatomi, Y. Shiraishi, S. Yoshimoto, "Iodine adlayer mediated gold electrooxidation in bis(trifluoromethylsulfonyl)amide-based ionic liquids". *Electrochimica Acta*, 371, (2021), 137811. <https://doi.org/10.1016/j.electacta.2021.137811>
- [24] K. W. Shah, L. Zheng, "Microwave-assisted synthesis of hexagonal gold nanoparticles reduced by Organosilane (3-Mercaptopropyl)trimethoxysilane". *Materials*, 12(10), (2019), 1680. <https://doi.org/10.3390/ma12101680>
- [25] P. Hasin, V. Amornkitbamrung, N. Chanlek, "Economical nanocomposites of cobalt or nickel species and polyaniline-derived n-doped mesoporous carbons for dye-sensitized solar cells as counter electrodes". *Journal of Catalysis*, 351, (2017), 19–32. <https://doi.org/10.1016/j.jcat.2017.03.021>
- [26] G. March, T. Nguyen, B. Piro, "Modified electrodes used for electrochemical detection of metal ions in environmental analysis". *Biosensors*, 5(2), (2015), 241–275. <https://doi.org/10.3390/bios5020241>

M. Safaei, "A sensitive voltammetric sensor based on AU nanoparticle decorated graphene nanosheets modified glassy carbon electrode for determination of acetylcholine in presence of dopamine". *Nanoarchitectonics*, 1(1), (2020), 43–52.
<https://doi.org/10.37256/nat.112020182.43-52>



ARID Journals

ARID International Journal for Science and Technology (AIJST)

ISSN: 2662-009X

Journal home page: <http://arid.my/j/aijst>

مَجَلَّةُ أُرَيْدُ الدَّوْلِيَّةُ لِلْعُلُومِ وَالتَّكْنُولُوجِيَا

المجلد 6 ، العدد 11 ، حزيران 2023 م

The Impact of Environmental Pollution on Congenital Anomalies of New Birth in Kirkuk City – Iraq

Rezan Hassan Mahammad

Department of Radiology and ultrasound, College of medical Technique, University of Alkitab,
Kirkuk ,Iraq

أثر التلوث البيئي على التشوهات الخلقية للمواليد الجدد في محافظة كركوك - العراق

ريزان حسن محمد
قسم الأشعة و السونار - كلية التقنية الطبية - جامعة الكتاب
كركوك - العراق

dr.rezanhasan@uoalkitab.edu.iq

arid.my/0008-0154

<https://doi.org/10.36772/arid.aijst.2023.6112>

ARTICLE INFO

Article history:

Received 05/11/2022

Received in revised form 30/11/2022

Accepted 02/12/2022

Available online 15/06/2023

<https://doi.org/10.36772/arid.aijst.2023.6112>

ABSTRACT

The Birth abnormalities or congenital malformations can emerge during the fetal development stage or from a parent's genetic composition. The main contributors to neonatal and childhood disease and impairment are congenital abnormalities. Increase the observation of congenital anomaly (CA) in Mama Village that belong to Kirkuk city has been made with information about frequency and nature of these abnormalities.

This study was conducted to estimate the prevalence of congenital anomaly in Mama Village that belong to Kirkuk city.

A Cross sectional study that includes 60 couples who are living in Mama Village for the duration from March 2020 to March 2022 to investigate the risk of congenital anomaly that increases in frequency in 2019. The data was collected by direct interview of the participants and took a full history of the performing ultrasonography.

The highest prevalence of CA that reach 55%, 96.7% of participant were cousin. Nearly two third of participant had single anomaly. Central nervous system anomaly was the most prevalent anomaly in the current study, and hydrocephalous was presented in 18.3% of them. Young age group mother, cousin marriage and history of infant death were a risk factor for CA.

It is concluded that a higher prevalence of congenital anomaly in the current study especially when compared with the number of area population. The central nervous system was more probable which shown to be substantially correlated with maternal history of prior previous child death, paternal consanguinity, and age. Higher prevalence of central nervous system could be related to the environment effect which is (weapon-related) occur in the studied area previously.

Key words: Congenital anomaly, cousin marriage, weapon explosion.

الملخص

يمكن أن تظهر تشوهات الولادة أو التشوهات الخلقية خلال مرحلة نمو الجنين أو من التركيب الجيني لأحد الوالدين، لكن زيادة ملاحظة التشوهات الخلقية في قرية ماما التابعة لقضاء الدبس / محافظة كركوك بنيت بمعلومات حول تكرار وطبيعة هذه التشوهات.

هدف الدراسة كان لتحديد أنواع مختلفة من التشوهات الخلقية وتكرارها بين العوائل الموجودة في قرية ماما التابعة لمحافظة كركوك وما إذا كانت هناك علاقة بين هذه التشوهات وانفجار الغاز غير معلومة المصادر وتحقيق في مخاطر التشوهات الخلقية التي تزداد وتيرتها منذ عام 2019.

دراسة المقطعية شملت 60 عائلة من الأزواج الذين يعيشون في قرية ماما من مارس 2020 إلى مارس 2022 وتم جمع البيانات عن طريق إجراء مقابلة مع المشاركين وإجراء فحص الموجات فوق الصوتية.

توصلت الدراسة لارتفاع معدل انتشار التشوهات الخلقية في الدراسة الحالية خاصة إذا ما قورنت بعدد سكان المنطقة وعلاقتها بانفجارات وتلوث البيئي في المنطقة.

I. Introduction

In wealthy nations, birth abnormalities continue to be the main contributor to perinatal death and childhood impairment. In contrast, poverty and infection are the major causes of death in several underdeveloped nations where infant mortality is still relatively high. However, due to limited diagnostic resources and the unreliability of medical records and health statistics, birth abnormalities in the poor countries are frequently underreported. Therefore, a rise in the occurrence of birth abnormalities should be treated with care as it can only be explained by the use of more accurate diagnostic tools or better medical records. [1]

Birth defects, commonly referred to as congenital malformations that include structural or functional malformations arising during pregnancy as a consequence of an anomaly or deficiency in the developmental period. [2] Congenital birth defects cause of death of

549 000 deaths in 2019, the global incidence was 62.9 cases per 1000 livebirths and estimated that 50.9 million of babies lived with birth defects in 2019. [3]

Congenital anomaly prevalence varies significantly by country that range 1- 8%. Geographic factors, sociocultural, racial, and ethnic factors are responsible for the variance in the incidence of congenital abnormalities. [4] In community based study the prevalence of birth defect in Saudi population was 0.04% [5] ,1.28% in Jordan [6] while the birth defect in Fallujah city was 14.7% .[7]

Single-system malformations and multiple-system malformations are two basic categories of congenital defects. Major congenital defects are those that, if left untreated, may significantly affect a person's ability to perform their regular bodily activities or even shorten their life

expectancy. Minor congenital abnormalities are those that are neither physically nor functionally disabling and can be considered to be typical variations. [8]

Birth abnormalities have been linked to a variety of reasons, including genetics, environmental teratogenic factors, a lack of certain micronutrients, and multifactorial inheritance. Familial marriage, maternal age, pharmaceuticals, smoking, alcohol intake, and maternal diseases are among the frequent risk factors mentioned in the literatures. Although genetic, viral, dietary, or environmental factors may contribute to congenital malformations, it is sometimes challenging to pinpoint their precise causes. [9] While the origins of the majority of birth abnormalities are still unclear, an increasing number of studies that suggested an environmental variable as contributor to genetic mutations and interact with genetic risk factors for birth defects. As a result, it can be said that the majority of birth abnormalities have multifactorial causes that result from a mix of genetic and environmental variables. [10] Previous studies showed that 37% of congenital abnormalities are related to genetic and environmental interactions, and 10% are linked to chemicals with teratogenic effects that have been scientifically proven. Only 40 of the 2500 compounds that have been identified as teratogenic agents are shown to produce teratogenic effects in humans, including carbon monoxide, ozone, lead chromate, lead acetate, lead phosphate, 1,2-dibromo-3-chloropropane, and 2-bromopropane. [11]

The majority of Iraqis marry in consanguineous relationships. According to the Central Organization of Statistics and Information Technology (COSIT) in 2044 about 33% of Iraqis were first cousin consanguineous. The incidence of consanguinity varies, however, tend to be higher in Arabic community that reach 56% in Saudi Arabia [12], 54% in Qatar [13] and 27.5% in Jordan. [14] Increase the autosomal recessive diseases as a result of the high rate of consanguinity that ranges from 20–60% of all their marriages. Congenital malformations were

substantially more common in children born to consanguineous parents than in non-consanguineous households. [15]

Since the introduction of depleted uranium in First Gulf War, study has concentrated on contamination caused by this substance as a probable factor in rising congenital abnormality (CA) and cancer rates. According to recent investigations, the US military may also employ conventional weapons in Iraq that have somewhat enriched uranium (U-235 mass percentage $>0.711\%$, 2%). [16] As a result, we refer to metallic uranium (of unknown isotopic composition) released to the environment in Iraq by the use of conventional weapons as "weaponized uranium". Studies on non-human in vivo animals have demonstrated that exposure to uranium oxides can cause teratogenic and carcinogenic consequences. Uranyl ions (the metabolism product of uranium oxides) easily interact with other molecules and are distributed throughout the body through systemic circulation and. The blood-brain barrier and the placental barrier are both permeable to uranium. It has been demonstrated that after absorption, uranium increases the presence of reactive oxygen species, breaks DNA strands, and changes gene expression, all of which have negative clinical implications. [17] Compared to veteran populations, local communities are more at risk of unfavorable health impacts from chronic exposure situations .[18]

Strategies to avoid babies with congenital defects also focus on the risk factors that are common to other unfavorable pregnancy outcomes, successfully seeking to cut down on reproductive waste and improve pregnancy outcomes. [19] The most efficient way to decrease the frequency of major congenital abnormalities and raise the survival rate of individuals born with these problems is through fetal anomaly screening. If a correctable anomaly is found, it may be advised that birth take place in a facility with pediatric surgical capabilities, and if a severe,

irreparable condition is found, a pregnancy termination option may be made available. If congenital abnormalities are not treated properly, survivors may have permanent physical, mental, visual, and auditory impairments. This can have a detrimental impact on the affected person's social and professional life, as well as the lives of their families and communities. Following the delivery of a child with significant defects, parents may experience emotions including denial, guilt, concern, sadness, and embarrassment. [2]

The aim of current research is to estimate prevalence of congenital anomaly in Mama Village which underwent Explosion in 2004.

II. Material and method

2.1 Study design:

A Cross sectional study that include 60 couples who live in Mama Village which belong to Dibs district in Kirkuk, during the duration March 2020 to March 2022 to investigate the risk of congenital anomaly that increase in frequency in 2019. The study included every couples who give birth to new born recently, willing to participate in the study and had no medical history that could cause a congenital anomaly to the child.

The data were collecting by direct interviewing the participant and took a full history about their age, degree of consanguinity with husband, number of living children, number of dead baby, presence of abortion or intrauterine death, presence of congenital anomaly, time of diagnosis and type of anomaly.

The ultrasonography done for every participant included in this study from first trimester till birth.

2.2 Statistical analysis:

The data was analyzed using the SPSS version 25.0 program, frequency percentage and charts were used to describe the data. The factors that contribute to congenital anomaly were identified using a logistic regression analysis.

III. Results

33 Newborn were born with congenital anomaly from 60 new born, the prevalence of anomaly in the current study was 55%.

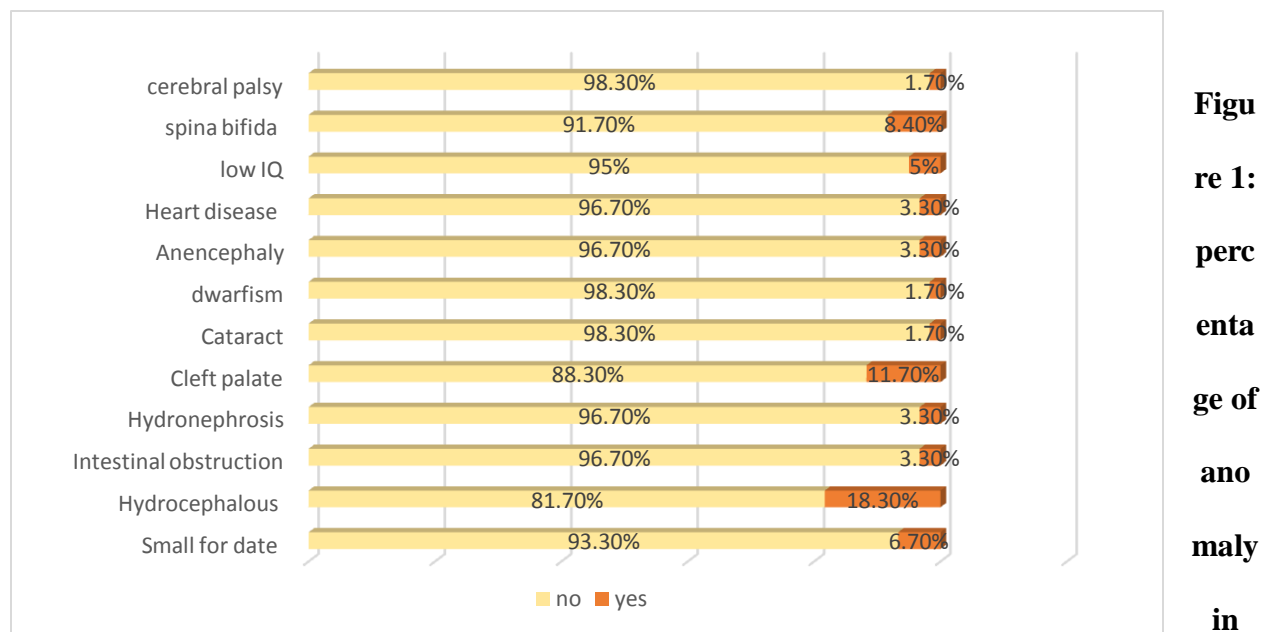
The age distribution shows that 18.3% were aged 15-20 yrs., 36.75 were 21-25 yrs., 10% were 26-30 yrs. and 35% were > 31. 96.7% were Relative to the husband. 35% had >4 children and 35% had 3-4 children. 25% had one previously dead baby and 13.3% had two previously dead baby. 15% had single abortion, 11.7% had two abortion and 1.7% had 3 previous abortion, only 8.3% had history of IUD.

Those who included in the study, 55% had congenital anomaly, 72.7% had single anomaly and 27.3% had multiple. Regarding time of diagnosis, 42.4% were diagnosed in 2nd trimester, 18.2% in the 3rd trimester and 39.4% after delivery, as presented in Table I.

Table(I): participant baseline data.

		N	%
Age group	15 – 20	11	18.3%
	21- 25	22	36.7%
	26 - 30	6	10.0%
	> 31	21	35.0%
Relative with his husband	No	2	3.3%
	Yes	58	96.7%
No. of children	no children	2	3.3%
	1-2 children	16	26.7%
	3-4 children	21	35.0%
	more than 4	21	35.0%
N. of dead baby	0	37	61.7%
	1	15	25.0%
	2	8	13.3%
No. of abortion	0	43	71.7%
	1	9	15.0%
	2	7	11.7%
	3	1	1.7%
No. of IUD	0	55	91.7%
	1	5	8.3%
Presence of congenital anomaly	No anomaly	27	45.0%
	Presence	33	55%
N. of congenital anomalies	Single	24	72.7%
	Multiple	9	27.3%
Time of diagnosis of abnormalities	2nd Trimester	14	42.4%
	3rd Trimester	6	18.2%
	After delivery	13	39.4%

The most common anomaly was hydrocephalous in 18.3%, followed by cleft palate in 11.7%, spina bifida in 8.4%, small for date baby in 6.7%, low IQ in 5%, heart disease, anencephaly, hydronephrosis and intestinal obstruction were presented in 3.3% in baby for each, as presented in figure 1



Figure(1): the babies of participant

The logistic regression analysis shows that being both parent relative had a statistical effect on presence of congenital anomaly, relative parents had 1.45 increase risk of having congenital anomalies in their baby in compare to non-relatives, p was 0.05.

Those with younger age group 15-20 years had 3.6 increase risk of anomaly, and those who aged 21-25 had 3.49 increase risk, p-value 0.01 and 0.05, respectively.

Presence of dead baby in the family increase risk of anomaly by 12 times in those with one dead child and by 12.9 in those with two dead child, p-value 0.003 and 0.02, respectively.

Both abortion and IUD were not a risk factors for anomaly in the current data, as presented in Table II.

Table(II): logistic regression analysis of Cousin Marriage, age group, history of dead baby, history of abortion and IUD on presentation of anomaly.

		Odd ratio	p-value
Cousin marriage	No	Reference	/
	Yes	1.45 (0.07-30.08)	0.05*
Age group	15-20	3.62 (0.73-17.87)	0.01*
	21-25	3.49 (0.96-12.60)	0.05*
	26-30	0.52 (0.21-2.60)	0.67
	≥ 31	Reference	
dead baby	No death	Reference	
	One	12.0 (2.34-61.52)	0.003*
	Two	12.92 (1.43-116.78)	0.02*
Abortion	No abortion	Reference	
	One	0.32 (0.07-1.507)	0.15
	Two	0.87 (0.17-4.44)	0.86
	three	1.0 (0.43-4.5)	0.09
IUD	No death	Reference	
	One	0.97 (0.14-6.56)	0.9

*p-value ≤ 0.05

IV. Discussions

Major congenital abnormalities often have a negative impact on a child's physical, mental, or social development, and they can raise their risk of morbidity due to a variety of medical conditions. A significant worldwide issue is the contribution of medications, infectious diseases, and environmental contaminants to congenital abnormalities.

The underlying reasons of the majority of congenital malformations are still unknown, though, and multifactorial inheritance is thought to be the root cause of the majority of common abnormalities.

The prevalence of congenital anomaly in current study was high and reach to 55%, the percentage was higher than the observed in other studies, 10.6% in Ethiopia [20], 2.4% in

Malaysia [21], 7.4% in Egypt [22], 0.02% in Fallujah city [23], 0.01% in Baghdad city [24] and 0.36% in Erbil city [2].

Congenital anomaly prevalence may vary over time or by region, which may be a result of intricate interplay between genetic and environmental factors as well as social and racial influences factors

Due to collecting the sample size from one village which is (Mama village) not from all Kirkuk city in the current study, the prevalence of congenital abnormalities could be high in comparison to other study.

An approximated proportion between those who aged 21-25 and those who are > 31 years, in Al-Alwani M et al [23] study, those who aged 20-29 years were forming nearly half of participant. While in Kamal NM et al [25] those who aged 26-35 years were forming one third of participant. Difference between the studies could be related to use different classification for age as well as cultural idea of community about age of marriage and having children.

Nearly all couples were Consanguineous (96.7%). The current percentage was higher than previously reports, Tayebi N et al [26] reported that cousin marriage was reported in 25% of participant, other study shows that 68% of participant were consanguineous [27], another study reported that 75.5% were consanguineous and 82.3% of those with consanguineous marriage were from rural area [28]. The high incidence of consanguineous marriage is ascribed to societal practices that involve planned marriages within families and general public ignorance of the negative implications of such a practice.

Although majority of participant report no previous neonatal death, abortion or intrauterine death, but one third report a history of dead baby and one forth report history of abortion and less

than 10% had IUD. Taye et al [29] reported lower number of child death, abortion and stillbirth. In Al-Musawi et al [30] study more than half of participant had history of abortion or IUD.

Over one third of participant who had a newborn with congenital anomaly discovered in the 2nd trimester and remaining discovered after delivery or in third trimester. Although majority had single anomaly, over one forth had multiple anomaly. Regarding each anomaly, hydrocephalous was the most common anomaly then cleft palate, spina bifida and small for date baby were also commonly presented, heart disease, anencephaly, hydronephrosis and intestinal obstruction all were common but in lesser extent than hydrocephalous. The most prevalent type of abnormality identified in this study was a malformation of the central nervous system, which can affect one or more systems, followed by cleft lip and palate deformity, genitourinary system, gastrointestinal, cardiovascular system, skeletal deformity and others.

In a study that was carried in India, musculoskeletal disorders were the commonest, followed by craniovertebral anomalies [31]. In Iranian study, skeletal abnormalities were the most common congenital followed by genitourinary system abnormalities [32], both were inconsistent with current study finding.

The similar observation was found in studies carried in Baghdad [24] , Al Mosul [33], Erbil [2] and Karbala. [34]

The high prevalence of central nervous system abnormalities may be explained by that the environment can play an important role. ‘Environment’ is a broad term that includes familiar contributors such as nutrition, adequacy of prenatal care, smoking and alcohol use, maternal age, and socioeconomic disparities, as well as less familiar contributors including pollution and chemical agents encountered both indoors and outdoors. In many cases, two or more

environmental factors may be interrelated or synergistic. [35] Etiological, epidemiological, or environmental factors that may contribute to, for example, the complex socioeconomic status of the general population in Iraq, or it may be due to a lack of medical services, particularly after the military operations in Iraq since 2003. Additionally, several genetic changes and mutations are anticipated as a result of the deployment of chemical weapons starting with the second Gulf War. [16]

Cousin marriage increase the risk of CA by 1.54 in current study population that agreed with previous studies [36-38]. The homozygous expression of recessive genes acquired from their common ancestors is most likely the cause of the increased occurrence of genetic abnormalities in the kids of consanguineous marriages. [39]

Mothers with aged below 20 had 3 times increase risk of newborn with CA that agreed with [40], but the result were different from Anele et al. [41], who observe association between CA and advance age of mothers ≥ 36 years, without regard to geographic area.

According to Tsehay et al. [42], young maternal age reflects risk for some particular CA.

Low maternal education is frequently linked to worse socioeconomic situations and is identified as a risk factor for pregnancy problems and reduced adherence to guidelines [34].

The small sample size and study design were a limitation point to the current study, a suggestion to the future research should focus on providing information to help women prevent congenital abnormalities as well as effectively treat patients with congenital malformations. Future studies should assess certain categories of congenital abnormalities, including their risk factors and prevalence rates, since more study is needed to determine the causes of the many forms of congenital malformations.

V. Conclusion

A higher prevalence of congenital anomaly in the current study especially if compared with number of area population. The central nervous system was more probable which shown to be substantially correlated with maternal history of prior previous child death, paternal consanguinity, and age. Higher prevalence of central nervous system could be related to the environmental effect (explosion occur in the studied area previously), consanguineous marriages due to exposure of parent to same environmental condition.

List of Abbreviations:

CA: Congenital anomaly

US: United State

IUD: Intra uterine death

COSIT: Central Organization of Statistics and Information Technology

Acknowledgement:

I would like to express my gratitude to Allah who gives me power and patience.

My great thanks and appreciation to Dr. Runak Taher for the encouragement.

I am highly grateful to Hemn Eyub for his help .

I would like to thank all people in Mama village especially Mr. Daham, Sabah and Abass for their help.

Reference

1. T.S. Al-Hadithi, J.K. Al-Diwan, A.M. Saleh, N.P. Shabila, "Birth defects in Iraq and the plausibility of environmental exposure: a review", *Conflict and health*, Dec;6(1) (2012) 1-7
2. S.K. Ameen, S.K. Alalaf, N.P. Shabila, "Pattern of congenital anomalies at birth and their correlations with maternal characteristics in the maternity teaching hospital, Erbil city, Iraq. BMC pregnancy and childbirth. 2018 Dec;18(1):1-8.
3. Congenital birth defects — Level 3 cause. healthdata.org. published 2019. Accessed September 20, 2022. https://www.healthdata.org/results/gbd_summaries/2019/congenital-birth-defects-level-3-cause.
4. Keerti Singh, Kandamaran Krishnamurthy, Camille Greaves, Latha Kandamaran, L.Anders. Nielsen, Alok Kumar, "Major Congenital Malformations in Barbados: The Prevalence, the Pattern, and the Resulting Morbidity and Mortality", *International Scholarly Research Notices*, vol. (2014), Article ID 651783, 8 pages, 2014. <https://doi.org/10.1155/2014/651783>.
5. A.M. Kurdi, M.A. Majeed-Saidan, M.S. Al Rakaf, A.M. AlHashem, L.D. Botto, H.S. Baaqeel, A.N. Ammari, "Congenital anomalies and associated risk factors in a Saudi population: a cohort study from pregnancy to age 2 years. BMJ open. Sep 1;9(9) (2019) e026351.
6. A. Albitoosh, M. Khasawneh, Y. Hussein, A.A. Zaghloul, A.M. Elsayed, H. Youssef, "Incidence of congenital anomalies of kidney using computed tomography: A retrospective hospital-based study". *Medical Science*.;26 (2022) e2336.
7. S.T. Alaani, M. Tafash, A.A. Murie, A.M. Al-Esawi, "High rates of birth defects in Fallujah, Iraq: radiological and chemical pollution of the affected children and their parents" *Asian Journal of Immunology*. Jan 9;1-0(2020) 210-216.
8. L.J. Anyanwu, B. Danborn, W.O. Hamman, "Birth prevalence of overt congenital anomalies in Kano Metropolis: overt congenital anomalies in the Kano. *Nature*;220 (25.55) (2015) 58-97.
9. W.H. Organization, "Congenital anomalies World Health Organization". Updated September (2016). (Accessed July 2018, 12, at <http://www.who.int/mediacentre/factsheets/fs370/en/>).
10. T.G. Beames, R.J. Lipinski, "Gene-environment interactions: aligning birth defects research with complex etiology". *Development (Cambridge, England)*. Nov 1;147(21) (2020) dev191064, 1-5.
11. M. Jaklin, J.D. Zhang, P. Barrow, M. Ebeling, N. Clemann, M. Leist, S. Kustermann, "Focus on germ-layer markers: A human stem cell-based model for in vitro teratogenicity testing". *Reproductive Toxicology*. Dec 1;98 (2020)286-98.
12. M.I. El-Mouzan, A.A. Al-Salloum, A.S. Al-Herbish, M.M. Qurachi, AA Al-Omar, "Regional variations in the prevalence of consanguinity in Saudi Arabia". *Saudi Med J*, 28 (2007)1881- 1884.
13. A. Bener, K.A. Alali, "Consanguineous marriage in a newly developed country: The Qatari population". *J Biosoc Sci*, 38 (2006) 239-246.
14. M.M. Islam, "Consanguineous marriage and its relevance to divorce, polygyny and survival of marriage: evidence from a population-based analysis in Jordan". *Annals of Human Biology*. Jan 2;48(1) (2021)30-6.

15. L. Romdhane, N. Mezzi, Y. Hamdi, G. El-Kamah, A. Barakat, S. Abdelhak, "Consanguinity and inbreeding in health and disease in North African populations". *Annu Rev Genomics Hum Genet*, Aug 31;20(1) (2019)155-79.
16. S. Alaani, M. Tafash, C. Busby, M. Hamdan, E. Blaurock-Busch, "Uranium and other contaminants in hair from the parents of children with congenital anomalies in Fallujah, Iraq, *Conflict and Health*. Dec;5(1) (2011)1-5.
17. S.A. Katz, "The chemistry and toxicology of depleted uranium", *Toxics*, Mar 17;2(1) (2014) 50-78.
18. A. Faa, C. Gerosa, D. Fanni, G. Floris, P.V. Eyken, J.I. Lachowicz, V.M. Nurchi, "Depleted uranium and human health". *Current medicinal chemistry*. Jan 1;25(1) (2018) 49-64.
19. World Health Organization, Regional Office for South-East Asia, "Prevention and control of birth defects in South-East Asia region Strategic framework (2013–2017). New Delhi, (2013).
20. F.B. Hadgu, L.G. Gebretsadik, H.G. Mihretu, A.H. Berhe, "Prevalence and factors associated with neonatal mortality at Ayder Comprehensive Specialized Hospital, Northern Ethiopia. A cross-sectional study", *Pediatric Health, Medicine and Therapeutics*, 11:29-37 (2020)
21. Lee KW, Ching SM, Hoo FK, Ramachandran V, Chong SC, Tusimin M, Nordin NM, Devaraj NK, Cheong AT, Chia YC. Neonatal outcomes and its association among gestational diabetes mellitus with and without depression, anxiety and stress symptoms in Malaysia: A cross-sectional study. *Midwifery*. 2020 Feb 1;81: 10:258-66.
22. H. ElAwady, A. AlGameel, T. Ragab, N. Hassan, "Congenital anomalies in neonates in Fayoum Governorate, Egypt", *Eastern Mediterranean Health Journal*, 27(8) (2021)790-7.
23. M. Al-Alwani, A.S. Alnuaimi, "Prevalence of major fetal defects in Fallujah, Iraq". *Open Journal of Obstetrics and Gynecology*. Jun 23 (2014) 9.
24. S.A. Mahdi, T.F. Kareem, D.F. Abdullah, "Preterm Detection of Congenital Anomalies by Ultrasound and Correlation with Possible Associated Risk Factors", *congenital anomalies*. Jan 1; 3:4. (2022), 268-274
25. N.M. Kamal, N. Othman, "Incidence and types of congenital anomalies in newborns in Sulaimaniyah City in Iraq", *Acta Medica Iranica*. 56 (2018)769-76.
26. N. Tayebi, K. Yazdani, N. Naghshin, "The prevalence of congenital malformations and its correlation with consanguineous marriages. *Oman medical journal*, Jan;25(1) (2010)37.
27. M. Gul, G. Nazir, A. Saidal, H. Bahadar, "Parental consanguinity increases the risk of congenital malformations", *Rehman Journal of Health Sciences*. Jul 12;3(1) (2021)48-51.
28. M. Iqbal, A. Aziz, M. Ihtesham, "Consanguinity and major genetic disorders in people of Peshawar, Pakistan: a community-based cross sectional study", *Journal of Medical and Health Sciences*, Feb 19;1(1) (2021) 13-20.
29. M. Taye, M. Afework, W. Fantaye, E. Diro, A. Worku, "Congenital anomalies prevalence in Addis Ababa and the Amhara region, Ethiopia: a descriptive cross-sectional study", *BMC pediatrics*. Dec;19(1) (2019) 1-1, 243
30. K.M. Al-Musawi, A.H. Shawq, Z. Majeed, S. Zaid, H. Ibraheem, "Risk factors for congenital anomalies in neonatal intensive care unit in Baghdad city", *Medico Legal Update* Jan;20(1) (2020) 1168-74.

31. Anne George Cherian, Dimple Jamkhandi, Kuryan George, Anuradha Bose, Jasmine Prasad, Shantidani Minz, "Prevalence of Congenital Anomalies in a Secondary Care Hospital in South India: A Cross-Sectional Study", *Journal of Tropical Pediatrics*, Volume 62, Issue 5, October (2016), Pages 361–367, <https://doi.org/10.1093/tropej/fmw019>.
32. M. Irani, T. Khadivzadeh, S.M. Asghari Nekah, H. Ebrahimipour, F. Tara, "The prevalence of congenital anomalies in Iran: A Systematic Review and Meta-analysis", *The Iranian Journal of Obstetrics, Gynecology and Infertility*, 21(Supple): (2018)29-41.
33. M. Al-Hamdany, "Post-war environmental pollution as a risk factor of congenital disorders in Iraq: A study review: Post-war environmental pollution as a risk factor of congenital disorders in Iraq: A study review", *Iraqi National Journal of Medicine*, Jan 15;2(1) (2020)1-2.
34. I.K. Ghaleb, T.A. Hassan, A.K. Shuwaikh, "The Prevalence of Congenital Anomalies and Its types among Births in Kerbala City/Iraq", *Annals of the Romanian Society for Cell Biology*, Apr 19 (2021) 7337-46.
35. T.S. Al-Hadithi, J.K. Al-Diwan, A.M. Saleh, N.P. Shabila, "Birth defects in Iraq and the plausibility of environmental exposure: a review", *Conflict and health*. 2012 Dec;6(1):1-7
36. T. Anbreen, L. Ali, S. Butt, T. Shah, "Congenital Anomaly Frequency, Risk Factor and Trends among Antenatal Patients Presenting at Tertiary Care Hospital in Pakistan", *Pakistan Journal of Medical Research*. Jul 9;60(2) (2021) 52-6.
37. S. Khalid, M. Naveed, H. Waseem, S. Nadeem, A. Hassan, "Association of consanguineous marriages with congenital anomalies", *Pakistan BioMedical Journal*. 2019 Jun 30;2(1).
38. S.A. Kazi, A. Memon, A.H. Radhan, "Frequency of congenital birth defects in newborn babies born at Hyderabad, Sindh", *The Professional Medical Journal*, Apr. 10;27(04) (2020)707-10.
39. L. Basel-Vanagaite, G.J. Halpern, L. Jaber, "General Health Topics Associated with Consanguinity; Genetic Disorders and Congenital Malformations; Benefits. Consanguinity-Its Impact", *Consequences and Management*. May 23 (2014)150.
40. M. Malik, W. Rizwan, A. Latif, "Frequency of Anomalies in Pediatric Population Presenting to Outpatients Department of a teaching hospital", *13: 2, APR – JUN 2019*, 297-300.
41. C.R. Anele, M.Z. Goldani, L. Schüler-Faccini, C.H. da Silva, "Prevalence of congenital anomaly and its relationship with maternal education and age according to local development in the extreme south of Brazil", *International Journal of Environmental Research and Public Health*, Jul 1;19(13) (2022) 8079.
42. B. Tsehay, D. Shitie, A. Lake, E. Abebaw, A. Taye, E. Essa, "Determinants and seasonality of major structural birth defects among newborns delivered at primary and referral hospital of East and West Gojjam zones, Northwest Ethiopia 2017–2018: case–control study", *BMC research notes*. Dec;12(1) (2019) 1-6.
43. B.S. Mensch, E.K. Chuang, A.J. Melnikas, S.R. Psaki, "Evidence for causal links between education and maternal and child health: systematic review", *Tropical Medicine & International Health*, May;24(5) (2019) 504-22.



ARID Journals

ARID International Journal for Science and Technology (AIJST)

ISSN: 2662-009X

Journal home page: <http://arid.my/j/aijst>

ARID

International Journal for Science and Technology

مجلة أريد الدولية للعلوم والتكنولوجيا

VOL. 6 NO. 11 JUNE 2023

ISSN: 2662-009X

ARID
ARID PUBLICATIONS
ARIDMYJST

مجلة أريد الدولية للعلوم والتكنولوجيا

المجلد 6 ، العدد 11 ، حزيران 2023 م

Preparation and Analysis of Heterocyclic Rings Made from (Thioxanthone) Derivatives Methods of Biological Activity, Thermal Analysis

Aseel Fadhil Kareem¹, Amal Talib Al Sa'ady²¹Dept. of Pharmaceutical Chemistry, College of Pharmacy, University of Babylon, Iraq.²Dept. Clinical Laboratory Sciences, College of Pharmacy, University of Babylon, Iraq

تحضير وتحليل الحلقات الهيدروكسيلية المصنوعة من مشتقات (ثايوكزانثون) وطرق النشاط البيولوجي والتحليل الحراري

أسيل فاضل كريم

فرع الكيمياء الصيدلانية/ كلية الصيدلة/ جامعة بابل/ العراق

أمل طالب السعدي

فرع العلوم المختبرية السريرية/ كلية الصيدلة/ جامعة بابل/ العراق

aseelpharmacy77@gmail.comarid.my/0007-3491<https://doi.org/10.36772/arid.aijst.2023.6113>

ARTICLE INFO

Article history:

Received 20/02/2023

Received in revised form 15/04/2023

Accepted 27/04/2023

Available online 15/06/2023

<https://doi.org/10.36772/arid.aijst.2023.6113>

ABSTRACT

In this study heterocyclic compounds were prepared from thioxanthone derivatives and determined their structure by measuring melting point (M.P) and infrared spectrum (FTR) and ¹HNMR for each one. These derivatives used for testing antibacterial activity *Streptococcus mutans*, *Staphylococcus saprophyticus*, *Enterococcus faecalis* (Gram positive bacteria) *Haemophilus influenzae* (Gram negative bacteria). Prepared compounds I,II,III,IV showed clear antibacterial activity against all tested bacteria either as solutions or powder. Solutions with DMSO have antibacterial activity greater than those with distilled. Compound I showed greater antibacterial activity than other compounds. On the other hand, Gram-positive bacteria showed higher sensitivity than Gram-negative ones to all solutions. The results of thermal analysis of the prepared derivatives showed stability at high temperatures (DSC and TG curves).

Key words: Thioxanthone, Schiff bases, antibacterial activity , imidazolidin-4-one , Oxazepine .

الملخص

في هذه الدراسة تم تحضير المركبات الحلقية غير المتجانسة من مشتقات الثايوكزانثون، وتم تحديد تركيبها عن طريق قياس درجة الانصهار (M.P) وطيف الأشعة تحت الحمراء (FTR) و $^1\text{H NMR}$ لكل منها. استخدمت هذه المشتقات لاختبار النشاط المضاد للبكتيريا *Streptococcus mutans*، *Staphylococcus saprophyticus*، *Enterococcus faecalis* (بكتريا موجبة الجرام) *Haemophilus influenzae* (بكتريا سالبة الجرام). أظهرت النتائج أن المركب المحضر أظهر نشاطاً مضاداً للبكتيريا واضحاً ضد جميع أنواع البكتيريا المختبرة. أظهرت نتائج التحليل الحراري للمشتقات المحضرة لها استقرار في درجات الحرارة المرتفعة من منحنيات (DSC) و (TG).

الكلمات المفتاحية: ثايوكزانثون ، حلقية غير متجانسة، قواعد شيف، نشاط مضاد للجراثيم اميدازولدين-4-اون، الاوكزازيبين.

1. INTRODUCTION:

Heterocyclic rings are cyclic compounds (organic) have contain one or more hetero atoms in structures, are (nitrogen, oxygen and sulphur) [1]. Most drugs are derivatives from heterocyclic compounds played widely role in living cells, DNA and RNA, hemoglobin and vitamins as (β -Lactams and Imidazole) [2]. All show has applications in different diseases as urinary antiseptics, antimicrobial herbicides and anti-inflammatory[3]. Schiff bases have more of application in multiplies fields such as, antibacterial, antifungal, anti-inflammatory, ant proliferative and antimalarial, [4] . Antiviral, antidepressant, antipyretic properties , ant tubercular, analgesic-anti-inflammatory , anticancer, anticonvulsant, antioxidant, anthelmintic, antiglycation, activities [5] . Four-membered rings (β -lactams) used as antibiotics, this involves penicillin derivatives, cephamycins, cephalosporins, monobactams and carbapenems. Beta-lactams one of the drugs which have clinical indications as (penicillin)[6]. Five (Imidazole) and seven (Oxazepine) - membered rings have (N,O) atoms in structural therefore spreads in nature, their heterocyclic exhibit a high spectrum in biological activity, anti-biotic, anticancer, anti-inflammatory and antimicrobial activity [7,8]. This study included preparation heterocyclic compounds as(imidazole, oxazepine and β -Lactam) from Schiff bases reactions by used Thioxanthone derivative as a principle material.

2. MATERIALS AND METHODS:

2.1. Chemical study :

2.1.1. Synthesis of 2-((4-hydroxy-3-methoxybenzylidene)amino)-9H-thioxanthen-9-one (I):

To prepare the mixture for recrystallization from 100% ethanol, vanillin (0.02 mole) was dissolved in (25 ml) of absolute ethanol, condensed with (0.02 mole) of (2-amino-9H-thioxanthen-9-one), and then added 1-2 drops of glacial acetic acid. This process was carried out while the mixture

was continuously shaken for 20-25 min on a magnetic stirrer at 65-70 °C. The mixture was evaporated and dried by Rotary evaporator to give compound (I). as displayed in **Scheme 1**.

2.1.2. Synthesis of 2-(4-hydroxy-3-methoxyphenyl)-3-(9-oxo-9H-thioxanthen-2-yl)-2,3-dihydro-1,3-oxazepine-4,7-dione (II):

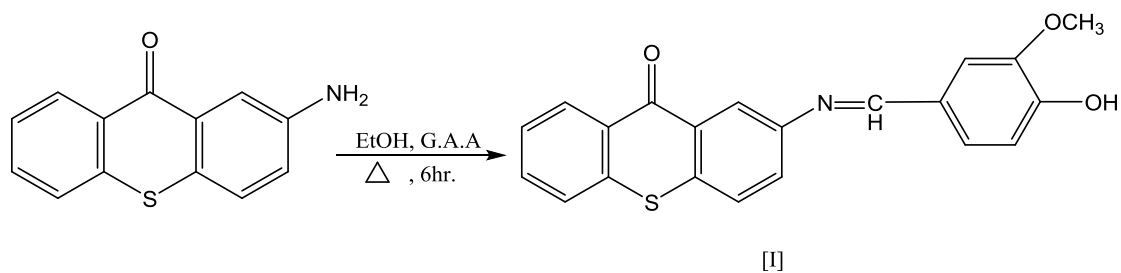
Maleic anhydride (0.02 mole) was added progressively after (0.02 mole) of compound (I) had been dissolved in (20 mL) of dry benzene to complete the reaction at 60–65 °C in 15 hours. For the purpose of preparing the mixture for recrystallization from 100% ethanol to provide compound (II) **Scheme 1**, the mixture was evaporated and dried using a Rotary evaporator.

2.1.3. Synthesis of 3-chloro-4-(4-hydroxy-3-methoxyphenyl)-1-(9-oxo-9H-thioxanthen-2-yl)azetidin-2-one (III):

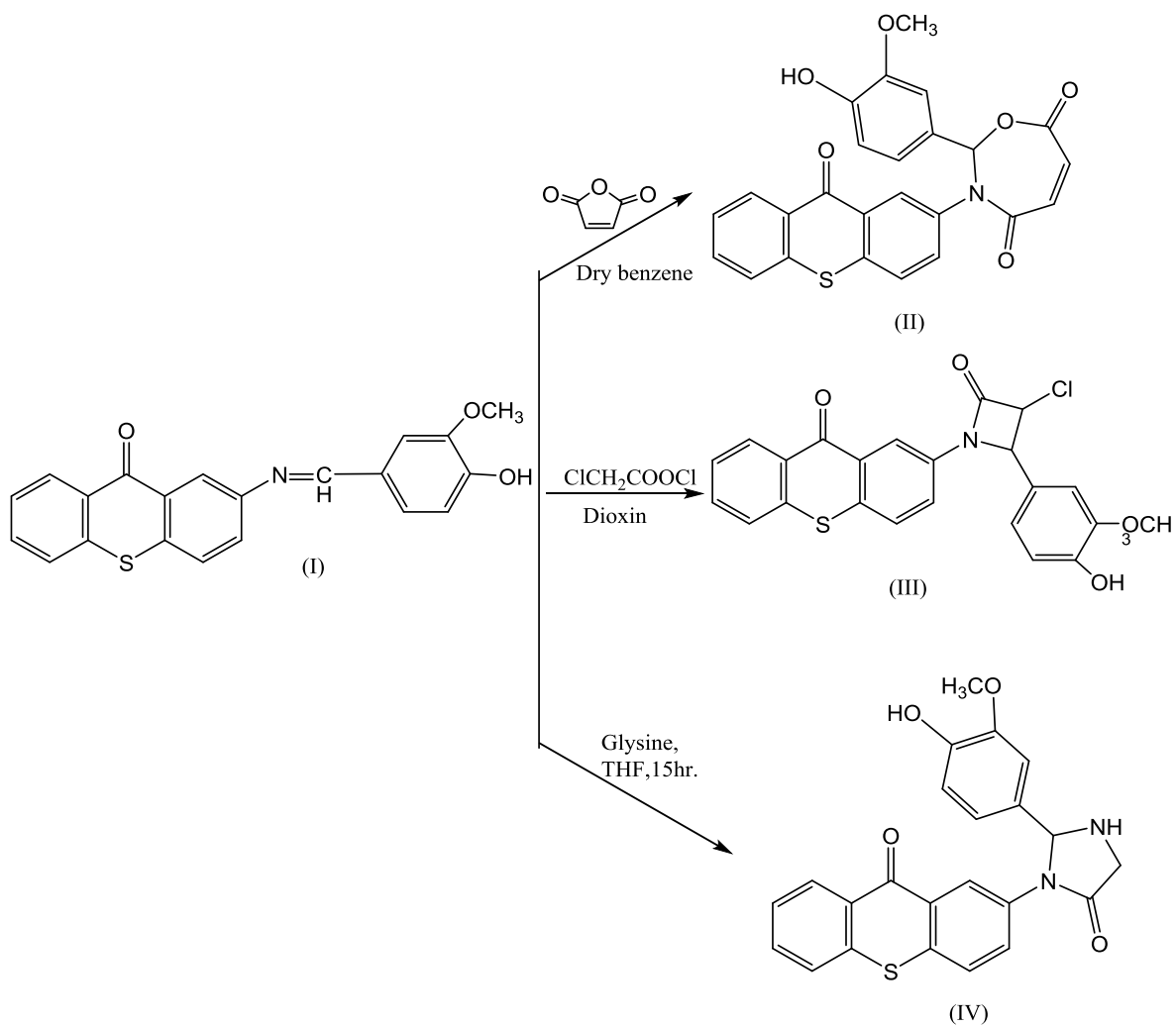
In order to complete the reaction at 10°C in 9 hours, (0.02 mole) of compound (I) was dissolved in 20 mL of dioxin before (0.02 mole) of triethylamine and (0.05 mole) chloroacetyl chloride were added progressively. In order to prepare the mixture for recrystallization from 100% ethanol to yield compound (III) **Scheme 1**, the mixture was evaporated and dried using a Rotary evaporator.

2.1.4. Synthesis of 2-(4-hydroxy-3-methoxyphenyl)-3-(9-oxo-9H-thioxanthen-2-yl)imidazolidin-4-one (IV):

(0.02mole) of compound (I) was dissolved in 20 mL of THF, and (0.02mole) of (Glycine) was added gradually to complete the reaction at(10°C) in 15 hours. The mixture was then evaporated and dried by a Rotary evaporator to prepare it for recrystallization from absolute ethanol to yield compound (IV). [9] **Scheme 1**. TLC was used on the finished result, and Table 1 has a list of all the compounds' physical characteristics .



Scheme(1)



Scheme(2)

Table (1): physical properties of synthesized compounds [I-IV].

Compound No	M.P (°C)	Color	Yield	Rf	Solvents (TLC)
[I]	187	Yellow	72	0.58	Ethanol:Toluene
[II]	193	Deep Yellow	76	0.68	Ethanol:Toluene
[III]	210	Orange	80	0.60	Ethanol:Toluene
[IV]	223	Yellowish Orange	82	0.64	Ethanol:Toluene

2.2. Antibacterial Activity Test:

The bacterial inoculum was prepared by 2–3 pure colonies (of already diagnosed bacterial isolates) were added into 5 ml of BHI (brain heart infusion broth), which is sterile. After incubation (at 37°C for 18 hrs), this broth culture was diluted with sterile normal saline in order to produce a standard bacterial suspension (turbidity equal to a standard McFarland tube). Bacterial suspension was used in the antibacterial activity test. The antibacterial activity test was performed by agar well diffusion method as detailed in Al-Sa'ady and Hussein[10] by using four bacterial isolates included *Streptococcus mutans*, *Staphylococcus saprophyticus*, *Enterococcus faecalis* (Gram positive bacteria) and *Haemophilus influenzae* (Gram negative bacteria). The compound solutions were prepared by using DMSO and Distilled Water as solvents for preparing two concentrations (125 mg/ml, 250 mg/ml) for each. Inoculum from the bacterial suspension was streaked on a Muller Hinton agar. On the streaked medium, four holes (6 mm) have been punched by a sterile cork borer(No.6), about 200 µl of each solution has been introduced in each hole. in addition to the powder (500 mg/ml) was used in this test. After incubation period (at 37°C for 18 hrs),diameter of inhibition zone was measured in millimeter.

3. RESULTS AND DISCUSSION :

3.1. Spectral Investigation :

Typically, melting points and FT-IR spectroscopy were used to study Schiff base (**I**) (**fig. 1**). With the appearance of a new stretching vibration at 1661 cm^{-1} , which is assigned to the azomethine group ($\text{CH}=\text{N}$), peak at 1677 cm^{-1} due to the $\text{C}=\text{O}$ group, peak at 787 cm^{-1} due to the $\text{C}-\text{S}$ group, the FT-IR spectrum revealed the elimination of absorption peaks induced by NH_2 and $\text{C}=\text{O}$ groups. By adding azomethine $\text{C}=\text{N}$ and maleic anhydrides in dry benzene, the (**II**) was created (**fig. 2**). New bands generated at 1558 as a result of the cyclic amid group ($\text{CO}-\text{N}$) in lactam. A lactone created a band at 1698 cm^{-1} , while OH was responsible for the band at $(3330-3442)\text{ cm}^{-1}$. The most recognizable proof of compound (**III**)'s FT-IR absorption bands is shown in **figure 3**. revealed that bands at 1776 cm^{-1} due to $\text{N}-\text{C}=\text{O}$ and 3462 cm^{-1} due to hydroxyl were among the other bands. [11-12] . The chemical [**IV**]'s FT-IR spectra is shown in **Figure 4**. displays absorption bands at 1541 cm^{-1} caused by the endocycle of ($\text{C}=\text{N}$) and an absorption band at 1608 cm^{-1} caused by ($\text{C}=\text{O}$) Amide.

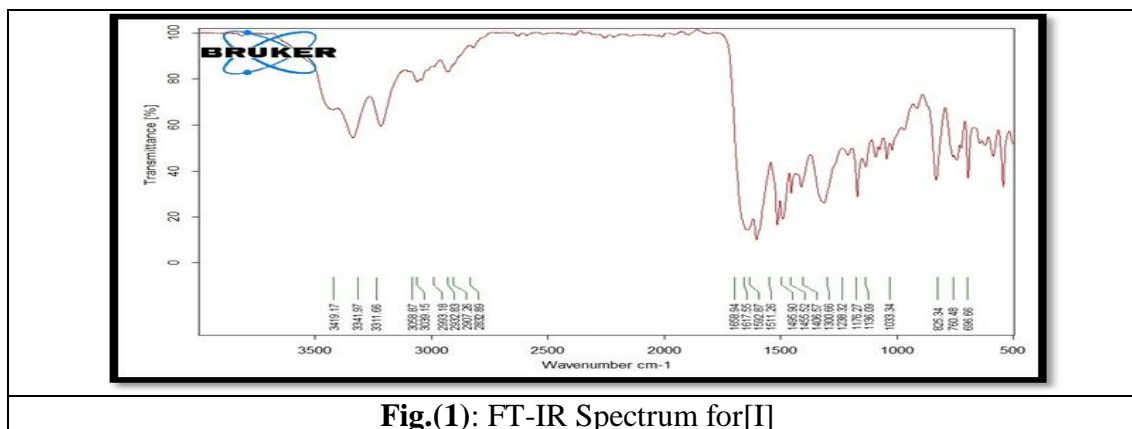


Fig.(1): FT-IR Spectrum for[I]

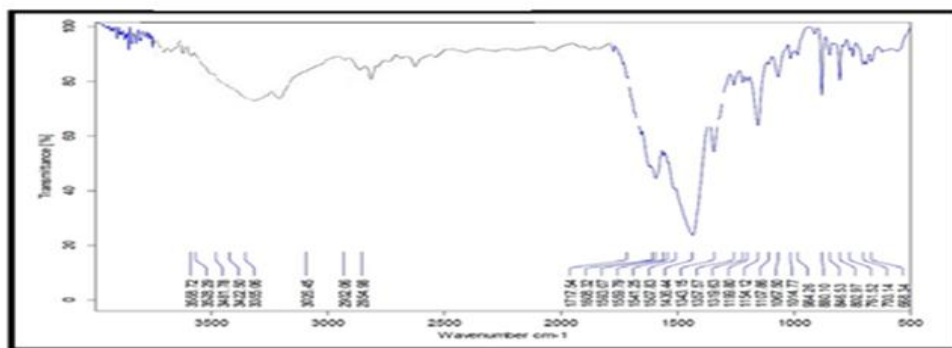


Fig.(2): FT-IR Spectrum for[II]

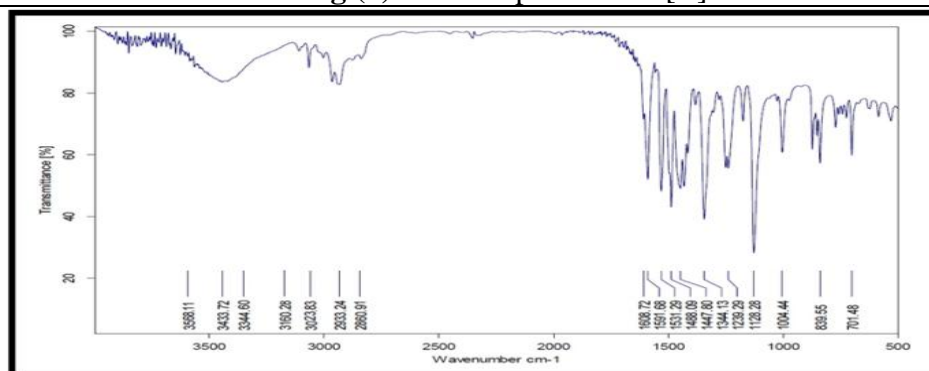


Fig.(3): FT-IR Spectrum for[III]

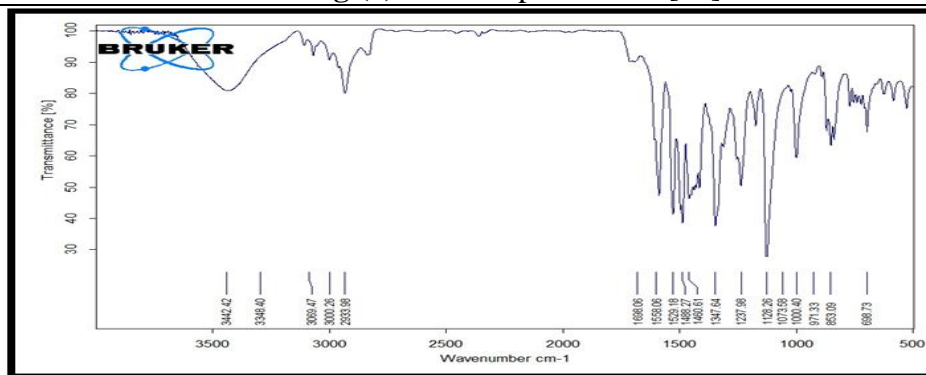


Fig.(4): FT-IR Spectrum for [IIV]

3.2. ¹H-NMR spectral identification

Compound [I],(fig.5) A singlet signal was found in the (^1H -NMR) spectrum (DMSO- d_6) for the proton of $\text{CH}=\text{N}$., Many signals indications at $\delta 6.9 - 7.4$ (ppm) resulting from aromatic protons.

Last but not least, the ^1H -NMR spectrum exhibits a signal peak at 13.4 of OH and an apparent

peak at 2.5 of solvent (DMSO-d₆) protons. The (¹H-NMR) spectrum of compound [II] (DMSO-d₆) revealed a sharp signal at 8.6 ppm for one proton of the N-CH-O oxazepine group and bands at 7.83–7.54 ppm that were identical to the CH=CH ring of the oxazepine ring and aromatic protons. Additionally, a singlet signal of methoxy group proton absorption at 4.2 PPM. Finally, the ¹H-NMR spectrum reveals peaks at δ10.2-13.0 to OH. Compound [IV]'s (¹H-NMR) spectra (DMSO-d₆) (**fig. 7**) revealed singlet signals for one proton of the NH endo cycle of the imidazole ring at 8.7 ppm and 3.0 3.5 ppm for the OCH₃ and CH₂ group rings. Finally, the ¹H-NMR spectrum shows an OH group band at 11.1 PPM and several signals indicative of aromatic protons between(6.6 and 7.6) PPM. [13-14].

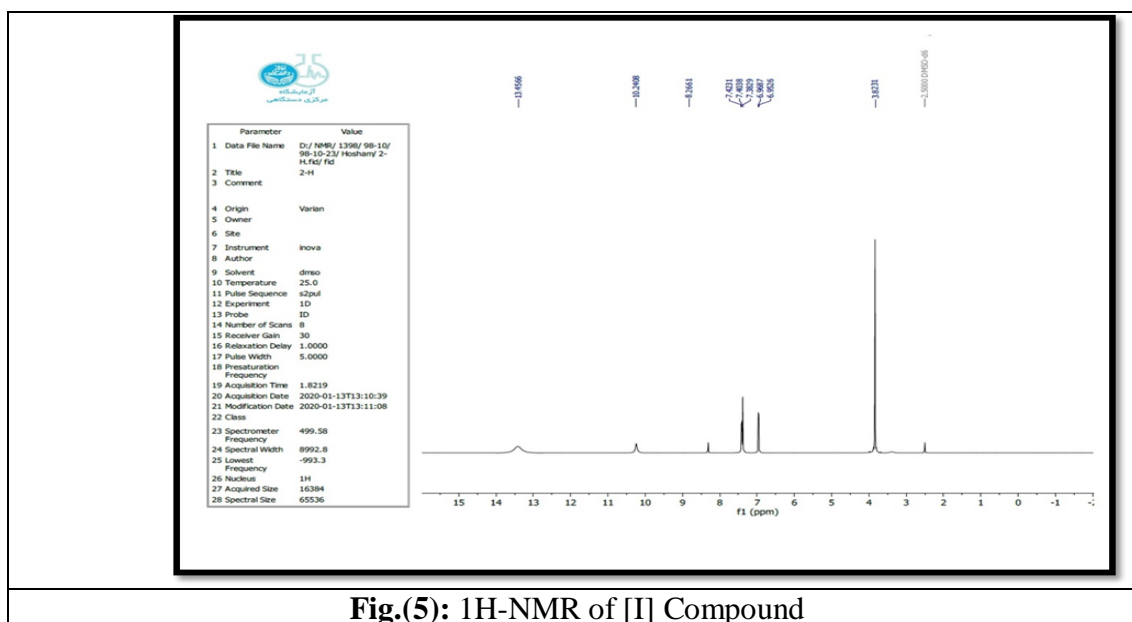
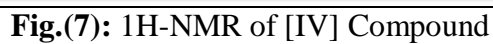


Fig.(5): ¹H-NMR of [I] Compound

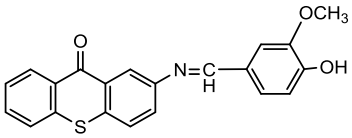
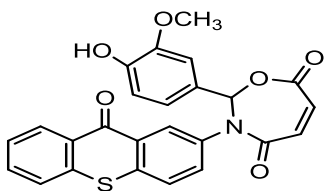
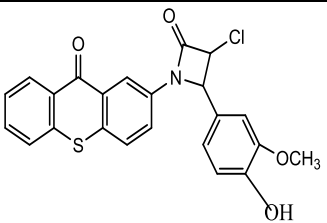
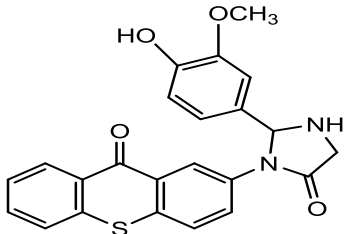


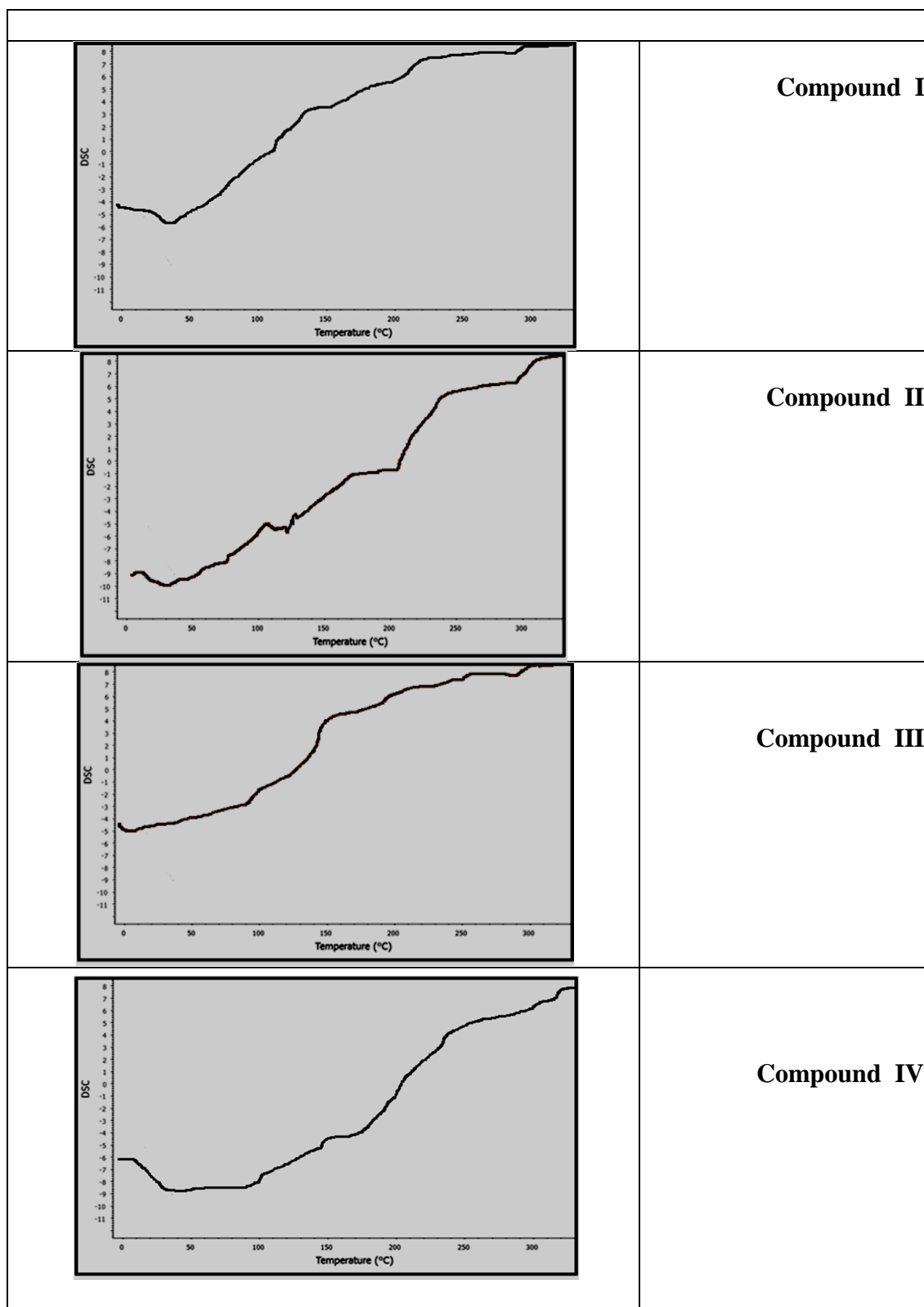
3.3. Thermal stability study of the synthesised compounds [I- IV].

These days, thermal analysis is a crucial instrument for researching the thermal stability of crucial goods including medications, polymers, and organic chemicals. TG and DSC techniques were used in the current investigation to examine thermal stability. One of the most fundamental and practical analytical techniques for thermal analysis is DSC, which is used to measure the weight loss of a tested sample as a function of temperature or of the amount of time it spends in a heated environment. The mass loss across the same temperature range is exactly proportional to the peak area of the DSC curve's (T_{initial} , T_{final}), and the peak height of the DSC curve at any temperature provides the mass loss rate. Because of this, understanding the DSC curve makes it possible to directly apply the rate function of the change in target sample weight to the study of derivatives that occur during differential scanning calorimetry analysis. shown in Fig. 8 , Table 2

The next step was completed for all compounds. Sometimes mechanical treatment can also produce metastable forms following ethanol crystallization, materials were ground in a mortar and pestle, compressed, and a DSC experiment was conducted [15]. The TG measurements were also performed to confirm the lack of solvates or breakdown. Figure 9 displays the DSC scans and TG for compounds. The melting of these compounds is observed for all runs due to their endothermic thermal impact. The temperatures are (462) K for ethanol crystallization, (462) K for toluene crystallization, and 462 K for post grinding and pressing. A shock cooling period was followed by the second measurement. DSC traces without solvate only display an endothermic peak at 462 K. In the inquiry temperature range, no mass loss in the TG analysis for any sample has suggested a decomposition process.

Table(2): DSC data of compounds [I-IV]

Compound No	Structure	Decomposition temperature range °C		Losing weight%
[I]		260	397	35.8
[II]		205	410	25.2
[III]		279	358	24.6
[IV]		280	350	25.2

**Fig.(8):** DSCcurves for compounds [I-IV]

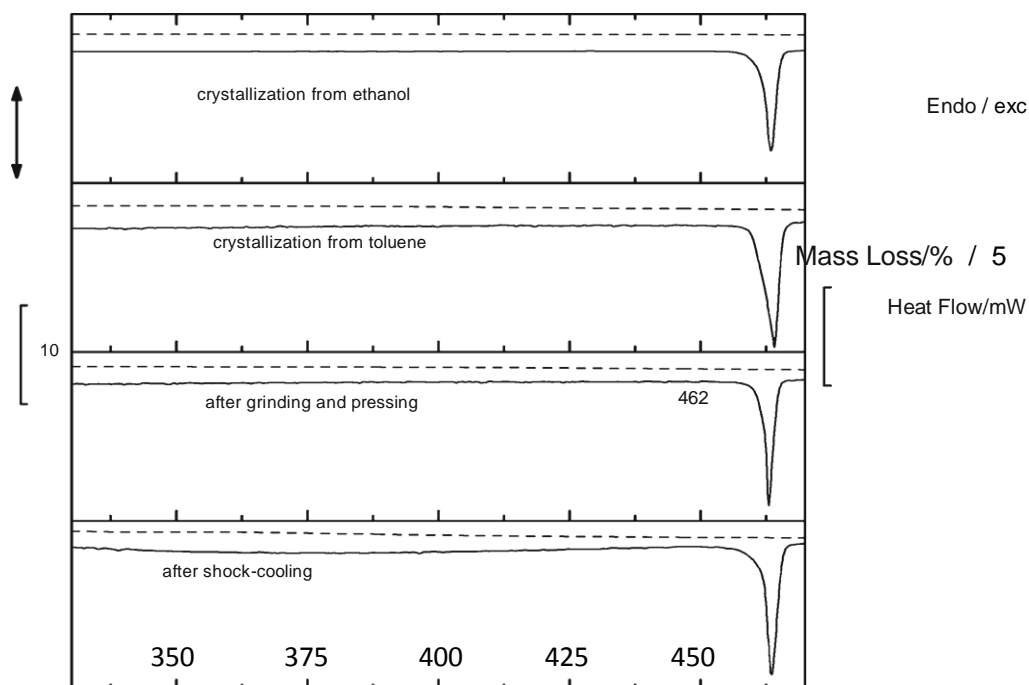


Fig.(9): (DSC and TG) traces for compounds [I–IV] at 5 K min⁻¹

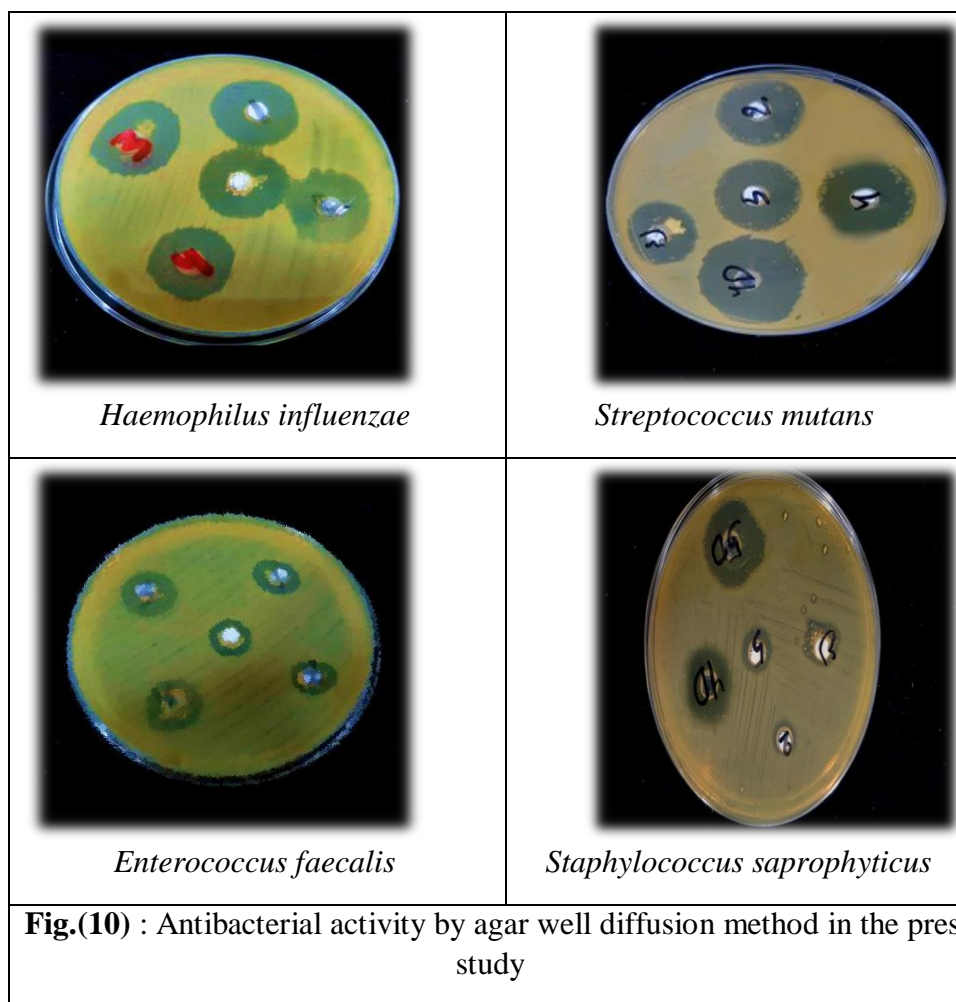
3.4. Antibacterial Activity Test

Recently, scientists and specialists have tended to search for more effective and safe alternatives compared to antibiotics due to the excessive increase in bacterial resistance to the most common antibiotics, which has become a major challenge for individuals and health institutions [16]. In the present study, prepared compounds I,II,III,IIV showed clear antibacterial activity against all tested bacterial species either as solutions or powder (DMSO and DW as solvents). Solutions with DMSO (as a solvent) have antibacterial activity greater than those with distilled water (table 3, figure 10), May be because DMSO is considered better solvent than DW which restrict the spread through agar resulting in less inhibition zone [17]. As detailed in table 3, Compound I showed greater antibacterial activity than other compounds II, III, and IIV and the powder. against microorganisms that are both(Gram-positive and Gram-negative). On the other hand, (

Gram-positive) bacteria displayed greater sensitivity to all solutions examined in this study than Gram-negative ones.

This finding is consistent with the published studies that have shown that thioxanthenes have *potential* antimicrobial activities In addition. It plays a unique part in boosting the effectiveness of antibiotics against bacteria that are multidrug resistant. This activity may be attributed to the properties of xanthenes which have been reported as inhibitors of the Bacterial efflux pumps and their rings contain (N, S, and O) atoms in their structures., which causes damage of the cell wall, inhibition of protein synthesis and RNA synthesis. In general, most of a drug's activity depends on the balance of hydrophilic and lipophilic characteristics, as well as substituent-dependent solubility, which improves a drug's lipophilicity, which could explain why nitrogen compounds have increased activity. [18,19,20]. In a study by Durães *et al.*, [21] The thioxanthone derivatives were suggested as potential bacterial efflux pump inhibitor, consequently, reduce the bacterial ability for antibiotic resistance.

Table(3): Antibacterial activity test of compounds I,II,III,IV prepared in the current study against Gram positive bacteria and Gram negative bacteria						
Solvent	Compound number	DMSO		Distilled Water		Powder
Conc. (mg/ml)		125	250	125	250	500 mg
<i>Streptococcus mutans</i>	I	26	28	22	25	15
	II	23	26	22	25	15
	III	23	24	18	22	9
	IV	20	21	15	19	9
<i>Staphylococcus saprophyticus</i>	I	25	27	19	23	14
	II	25	27	18	23	15
	III	23	25	18	23	9
	IV	21	22	14	20	10
<i>Enterococcus faecalis</i>	I	26	28	18	22	11
	II	23	25	15	20	9
	III	23	25	15	20	9
	IV	22	25	14	20	10
<i>Haemophilus influenza</i>	I	22	24	18	20	9
	II	21	24	17	21	9
	III	21	24	16	22	9
	IV	20	23	15	21	8
The data in this table represent the diameter of inhibition zone by mm						



4. CONCLUSION

This research suggests that all rings synthesized have a strong antibacterial activity, suggesting that they could be used to combat a wide range of diseases in the future. To characterize solid states, differential thermal analysis (DSC) has been employed. Additionally, calculations using the Density Functional Theorem (DFT) were carried out. Controlling crystal clarity is crucial for the pharmaceutical sector. Our study's objective was to identify the existence of different solid-state forms. Theoretical calculations indicate that all chemicals are capable of forming hydrogen bonds with ethanol as a solvent. . Since it is stable at high temperatures, it can be used as a ligand in inorganic chemistry to create complexes. The byproducts of the processes can also be

used as activators or sensitizers in the photo-polymerization of ethylenically unsaturated monomers or in the preparation of pharmaceutical products for use in the field of psychotherapy.

Table 4 List of abbreviations

DMSO	Dimethyl sulfoxide
DSC	Differential scanning calorimetry
DW	Distill Water
M.P	Melting point
Rf	Retention factor
TG	Thermogravimetric
TLC	Thin layer Chromatography
THF	Tetra Hydro Furan

REFERENCES

1. A. L. Jarallah , A.F.Kareem, "Synthesis, Examination of Various Seven Rings, and Effects on Corrosion and Fungus", *Journal of Medicinal and Chemical Sciences*, 2023 6 (3) 532-539 DOI:10.26655/JMCHMSCI.2023.3.10.
2. M. M. Redha, N. M.Aljamali, "Preparation, Spectral Investigation, Thermal Analysis, Biochemical Studying of New (Oxadiazole - Five Membered Ring)- Ligands " , *Journal of Global Pharma Technology*, 201810(1) 20-29.
3. A.T. Chinillach, R.Chinillach, " Synthesis of xanthine, thioxanthone by using visible light &molecular oxygen" ,*Molecules*, 2021 26(1) 1-10.
4. A.F.Kareem, H.T. Ghanim, " Antimicrobial studying of (Imidazole) derivative from pyrimidine" *International Journal of Pharmaceutical Research*, 2020 12 (4) 913- 917.
5. A.F.Kareem, H.T. Ghanim, "Antimicrobial Study against Seven Cycles Compounds Derivatives from Pyrimidine", *Indian Journal of Forensic Medicine & Toxicology*, 2020 14 (3) 794.
6. M.N. Prasad, P. Arena, "Decolourization of selected procaine dye using fungi acrimonious chrysogenum" ,*Int. J. lied Bio & pharm. Teche*, 2013 4(3) 327-33.
7. R.M .Obaid , H.T. Ghanim, "Synthesis and Characterization of Heterocyclic Compounds from 8-Hydroxyquinoline" ,*Journal of Kufa for Chemical Scienc*, 2017 2(3) 66-83.
8. N.J. ALganab , N.J. Rasool, "Synthesis and characterization of Some New Sulfadiazine derivatives", *J. Pharm. Sci. & Res*, 2018 10(11) 2796-2799.
9. A.F.Kareem, ,, Synthesis and Chemical Characterization of Cycles from Oxadiazol- Indole Derivatives" , *International Journal of Biology,pharmacy and allied sciences*,2016 5(6) 1455-1467.
10. A.T.Al-Sa'ady, H.H, " Nanomedical Applications of Titanium Dioxide Nanoparticles as Antibacterial Agent against Multi-Drug Resistant Streptococcus Pneumoniae" , *Systematic Reviews in Pharmacy*, 2020 11(10) 53-63, doi:10.31838/srp.2020.10.11.
11. A.F.Kareem, S. Ahmed, ,,Antimicrobial Study of Azo-imidazole (five cycles) Compounds",*Muthanna Medical Journal*, 2017 4(2) 97-104.
12. R.M.U .Mahmood, R.A.A. Ghafil , "Synthesis and Characterization some Imidazolidine Derivatives and Study the Biological Activity, *Annals of R.S.C.B*, 2021 5(3) 569 – 584.
13. A.K. Mahdi, N.M. Aljamali, "Heterocyclic- Derivatives with Aspirin Drug Synthesis, Characterization, Studying of Its Effect on Cancer Cells" , *International Journal of Cell Biology and Cellular Processes*, 2020 6(2) 1-20.
14. A.M .Jawad, ,, Innovation, Preparation of Cephalexin Drug Derivatives and Studying of Toxicity & Resistance of Infection" , *International Journal of Psychosocial Rehabilitation*, 2020 24(4), DOI: 10.37200/IJPR/V24I4/PR201489.
15. A.F. Kareem, ,, Chemical Studying of New Organic Heterocyclic Compounds" ,*Iraqi National Journal of Chemistry*, 2019 19(2019) 12.
16. A. T . Al-Sa'ady, ,,Detection of vancomycin resistance in multidrug-resistant Enterococcus faecalis isolated from burn infections" , *Drug Invention Today*, 2019 11(11) 2984-2989
17. S.M .Al-Araji,R.S . Dawood, ,,Synthesis and characterization of new heterocyclic thioxanthone,, , *Baghdad Science Journal*, 2013 10(3) 779-789.

18. M.M.M. Pinto, A.Palmeira, C.Fernandes, D.I.S.P .Resende,E. Sousa, H . Cidade,M.E Tiritan, M.Correia-da-Silva, S.Cravo, „From Natural Products to New Synthetic Small Molecules” ,*Molecules*, 2021 2 (2) 431.
19. F. Durães, D.I.S.P .Resende, A.Palmeira, N. Szemerédi, M.M.M .Pinto, G . Spengler, E .Sousa, ”Xanthoness Active against Multidrug Resistance and Virulence Mechanisms of Bacteria”, *Antibiotics*, 2021 10(2) 600.
20. A.S .Hassan, A.S .Hame, ” Study of antimicrobial activity of new prepared seven membered rings Oxazepine” , *Research Journal of Biotechnology*, 2019 14 (1) 109-118.
21. F. Durães,A.Palmeira, B.Cruz, B. Freitas-Silva, J. N. Szemerédi, L.Gales, P.M. daCosta, F. Remião, R.Silva, M. Pinto, G.Spengler , E. Sousa, ”Antimicrobial Activity of a Library of Thioxanthoness and Their Potential as Efflux Pump Inhibitors” ,**Pharmaceuticals**, 2021 **14** 572. <https://doi.org/10.3390/ph14060572>



ARID Journals

ARID International Journal for Science and Technology (AIJST)

ISSN: 2662-009X

Journal home page: <http://arid.my/j/aijst>

ARID

International Journal for Science and Technology
مجلة أريد الدولية للعلوم والتكنولوجيا

VOL. 6 NO. 11 JUNE 2023

ISSN: 2662-009X

ARID
ARID PUBLICATIONS
ARIDMYJST

مجلة أريد الدولية للعلوم والتكنولوجيا

المجلد 6 ، العدد 11 ، حزيران 2023 م

Effect of Seawater Irrigation on Germination and Growth of Bauhinia Variegata Seedlings and Seed Treatment with Gibberellins

Sami Mohammed Salih^{1*}, Ahmed AmrajaaAbdulrazziq¹ and Sameer Salih Mohammed²

Department of Biology, Faculty of Education, Omar Al-Mukhtar University, Al-Bayda, Libya

²Sector Agriculture of Labraq, Ministry of Agriculture, Libya

تأثير الري بمياه البحر على إنبات ونمو شتلات أشجارخف الجمل *Bauhinia variegata* ومعالجة البذور بالجبرلين

سامي محمد صالح^{1*}، أحمد امراجع عبد الرازق¹ وسمير صالح محمد²¹قسم الأحياء، كلية التربية، جامعة عمر المختار، البيضاء، ليبيا.²قطاع الزراعة الأبرق، وزارة الزراعة، ليبيا.sami.mohammed@omu.edu.lyarid.my/0008-0419<https://doi.org/10.36772/arid.aijst.2023.6114>

ARTICLE INFO

Article history:

Received 03/03/2023

Received in revised form 11/03/2023

Accepted 22/03/2023

Available online 15/06/2023

<https://doi.org/10.36772/arid.aijst.2023.6114>

ABSTRACT

The sea height level along Libyan coasts is considered one of the environmental pressures that lives in soil vegetation characteristics. Therefore, two experiments were conducted (laboratory - pots) to find out the effect of irrigation with seawater at the concentration (10%, 20%, 40%, 60%) on germination of seeds and seedlings of *Bauhinia variegata* trees with an age of 6 months, and treated using pre-soaking in gibberellin acid (GA3) 500ppm for 24 hours. The results showed that the exposure of seeds and seedlings of *B.variegata* trees to salinity led in two experiments to a significant decrease in percentage germination, an increase in means germination time, moreover, a decreased seedlings lengths, number of leaves/plant, shoot and root lengths, fresh and dry weight of seedlings compared with a control. The results also showed that the seeds and seedlings of *B.variegata* trees were able to germinate in different concentrations of seawater, except for 60% concentration which caused in death of seeds and seedlings, while pre-soaking treatment of seeds with gibberellin acid was not successful to overcome the salt stress, although slightly improved some studied traits. The results concluded that the possible seeds and seedlings agriculture of *B.variegata* trees in coastal locations in which seawater concentration did not exceed 40%, existed to be used in reforestation of degraded lands.

Key words: *Bauhinia variegata*, seawater, GA3, Libyan coasts.

الملخص

يعد ارتفاع مستوى سطح البحر على طول السواحل الليبية، من أكثر الضغوطات البيئية التي تؤثر على خصائص التربة والبيئة النباتية، لذلك أجريت تجربتان (مختبرية - أصص) بهدف معرفة تأثير الري بماء البحر بتركيز (10%، 20%، 40%) على إنبات بذور وتحمل شتلات أشجار خف الجمل *Bauhinia variegata* بعمر 6 شهور ومعالجتها باستخدام معاملة النقع المسبق بحمض الجبرلين (GA3) 500 ppm لمدة 24 ساعة. أشارت النتائج إلى أن تعرض بذور وشتلات أشجار خف الجمل للملوحة في التجربتان أدت إلى انخفاض معنوي في النسبة المئوية للإنبات، وزيادة متوسط زمن الإنبات، وانخفاض أطوال الشتلات، وعدد الأوراق/نبات، وأطوال المجموعتين الخضري والجذري، والوزنين الطازج والجاف للشتلات مقارنة مع الشاهد، كما بينت النتائج أن بذور وشتلات أشجار خف الجمل كانت قادرة على الإنبات في مختلف تراكيز ماء البحر باستثناء التركيز 60% الذي تسبب في موت البذور والشتلات، بينما كانت معاملة النقع المسبق للبذور بحمض الجبرلين غير ناجحة في التغلب على الإجهاد الملحي، مع أنها حسنت قليلاً من بعض الصفات المدروسة، وخلصت النتائج إلى إمكانية زراعة بذور وشتلات أشجار خف الجمل في المواقع الساحلية التي لا يزيد تركيز ماء البحر فيها عن 40% لاستغلالها في إعادة تشجير الأراضي المتدهورة.

الكلمات المفتاحية: خف الجمل، ماء البحر، حمض الجبرلين، السواحل الليبية.

المقدمة:

تعد ملوحة التربة من المشاكل التي تهدد أكثر من مليار هكتار من الأراضي في أكثر من 100 دولة [1]، وفي ليبيا تقدر مساحة الأراضي المتأثرة بالملوحة حوالي 51.9% [2]. يشاهد تسرب مياه البحر في المناطق الساحلية الليبية، نتيجة لارتفاع مستوى سطح البحر [3]، مما أدى إلى تدهور التربة في المناطق الجافة وشبه الجافة وتكوين السبخات الملحية وبالتالي انخفاض إنتاجية التربة، وانعدام الغطاء النباتي [4] نظراً لتأثيرها السلبي على الصفات المورفولوجية والفسولوجية للنباتات من خلال تعطيل وإتلاف العمليات والمكونات الخلوية جراء اختلال التوازن الاسموزي والأيوني، وإنتاج أنواع الأكسجين التفاعلية [5]. تنتمي أشجار خف الجمل *Bauhinia variegata* للعائلة الفرعية *Cesalpiniaceae* العائدة للعائلة البقولية *Fabaceae*، من أشجار الزينة المنتشرة عالمياً، والتي يصل طولها إلى 8 أمتار [6, 7]، وتعرف بأشجار خف الجمل نسبةً لأوراقها التي تأخذ شكل قدم الأبل [8]، تستخدم زراعياً في إعادة تشجير الأراضي المتدهورة، وصناعياً لتصنيع الأخشاب والزيت، والصمغ، وطبياً لعلاج العديد من الأمراض لما لها من أنشطة مضادة للأورام، والميكروبات، والالتهابات [9, 10].

يوجد عدة طرق لاستصلاح الأراضي الواقعة تحت الملوحة، على سبيل المثال غسيل التربة بالمياه العذبة كمحاولة لإزالة الأملاح السطحية المتراكمة [11]، كذلك طريقة الري بالتنقيط [12]، واستخدام المواد الكيميائية المضافة للتربة [13]، ولكن تظل هذه الطرق باهظة الثمن وغير مستدامة، لذلك توجهت الدراسات الحديثة إلى انتخاب أنواع من النباتات المقاومة، بواسطة خفض منسوب المياه الجوفية المالحة [14]، حيث دعت دراسة أجريت في إيران إلى إمكانية زراعة شتلات أشجار *Rhizophora mucronata* (Lam) لمقاومتها مستويات الملوحة المعتدلة، ولمساهمتها في انخفاض الطلب على الماء لهذه الأشجار [15]، وفي بنما أجريت دراسة بينت أن الأشجار الساحلية هي الأكثر تكيفاً من تلك الاستوائية تحت تراكيز الملوحة المتزايدة [16]، لذلك هدفت هذه الدراسة إلى اختبار تأثير الري بمستويات مختلفة من مياه البحر على إنبات بذور ونمو شتلات أشجار خف الجمل *Bauhinia variegata* ومعالجتها بالنقع المسبق بحمض الجبرلين.

المواد وطرق البحث

- التجربة المختبرية

- تجميع ومعالجة البذور:

جمعت عينات البذور الناضجة من ثلاث أشجار لنبات خف الجمل *Bauhinia variegata* من ثلاث مواقع بمدينة البيضاء شرقي ليبيا خلال العام 2020-2021 وتم انتقاء البذور المتجانسة قدر الإمكان، ونظفت من الشوائب، واختبرت حيويتها من خلال نقعها في الماء المقطر للتخلص من البذور الفارغة الطافية على سطح الماء، ونقعت في محلول هايپوكلوريد الصوديوم 3% لمدة 5 دقائق وغسلت بالماء المقطر.

المعاملات المستخدمة:

- 1 - الشاهد الأول: بدون معاملة (ماء مقطر معقم).
 - 2 - الشاهد الثاني: نقع في الجبرلين 24 ساعة.
 - 3 - معاملة مستويات الملوحة: الري بماء البحر بتركيز (10%, 20%, 40%, 60%).
 - 4 - معاملة النقع المسبق في هرمون الجبرلين (GA3): نقعت بذور خف الجمل مسبقاً قبل معاملتها بالملوحة في الجبرلين 500ppm لمدة 24 ساعة، وحضر التركيز المذكور بإذابة 0.5غم من الجبرلين في حجم لتر ماء مقطر.
- وزعت البذور المعقمة في أطباق بتري زجاجية قطرها 15سم معقمة مبطنة بورق ترشيح بمعدل 20 بذرة/ طبق، وأضيف لكل طبق 2.5 مل من المحاليل الملحية لمياه البحر بتركيز (10%, 20%, 40%, 60%)، وكررت كل معاملة ثلاث مرات، وتم متابعة الإنبات من حيث إضافة المحلول الملحي حسب الحاجة لكل طبق مع استعمال الماء المقطر للشاهد، مع مراعاة تغيير أوراق الترشيح لمنع تراكم الملح وخضعت الأطباق للملاحظة اليومية لمدة 10 أيام، وتم حساب الإنبات بتسجيل عدد البذور النابتة في جميع المعاملات بدءاً من اليوم الثالث، وهو اليوم الذي حدث فيه أول إنبات علماً بأن معيار الإنبات هو خروج الجذير خارج غلاف البذرة [17]، وفي نهاية التجربة أخذت النتائج النهائية للصفات التالية:

$$\text{نسبة الإنبات} \% = \frac{\text{عدد البذور النابتة}}{\text{العدد الكلي للبذور}} \times 100X$$

- متوسط زمن الإنبات = مجموع عدد البذور النابتة في كل يوم / مجموع عدد البذور النابتة في نهاية التجربة [18].

تجربة الأصص:

عقمت تربة طميية طينية عند درجة حرارة 90م لمدة 48 ساعة، ووضعت في أصص مملوءة بخمسة كيلوغرامات من التربة الطينية الرملية الجافة بنسبة 1:2 وزرعت 5 بذور/أصص، وتحت ظروف أشعة الشمس، تم ري الأصص بماء الصنبور العادي حسب الحاجة، وبعد 6 شهور من الزراعة، قسمت الأصص إلى ثلاث مجموعات، وثلاث مكررات، (بذور الشاهد بدون معاملة، بذور عوملت بمستويات الملوحة المختلفة لماء البحر، وبذور منقوعة مسبقاً في الجبرلين تحت تأثير مستويات ملوحة ماء البحر)، وتم ري مجموعة الشاهد بماء الصنبور أما باقي المجموعات رويت بتركيزات مختلفة من المحاليل الملحية لماء البحر (10%, 20%, 40%, 60%)، وبعد 30 يوماً من المعاملة تم اقتلاع الشتلات وغسلت بماء الصنبور لإزالة جزيئات التربة الملتصقة، ثم بالماء المقطر، ونظفت برفق باستخدام ورق الترشيح، ثم أخذت النتائج النهائية للصفات التالية:

- طول الشتلة وطول المجموع الخضري والجذري (سم): أخذت القياسات باستخدام مسطرة مدرجة، وتم حساب المتوسطات في ثلاث مكررات.

- عدد الأوراق/نبات .

- الوزن الطازج والجاف للشتلات (جم): تم تحديد الأوزان الطازجة لخمس شتلات، بعد ذلك وضعت في الفرن عند

65⁰م لمدة 72 ساعة لأخذ الأوزان الجافة لها.

التحليل الإحصائي:

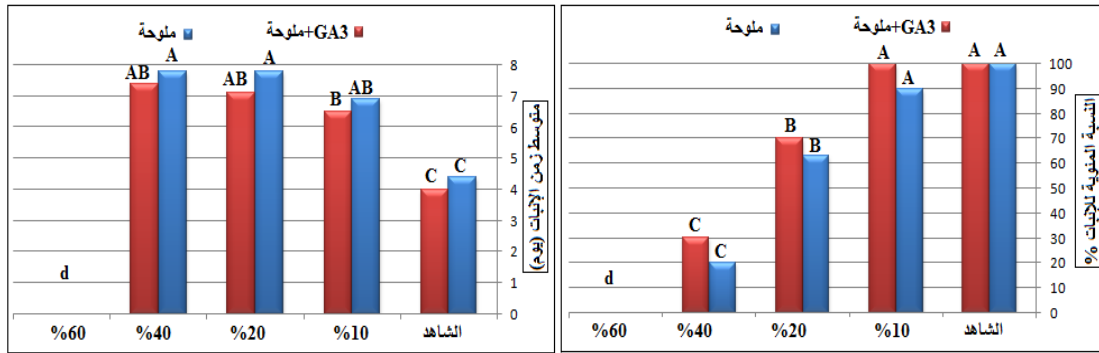
تم تصميم تجارب الدراسة وفقاً للتصميم كامل العشوائية (CRD)، وأجري التحليل الإحصائي باستخدام برنامج (Minitab

17) وجداول تحليل التباين ANOVA، وتم مقارنة المتوسطات باستخدام اختبار (Tukey's) عند $P < 0.05$.

النتائج والمناقشة:

التجربة المختبرية:

أشارت البيانات الواردة في الشكل (1) إلى تأثير مستويات الملوحة المختلفة لماء البحر بتركيز (10%، 20%، 40%، 60%)، على النسبة المئوية للإنبات، ومتوسط زمن الإنبات لأشجار خف الجمل *B. variegata* بعد 10 أيام من بداية التجربة، حيث بينت النتائج الإحصائية عدم وجود أي فروق معنوية في النسبة المئوية للإنبات للتركيز 10% والشاهد في حين كانت هناك زيادة واضحة في متوسط زمن الإنبات من (4.4 يوم) للشاهد إلى (6.9 يوم)، وبزيادة تراكيز الملح لمياه البحر أخذت النسب المئوية في الانخفاض بشكل عام، مما نتج عنه تأخير متوسط زمن الإنبات، حيث أعطى التركيز 20% نسبة إنبات بلغت (63%) وبمتوسط زمن إنبات (7.8 يوم)، بينما سجل التركيز 40% نسبة إنبات وصلت (20%) وبمتوسط زمن إنبات (7.8 يوم)، كما أظهر الإجهاد الملحي سميته على إنبات بذور خف الجمل للتركيز 60% والذي لم يظهر معه أي إنبات مسبب في موت البذور وتعفنها، تؤيد هذه النتائج ما ذكره [17] بإمكانية نمو بذور العديد من الأشجار الاستوائية بشكل طبيعي تحت مستويات الملوحة المنخفضة، كما اتفقت هذه النتائج مع ما قدمه [19] بأنه لا يمكن زراعة بذور أشجار الخروب في المواقع الساحلية التي يزيد تركيز ماء البحر فيها عن 50% لما تسببه التراكيز العالية من تثبيط واضح لإنبات البذور، وقد يرجع التأثير السام للملوحة كونها تقلل محفزات الإنبات كالجبرلين GA_1 و GA_2 والتي بدورها تضعف نشاط أنزيم α -amylase و protease المسؤولين عن تحلل وتحول المواد المخزنة في الجنين [20] كما تشير النتائج أيضاً من الشكل (1) لمعاملة النقع المسبق لبذور خف الجمل *B. variegata* بحمض الجبرلين بتركيز 500ppm لمدة 24 ساعة، والتي بينت فيها التحاليل الإحصائية عدم وجود فروق معنوية بينها وبين مستويات الملوحة لماء البحر، مع أنها حسنت قليلاً من أداء البذور تحت مستويات الملوحة، بنسبة إنبات (100%) وبمتوسط زمن إنبات (6.5 يوم) للتركيز 10% مقارنة بالبذور الغير معاملة، كما أعطى التركيز 20% زيادة في النسبة المئوية للإنبات بلغت (70%) وبمتوسط زمن إنبات (7.1 يوم) مقارنة بالبذور غير المعاملة، وارتفعت نسبة الإنبات للتركيز 40% لتصل (30%) وبمتوسط زمن إنبات (7.4 يوم) بينما لم يظهر للتركيز 60% أي إنبات للبذور، اختلفت هذه النتائج مع [21]، الذين أكدوا أن معاملة حمض الجبرلين تزيد من تكيف نمو أشجار *Carica papaya* L ضد الإجهاد الملحي.

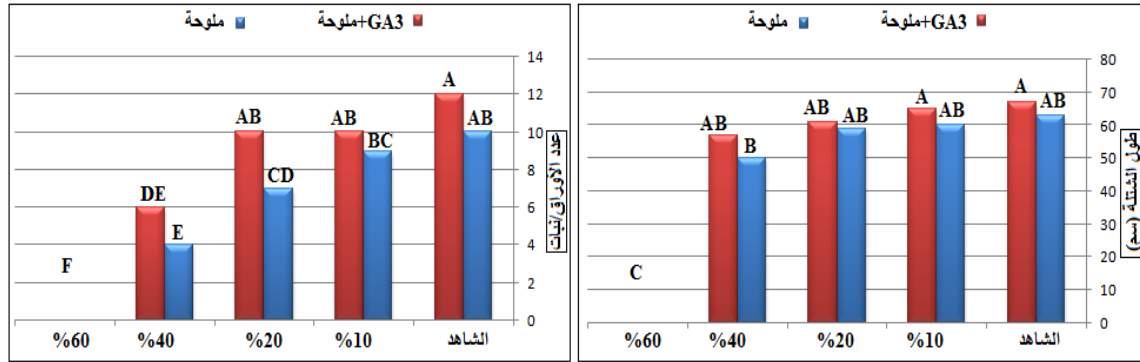


شكل (1): تأثير مستويات ملوحة ماء البحر والنقع في الجبرلين على النسبة المئوية

ومتوسط زمن الإنبات لأشجار خف الجمل *B. variegata*.

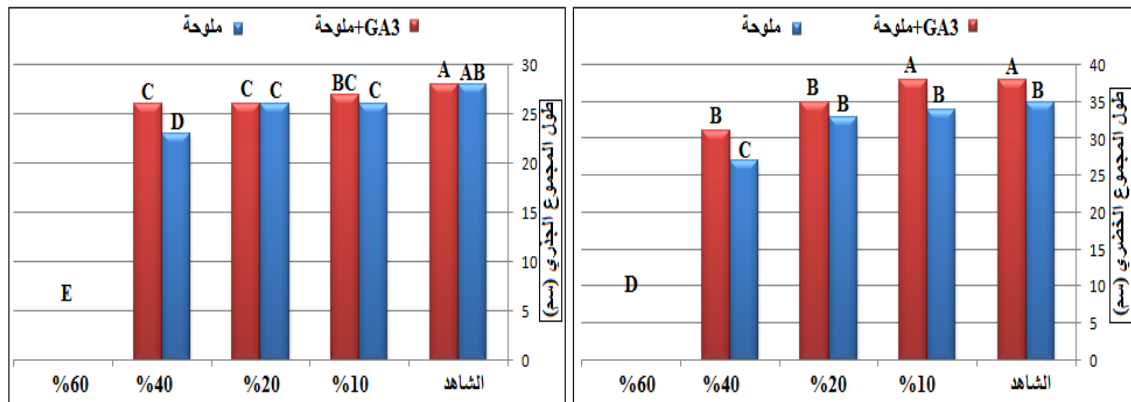
تجربة الأصص:

أشارت البيانات من الشكل (2) إلى تأثير مستويات الملوحة المختلفة لماء البحر بتركيز (10%, 20%, 40%, 60%) على طول الشتلة وعدد الأوراق/نبات لخف الجمل، بعد 30 يوما من بداية التجربة، بينت النتائج أن معاملة الشتلات بالملوحة أدت إلى انخفاض أطوالها من (63سم) للشاهد إلى (50, 59, 60سم) للتركيز 10%, 20%, 40% على التوالي، كما يلاحظ أن التركيزات المختلفة من الملوحة عجلت من ذبول الأوراق وتساقطها لتصل إلى (9, 7, 4 أوراق/نبات) لنفس التركيزات السابقة على التوالي، مقارنة بالشاهد (10 أوراق/نبات، وتقاربت هذه النتائج مع مذكره [22] بانخفاض أطوال شتلات المورينجا وانخفاض أوزان أوراقها عند معاملتها 50 يوماً بمستويات الملوحة، في حين تسبب التركيز 60% في سقوط جميع الأوراق وموت الشتلات، وهذا مقارب لما وجدته [23]، بسقوط أوراق وموت شتلات أشجار *Xylocarpus granatum* عند تعرضها لإجهاد ملحي يزيد عن 25 PSU، بسبب التأثير المثبط للملح على انقسام الخلايا وتضخمها، كما بينت النتائج أيضاً من الشكل (2) تفوق معاملة النقع المسبق للبذور بحمض الجبرلين في إعطاء أفضل المعدلات لأطوال الشتلات بارتفاع (54, 61, 65سم) وبزيادة قدرها (5, 2, 4سم) للتركيز 10%, 20%, 40% على التوالي، مقارنة بالشتلات غير المعاملة، كما سجلت بيانات عدد الأوراق/نبات عدد (10, 10, 6/نبات) وبزيادة مقدارها (1, 3, 2 نبات) لنفس التركيزات السابقة على التوالي، مقارنة بالشتلات غير المعاملة.



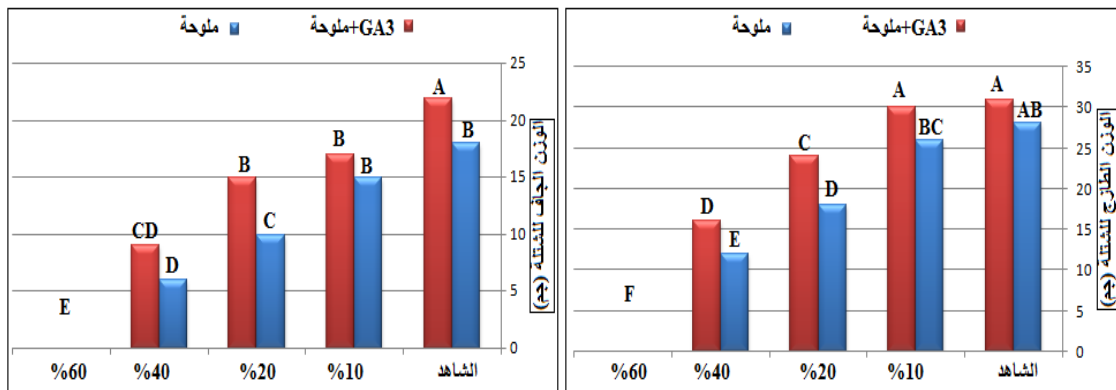
شكل (2): تأثير مستويات ملوحة ماء البحر والنقع في الجبرلين على أطوال الشتلات وعدد الأوراق/نبات لأشجار خف الجمل *B. variegata*.

كما أشارت البيانات من الشكل (3) و(4) إلى تأثير مستويات الملوحة المختلفة على أطوال المجموع الخضري والجذري، والوزنين الطازج والجاف للشتلات، حيث أظهرت النتائج عدم وجود أي فرق معنوي بين معاملات الملوحة المختلفة لأطوال المجموع الخضري، باستثناء التركيز 40% الذي أعطى ارتفاعاً قدره (27سم) مقارنة بالشاهد (35سم)، كما لوحظ تدني أطوال المجموع الجذري إلى (26, 26, 23سم) مقارنة بالشاهد (29سم)، كما ساهمت الملوحة في تثبيط الأوزان الطازجة للشتلات من (28جم) إلى (26, 18, 12جم) والأوزان الجافة من (18جم) إلى (15, 10, 6جم) للتركيزات 10%, 20%, 40% على التوالي، وتقاربت نتائجنا مع [24] بهذا الخصوص عندما تعرضت شتلات السنط العربي *Vachellia nilotica* (L.) للإجهاد الملحي.



شكل (3): تأثير مستويات ملوحة ماء البحر والنقع في الجبرلين على أطوال المجموعين الخضري والجذري لأشجار خف الجمل *B. variegata*.

كما بينت النتائج أيضا من الشكل (3) عدم وجود أي فروق معنوية بين معاملة النقع المسبق للبذور بحمض الجبرلين ومستويات الملوحة باستثناء التركيز 10% لأطوال المجموعين الخضري والجذري، حيث سجلت معاملة الجبرلين ارتفاع (38, 35, 31 سم) بزيادة قدرها (4, 2, 4 سم) للتركيز 10%, 20%, 40% على التوالي، للمجموع الخضري مقارنة بالشتلات غير المعاملة، كما بلغت معدلات أطوال المجموع الجذري، (27, 26, 26 سم) لنفس التراكيز السابقة على التوالي، مقارنة بالشتلات غير المعاملة، كما أظهرت النتائج من الشكل (4) وجود فرق معنوي لمعاملة النقع بالجبرلين في التغلب على مستويات الملوحة للوزن الطازج بمعدلات بلغت (30, 24, 16 جم) وبزيادة قدرها (4, 5, 4 جم) 10%, 20%, 40% على التوالي، مقارنة بالشتلات غير المعاملة، كما سجلت معدلات (17, 15, 9 جم) بزيادة قدرها (2, 5, 3 جم) لنفس التراكيز السابقة على التوالي، مقارنة بالشتلات غير المعاملة.



شكل (4): تأثير مستويات ملوحة ماء البحر والنقع في الجبرلين على الوزنين الطازج والجاف لشتلات أشجار خف الجمل *B. variegata*.

بينت النتائج أن تعرض بذور وشتلات خف الجمل للملوحة أدت إلى انخفاض معنوي في النسبة المئوية للإنبات، وزيادة متوسطات زمن الإنبات، وانخفاض أطوال الشتلات، وعدد الأوراق/نبات، وأطوال المجموعين الخضري والجذري، والوزنين الطازج والجاف للشتلات مقارنة مع الشاهد، واتفقت هذه النتائج مع [25, 26, 27] بحساسية أشجار بعض الأجناس التابعة للبوهدينيا للإجهاد الملحي، كما يلاحظ أن بذور وشتلات خف الجمل كانت قادرة على الإنبات في جميع مستويات ملوحة ماء البحر باستثناء التركيز 60% الذي تسبب في موت البذور والشتلات، كما أظهرت نتائج التحليل الإحصائي أن معاملة النقع المسبق للبذور بحمض الجبرلين حسنت قليلاً من بعض الصفات المدروسة ولكنها لم تكن ناجحة في التغلب على الإجهاد الملحي، لأغلبية التراكيز.

الاستنتاجات:

نستنتج من هذه الدراسة أن بذور وشتلات خف الجمل كانت متسامحة لملوحة ماء البحر للتركيز المنخفضة، بينما كانت حساسة للتركيز العالية، وكان التركيز 60% هو التركيز المميت للبذور والشتلات، وكانت معاملة النقع المسبق للبذور بحمض الجبرلين غير ناجحة في التغلب على إجهاد الملوحة، لذا يوصي الباحث بزراعة بذور وشتلات أشجار خف الجمل *Bauhinia variegata* في المواقع الساحلية الليبية التي لا يزيد تركيز ماء البحر فيها عن 40% كمحاولة لإعادة تشجير الأراضي المتدهورة وتثبيت التربة.

قائمة المراجع والمصادر:

- 1- A. Singh, Soil salinity: A global threat to sustainable development. *Soil Use and Management*, 38(1) (2022) 39-67.
- 2- K. Ben-Mahmoud, "Libyan Soils." First Edition. Tripoli: National Research Scientific Organization.(1995).
- 3- H. A. Zurqani, E. A. Mikhailova, C. J. Post, M. A. Schlautman, and A. R. Elhawej, A Review of Libyan Soil Databases for Use within an Ecosystem Services Framework. *Land*, 8(5) (2019) p.8.
- 4- A. R. Mohamed, and A. M. Elssaidi, Soil and Water Physical and Chemical Properties of Tragen Sabkha Area, Southwest Libya, *Al-Mukhtar Journal of Sciences* 35 (1) (2020) 46-59.
- 5- D. Singh, Juggling with Reactive Oxygen Species and Antioxidant Defense System—A coping mechanism under salt stress. *Plant Stress*, (5) (2022) 100093 .
- 6- V. C. Filho, Chemical composition and biological potential of plants from the genus *Bauhinia*. *Phytotherapy Research*, 23(2009) 1347- 1354.
- 7- O. N. Allen, and E. K. Allen, *The Leguminosae: A source book of characteristics, uses and nodulation*. USA, Wisconsin: UW Press (1981).
- 8- A. H. Elbanna, E. A. H. Mahrous, A. E. S. Khaleel, and T. S. El-alfy, Morphological and anatomical features of *Bauhinia vahlii* Wright & Arnoot. Grown in Egypt. *Journal of Applied Pharmaceutical Science*, 6(12) (2016) 084-093.
- 9- P. Khare, K. Kishore, and D. K. Sharma, A study on the standardization parameters of *Bauhinia variegata*. *Asian Journal of Pharmaceutical and Clinical Research*, 10(4) (2017) 133-136.
- 10- R. G. Mali, and A. S. Dhake, *Bauhinia variegata* Linn. (Mountain Ebony): a review on ethnobotany, phytochemistry and pharmacology. *Advances in Traditional Medicine*, 9(3) (2009) 207-216.
- 11- I. Sastre-Conde, M. C. Lobo, R. I. Beltran-Hernandez, and H. M. Poggi-Varaldo, Remediation of saline soils by a two-step process: Washing and amendment with sludge. *Geoderma*, 247(2015) 140-150 .
- 12- Y. Roupahel, M. Cardarelli, E. Rea, A. Battistelli, and G. Colla, Comparison of the subirrigation and drip-irrigation systems for greenhouse zucchini squash production using saline and non-saline nutrient solutions. *Agricultural water management*, 82(1-2) (2006) 99-117.
- 13- E. A. Hasoon, F. S. Al-kinany, S. R. Al-Jeboory, and A. H. Al-hadithy, Effect of irrigation water of the main out full with addition Gypsum Phosphate on growth of barley (*Hordeum Vulgare*). *Journal of Kerbala for Agricultural Sciences*, 4(2) (2019) 133-144.
- 14- S. Imada, N. Yamanaka, and S. Tamai, Effects of salinity on the growth, Na partitioning, and Na dynamics of a salt-tolerant tree, *Populus alba* L. *Journal of arid environments*, 73(3) (2009) 245-251 .
- 15- M. Moslehi, T. Pypker, A. Bijani, A. Ahmadi, and M. H. S Hallaj, Effect of salinity on the vegetative characteristics, biomass and chemical content of red mangrove seedlings in the south of Iran. *Scientia forestalis*, 49(2021) (132).
- 16- A. De Sedas, Y. González, K. Winter, and O. R. Lopez, Seedling responses to salinity of 26 Neotropical tree species. *AoB Plants*, 11(6) (2019) plz062.
- 17- K. O. Yongkriat, N. Leksungnoen, D. Onwimon, and P. Doornil, Germination and salinity tolerance of seeds of sixteen Fabaceae species in Thailand for reclamation of salt-affected lands. *Biodiversitas Journal of Biological Diversity*, 21(5) (2020).

- 18- M. Das, M. Sharma, and P. Sivan, Seed germination and seedling vigor index in *Bixa orellana* and *Clitoria ternatea*. *Int. J. Pure App. Biosci*, 5 (5) (2017) 15-19.
- 19- A. Kheloufi, and L. M. Mansouri, Effect of seawater irrigation on germination and seedling growth of Carob tree (*Ceratonia siliqua* L.) from Gouraya National park (Bejara, Algeria). *Reforesta*, (10) (2020) 1-10.
- 20- L. Liu, W. Xia, H. Li, H. Zeng, B. Wei, S. Han, and C. Yin, Salinity inhibits rice seed germination by reducing α -amylase activity via decreased bioactive gibberellin content. *Frontiers in Plant Science*, 9(2018) 275.
- 21- S. J. Alvarez-Mendez, A. Urbano-Gálvez, and J. Mahouachi, Mitigation of salt stress damages in *Carica papaya* L. seedlings through exogenous pretreatments of gibberellic acid and proline. *Chilean journal of agricultural research*, 82(1) (2022) 167-176.
- 22- A. K. Atteya, R. S. El-Serafy, K. M. El-Zabalawy, A. Elhakem, and E. A. Genaidy, Exogenously supplemented proline and phenylalanine improve growth, productivity, and oil composition of salted moringa by up-regulating osmoprotectants and stimulating antioxidant machinery. *Plants*, 11(12) (2022) 1553.
- 23- M. R. H. Siddique, S. Saha, S. Salekin, and H. Mahmood, Salinity strongly drives the survival, growth, leaf demography, and nutrient partitioning in seedlings of *Xylocarpus granatum* J. König. *iForest-Biogeosciences and Forestry*, 10(5) (2017) 851-856.
- 24- M. S. Yousaf, I. Ahmad, M. Anwar-ul-Haq, M. T. Siddiqui, T. Khaliq, and G. P. Berlyn, Morphophysiological response and reclamation potential of two agroforestry tree species (*Syzygium cumini* and *Vachellia nilotica*) against salinity. *Pak. J. Agri. Sci*, 57(5) (2020) 1393-1401.
- 25- O. S. Tomar, P. S. Minhas, V. K. Sharma, Y. P. Singh, and R. K. Gupta, Performance of 31 tree species and soil conditions in a plantation established with saline irrigation. *Forest Ecology and Management*, 177(1-3) (2003) 333-346.
- 26- J. Gupta, R. K. Dubey, N. Kaur, and O. P. Choudhary, Physiological response of ornamental tree species to induced salinity. *Indian Journal of Agricultural Sciences*, 87, 5(2017).
- 27- J. Gupta, R. K. Dubey, O. P. Choudhary, and N. Kaur, Effects of salinity on growth and physiology of some sub-tropical ornamental trees in punjab. *Agric Res J* 56 (3) (2019) 480-492.



ARID Journals

ARID International Journal for Science and Technology (AIJST)

ISSN: 2662-009X

Journal home page: <http://arid.my/j/aijst>

ARID

International Journal for Science and Technology

مجلة أريد الدولية للعلوم والتكنولوجيا

VOL.6 NO.11 JUNE 2023

ISSN: 2662-009X

ARID
ARID PUBLICATIONS
ARIDMYJST

مَجَلَّةُ أُرِيدُ الدَّوْلِيَّةُ لِلْعُلُومِ وَالتَّكْنُولُوجِيَا

المجلد 6 ، العدد 11 ، حزيران 2023 م

Passive Cooling Strategies in the Hot-humid Climate: A Review Study

Maryam Qays Oleiwi*

Mohd Khairul Azhar Mat Sulaiman

Mohd Farid Mohamed

Department of Architecture and Built Environment - National University of Malaysia- Selangor-Malaysia

استراتيجيات التبريد السلبي للمباني في المناخ الحار الرطب: دراسة مرجعية

محمد فريد محمد

خيروال الازهر مت سليمان

مريم قيس عليوي *

قسم العمارة والبيئة المبنية - الجامعة الوطنية الماليزية - سلانكور - ماليزيا

mar_mka@yahoo.com*arid.my/0001-1034<https://doi.org/10.36772/arid.aijst.2023.6115>

ARTICLE INFO

Article history:

Received 12/03/2022

Received in revised form 23/02/2023

Accepted 29/04/2023

Available online 15/06/2023

<https://doi.org/10.36772/arid.aijst.2023.6115>

ABSTRACT

Recently, passive cooling strategies have gained more attention as an alternate method of cooling and ventilating indoor areas as part of a push toward more sustainable architecture. Passive cooling relies on free and sustainable energy sources such as the sun and wind to provide the necessary cooling, ventilation, and lighting for buildings to provide a comfortable indoor environment, therefore, the electrical energy that required for mechanical cooling can be reduced. The studies showed that these solutions have the potential to save good amount of building's cooling energy annually -about 23.6%-, depending on building type, construction materials, windows' area and other specifications. In spite of that, the specifications need to be implemented and well-designed in an integrated system. This paper aims to review and discuss the possible passive cooling strategies that can be implemented in the hot-humid climate as a step towards decreasing energy consumption. A review of the literature has been done by searching for the appropriate keywords. It was found that many studies have highlighted the significance of using several types of passive cooling strategies for enhancing thermal comfort inside the buildings in the hot-humid climate, while some other strategies are not recommended. Protecting the buildings from direct solar radiation and applying natural ventilation to the buildings are the most effective passive cooling strategies that can be used in the hot-humid climate. The study recommended to review the appropriateness of several types of passive cooling strategies in different types of climates to highlight the most appropriate passive cooling strategies for each type of climate.

Keywords: Passive cooling, Natural ventilation, Green building, Thermal comfort, Building sustainability.

الملخص

اكتسبت استراتيجيات التبريد السلبي للمباني مزيداً من الاهتمام في العقد الأخير كطريقة بديلة لتبريد وتهوية المناطق الداخلية سعياً للتوجه نحو أبنية أكثر استدامة، حيث يعتمد التبريد السلبي على مصادر الطاقة المجانية والمستدامة مثل الشمس والرياح لتوفير التبريد والتهوية والإضاءة اللازمة للمباني لتوفير بيئة داخلية مريحة، حيث يمكن تقليل الطاقة الكهربائية المطلوبة للتبريد الميكانيكي. وأظهرت الدراسات أن هذه الحلول لديها القدرة على توفير كمية جيدة من طاقة تبريد المبنى سنوياً - حوالي 23.6% - اعتماداً على نوع المبنى ومواد البناء ومساحة النوافذ والمواصفات الأخرى. وعلى الرغم من ذلك، فإن هذه المواصفات تحتاج إلى تنفيذ وتصميم جيد في نظام متكامل. وتهدف هذه الورقة إلى مراجعة ومناقشة استراتيجيات التبريد السلبي التي يمكن تنفيذها في المناخ الحار الرطب كخطوة نحو تقليل استهلاك الطاقة. حيث تم إجراء مراجعة للأدبيات باستخدام الكلمات المفتاحية المناسبة. وقد وُجد أن العديد من الدراسات قد ناقشت أهمية استخدام أنواع عديدة من استراتيجيات التبريد السلبي لتعزيز الراحة الحرارية داخل المباني في المناخ الحار الرطب. وقد تم إجراء هذه الدراسة لتمهيد الطريق لاختيار استراتيجيات التبريد السلبي المناسبة التي يمكن أن توفر الراحة الحرارية وتحقيق أفضل توفير للطاقة في المناخ الحار الرطب.

الكلمات المفتاحية: التبريد السلبي، التهوية الطبيعية، المباني الخضراء، الراحة الحرارية، استدامة المباني.

1. Introduction:

The world's most pressing environmental issues are global warming and ozone depletion, as well as lack of energy supplies [1-4]. The overreliance on fossil fuels have the large portion of global energy demand recently. As a result, energy resources, which are non-renewable, is expected to be drained in the near future. Therefore, non-renewable energy resources are expected to be depleted. Energy consumption is expected to rise in the coming years as a result of population growth and technological advancement [5]. Changing in the climate and growing in the economic will increase the demand on cooling energy in the tropical region (which is described as a hot region all over the year), necessitating immediate adaptation in the construction sector to mitigate the issues posed by future increment in cooling energy demand [6]. High energy consumption will also harm the environment and worsen the effects of climate change. Tropical and semitropical areas use significantly more energy than other regions, primarily to meet cooling needs. However, cooling loads can be reduced by using energy-efficient designs and methods [7-10]. Passive cooling has been introduced as an environmentally friendly energy saver, and its effectiveness and sustainability have been investigated [11].

In contrast to the use of active mechanical equipment for cooling and ventilation, passive cooling is typically considered as a combination of natural techniques and approaches for lowering indoor temperatures. Passive cooling solutions have demonstrated excellent efficiency in buildings and can contribute significantly to reduce building cooling loads. Numerous studies have tested and evaluated effective passive techniques. In addition, Passive cooling has demonstrated good thermal comfort and indoor air quality while using low amount of energy. Buildings that use passive cooling methods have shown a reduction in their cooling load by up to 70% [12]. The term "passive cooling systems" has been defined by Givoni [13] as "various

simple cooling techniques that enable the indoor temperatures of buildings to be lowered through the use of natural energy sources". Moreover, Givoni clarified that using a fan or a pump is not excluded when their application could improve the performance.

The study of Santamouris and Asimakopoulos [12] showed that there are three main categories of passive cooling techniques. The first technique depends on protecting buildings' envelopes from solar radiation and heat gain by using landscaping and vegetation, using outdoor and semi-outdoor spaces, building form, layout and external finishing, colour of buildings' envelop, shading of building surfaces, thermal insulation, windows' size and window to wall ratio, orientation, etc.

The second method that mentioned by Santamouris and Asimakopoulos [12] depends on controlling thermal storage capacity of building structure. This strategy can reduce cooling load peaks and modulates the internal temperature with the heat discharge later. The greater the temperature swings in the outside, the greater the impact of this storage capacity. In order to avoid overheating in the discharge phase, the cycle of heat storage and discharge should be combined with means of heat dissipation, such as night ventilation.

While the third method depends on heat dissipation, which treats with the potential for the disposal of building's excess heat to a lower temperature environmental sink and the establishment of a suitable thermal coupling between the building and the sink as well as an effective temperature variances for the transfer of heat. The potential of heat dissipation techniques are strongly depending on climate conditions. The techniques are known as hybrid cooling if heat transfer is supported by mechanical devices.

Several scholars have outlined various passive cooling strategies in different climate conditions for buildings in order to improve building energy performance. Some of these strategies are old, while others have only been around for a few years. Numerous analyses, simulations, case studies, experimental and modeling investigations have been conducted [14-20].

Other researchers have focused on the possibility of achieving passive cooling strategies in hot-humid climate as options for reducing the energy and environmental impacts of air-conditioning, which is critical in the future [21-24]. The study of Gamero-Salinas et al. [25] underlined the need of passive cooling and overheating prevention design solutions in tropical regions. Al-Tamimi & Fadzil simulation study [26] discussed using shading devices as a solution for minimising solar heat gain through building design in the hot-humid climate of Malaysia. Sulaiman's experimental study [27] examined the use of green façade in Malaysia's hot-humid climate as well. Applying natural ventilation strategies for windows opening have been discussed by other researchers [28, 29]. Using solar chimney in reducing indoor air temperature and increasing air velocity were also discussed by Agung Murti Nugroho [30] which is proved to be effective strategies to increase indoor thermal comfort and minimising energy consumption in the hot-humid climate of Malaysia.

The study of Mirrahimi et al. [31] reviewed the findings of previous studies to determine the proper building envelope parameters for high-rise residential buildings in tropical climate. The study showed that passive cooling strategies are very effective for cooling the buildings in the hot-humid climate. In addition, the study revealed that there is strong effect of different building components, including shading devices, external wall, external roof and external glazing and

insulation, and reducing the energy that used for cooling. Moreover, in order to eliminate the dependency on mechanical systems in the buildings, the study recommended to consider the total thermal performance of all components of building's envelope, such as an optimal window-to-wall ratio, appropriate material for glazed windows, and the appropriate shading equipment. Briefly, the study focused on the effect of building envelop on indoor thermal comfort.

Another study conducted by Bhikhoo, Hashemi, and Cruickshank [32] in the hot-humid climate (Thailand) and used IES-VE (Integrated Environmental Solutions-Virtual Environment) simulation software proved that indoor overheating can be reduced in the tropics if proper building design principles for these climate zones are used. Moreover, the same study revealed that roof material and the presence of balconies were found to have the greatest influence on indoor thermal comfort. On the other hand, the study of Tong et al. [33] that was conducted in the hot-humid climate (Singapore) and used parametric method proved that reducing façade's window-to-wall ratio have a good impact on deceasing indoor air temperature.

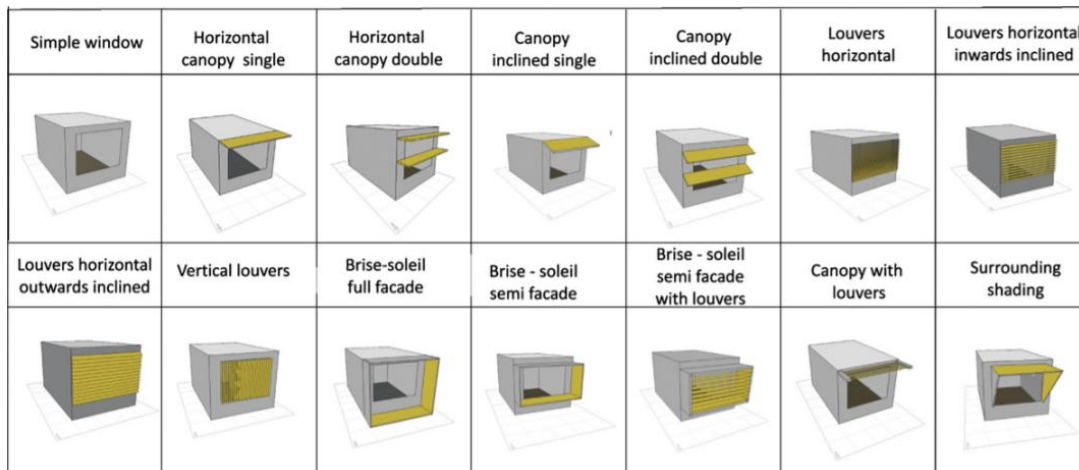
2. Methodology

This study has been conducted to give a sufficient review of the possible passive cooling strategies that can be used in the hot-humid climate to reduce the load on mechanical means and reduce energy consumption, based on the categories of passive cooling strategies that mentioned in the study of Santamouris and Asimakopoulos [12]. The three categories and their passive cooling strategies can be explained as follows:

2.1 The first strategy that depends on protecting buildings' envelops from solar radiation. The following strategies can be used for this purpose.

a- Shading devices: Normal and louvered shading devices can be placed on buildings' façades and can be designed in variety of shapes and sizes in order to block direct solar radiation while allowing wind to pass through the windows and cool the interior environment. They can be positioned horizontally and vertically, or can be louvered which can be adjusted and rotated to provide the optimum results [34]. Figure (1) shows different designs of shading devices.

Another study [35] proved that -in the tropical climate- protecting the windows from solar radiation by adding shading devices and closing the curtains resulted in the lowest indoor operative temperature compared to other investigated strategies that were examined in the study.



Figure(1): Different designs of shading devices.

Source: [36]

b. Double glazing: Windows are the main element of exchanging large amounts of heat between building's structure and outside environment. However, when compared to single-glazed windows, double glazing has been shown to be effective at reducing heat transfer. The distance between the two glass panels determines how well windows are insulated. The cavity between the two glass panels can be vacuumed or filled with gas [34, 37]. Figure (2) shows the double glazed windows.

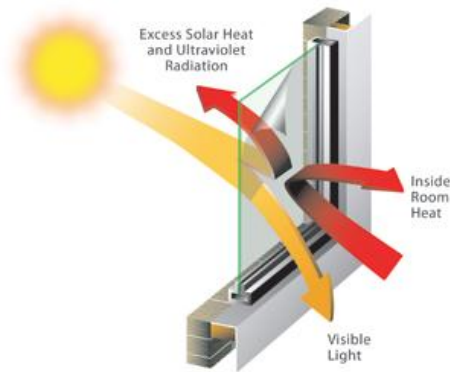


Figure(2): Double glazed windows
Source: [37]

c. Solar reflective film for windows: Solar control film comes in a variety of grades and types, each with a particular amount of performance. Each film is created with the goal of reducing heat transfer by reflecting a portion of the sun's solar radiation. The film can assist to reduce the inside temperature from rising to uncomfortable levels by efficiently rejecting a percentage of the heat that comes from solar radiation [38].

The numerical study of Xamán et al. [38] that was conducted in the hot-humid summer in Mexico revealed that employing solar control film in a double glazed window in hot- humid climates might lower energy consumption within the building by approximately 52% when compared to a regular double glazed window. Moreover, the simulation study of Al-Tamimi and Qahtan [39] that was conducted in the hot-humid climate (Malaysia) recommended the

use of reflective single or double glass can decrease indoor air temperature throughout the day. Figure (3) shows how solar reflective film works.



Figure(3): Solar reflective film for windows.

Source: [40]

d. Using light colours in coatings with high reflection: Exterior walls are exposed to solar radiation, and can transfer a significant amount of heat to a building; as a result, the temperature of interior environment and the level of comfort can be affected [41]. Solar reflective coating can be used to minimise heat transmission and lower the temperature of the interior space. However, the colour of coating depends on the climate and the type of material utilised. Considering these parameters can lead to energy being saved, especially during the peak time. When bright colour of the exterior walls are compared to dark colour, there is a significant difference, demonstrating the importance of solar reflectance of building envelop [29].

Taleb [34] used three different types of coatings to determine the impact of each type on energy consumption. The first type was standard coating, whereas the second and third had a higher rate of reflection. These various types of coatings were applied to three different walls in order to determine the surface and indoor temperatures, as well as their impact on energy efficiency. The reflection levels for each coating were 32%, 42% and 61% respectively. The study concluded

that coating the building with highly reflective coatings can limit heat transfer from the exterior walls to the interior space. This had an effect on the building temperature and as a result, increased thermal comfort inside the building. In addition, using a paint with a 61% reflection of the spectrum had a beneficial effect on energy saving. On the other hand, a recent experimental study conducted by Wang et al. [42] in the hot climate of China proved that using retro-reflective (RR) coatings can give better cooling potential than the Highly-reflective (HR) coatings in the high-density areas.

e. Green roofs and walls: Buildings' roofs are the most elements that exposed to solar radiation, thus, protecting roofs from solar radiation is necessary to avoid indoor overheating. Cooling is a crucial demand of buildings, particularly in the hot-humid climate [43]. Therefore, green roofs have been introduced by the researchers as a sustainable passive cooling strategy. According to Jaffal et al. [44] green roof can be defined as a "building roof covered by grasses or plants which lie over a waterproof membrane". A review of the literature indicated that green roofs are the most effective way to insulate roofs. As mentioned previously, the roof is one of the main surfaces of the building that exposed to high solar heat, so employing a high amount of insulation can help to limit heat transmission to the inside. Besides, there are other significant sustainable advantages that green roofs can provide such as providing oxygen to the environment, reducing the urban heat island effect, and lowering air temperature [34, 45].

Green walls, on the other hand, have recently become a topic of discussion. Green walls can be classified into different types based on the local environment, plant species, and the type of the building itself [46]. Sulaiman [27] discussed in details several types of plants and the shading that each type can provide to achieve the best air temperature reduction inside buildings in the hot-humid climate of Malaysia.

f. Orientation: Studies concluded that in the tropical hot-humid climate, façades that facing the north and south is preferable over façades facing east and west. Therefore, it is recommended to provide the north and south sides of the buildings with large openings for cross ventilation, while protecting the east and west external walls with appropriate building construction materials to avoid high solar heat gains [47]. Additionally, when combining Polymer Dispersed Liquid Crystal (PDLC) glazing with southern and the northern windows' orientation for the tropical climate of Singapore, energy consumption was the less as solar radiation was less in these two orientations [48]. However, the study of Dutta et al. [49] that was conducted in India found that in a tropical climate of the northern hemisphere, heat gain through south-facing windows is the greatest, followed by east, west, and north-facing windows. The differences in the results of these studies could be attributable to different locations where the studies have been conducted (Singapore and India).

g. Insulation and using proper construction materials: To limit heat loss or gain throughout buildings' envelopes, passive design should include insulation. Insulation functions as a thermal barrier, preventing heat gain from the outside. As a result, insulation is used in the walls, ceilings, and floors, and it comes in a variety of forms [50].

According to Mirrahimi et al. [31], applying appropriate thermal insulation in building envelope is the one of most effective method to reduce heat transmission through the envelop and reduce energy consumption of internal cooling and heating.

Understanding the environmental influence on buildings and the thermal comfort of their occupants is necessary for designing passive energy solutions. In hot-humid climates, building materials absorb heat for the majority of the day [51]. Construction materials play significant role in achieving thermal comfort [52, 53]. The indoor thermal environment is greatly influenced

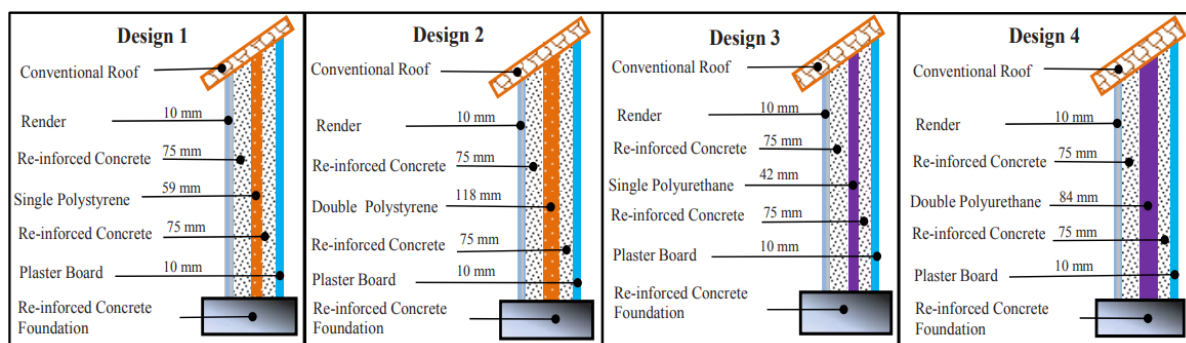
by the local climate. As building envelope separates the inside space from the outer environment and limits the amount of heat flow through itself, selecting the appropriate building envelope material that appropriate for the outdoor climate is highly effective parameter that impacts the indoor environment [54-56].

Furthermore, building's characteristics influence the effect of the outer environment and play an important part in determining the indoor thermal conditions. The influence of local climate on indoor thermal comfort, according to Raja et al. [57], manifests in heat transmission from the outer environment through building materials, where building envelope adjusts heat transmission based on its thermal mass and insulation.

Aldawi et al. [55] found that the new design wall systems -which used different construction materials- required less cooling and heating energy for 9 cities in Australia -including the cities that located in the hot- humid climate- when compared to the old traditional building method of brick veneer and weatherboard houses. Figure (4) shows the traditional building methods in Australia. Figure (5) shows the new design wall systems that suggested by the mentioned study.



Figure(4): Brick veneer and weather board walls in Australia (Traditional method).
Source: [55]



Figure(5): New house wall designs with different insulation materials and thickness.
Source: [55]

In comparison to polystyrene insulation material, the same study [55] found that polyurethane insulation material saves much more energy (almost 40%). However, doubling the thickness of both materials reduces energy use by 5 to 10%. Based on these results, economic analysis and life cycle evaluation should be conducted to determine which of these two materials is better to be used as thermal insulation.

The experimental study of Kolokotroni et al. [54] that was conducted in the tropical climate [Jamaica, Northeast Brazil and Ghana] mentioned that the thermal characteristics of materials used for external walls and roofing can have a substantial impact on the surface temperature as well as the amount of heat transferred across building surface.

The effect of building materials in enhancing thermal comfort in hot-humid conditions has been extensively discussed in a review study by Latha et al. [58]. The study focused on the use of certain materials in building's envelope to improve thermal comfort, such as vacuum insulation panels (VIPs), phase change materials (PCMs), autoclaved cellular concrete (ACC), and polymer skin. Light-coloured external surfaces, reflecting paints, window

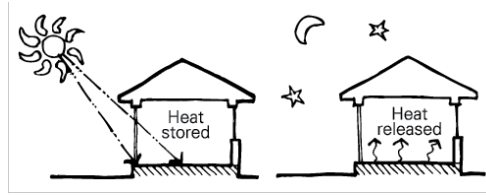
treatments, and roof gardens are also mentioned in the same study as popular methods for reducing buildings' heat load.

From the previous literatures, it can be conclude that protecting the buildings from solar radiation and using appropriate insulation and building materials in the countries that have high solar radiation is effective to reduce indoor temperature and cooling loads.

2.2 The second strategy is contingent upon controlling thermal storage capacity of building structure which can be achieved through using high thermal storage materials (or thermal mass). As mentioned previously, this strategy depends on reducing cooling load peaks while modulating the internal temperature with the heat discharge later by combining it with another cooling method during the discharge phase to avoid overheating inside the buildings. Brick, concrete and tiles as high thermal mass materials, act as a storage for heat as they heat up and cool down relatively slowly [12].

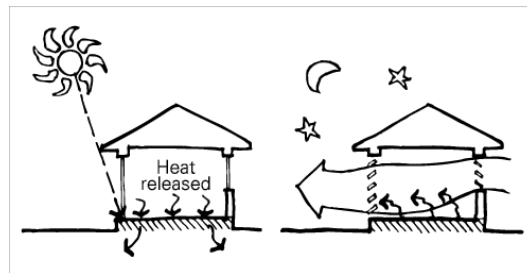
Thermal mass can be defined as “the ability of a material to absorb, store and release heat energy”. Thermal mass absorbs thermal energy when the environment is hotter than the mass and gives it back when the environment is cooler, but it never reaches thermal equilibrium [59].

In winter, thermal mass can absorb heat from direct sunlight or radiant heaters during the day. The warmth is then re-radiated into the residence throughout the night. Figure (6) shows thermal mass performance in winter.



Figure(6): Thermal mass performance in winter.
Source: [60]

The same performance in summer, however, allowing cool night breezes and/or convection currents to pass over the thermal mass through natural ventilation, removing out all the stored heat. During the day, using shading and insulation to shield the thermal mass from the hot solar radiation is preferable. Figure (7) shows thermal mass performance in summer.



Figure(7): Thermal mass performance in summer.
Source: [60]

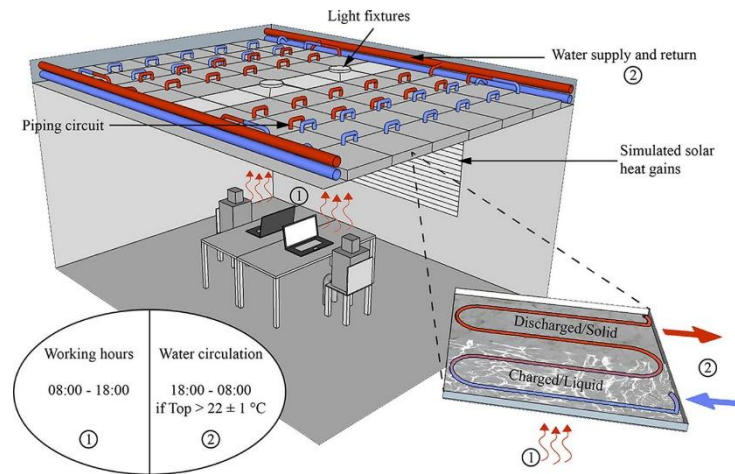
Sharaf [61] found that in a semi-arid hot climate, high thermal mass construction materials such as clay-bricks help to keep the indoor environment within the human thermal comfort zone. As a result, the amount of energy required to maintain the room's thermal comfort is considerably lowered.

The usage of thermal mass was investigated in both temperate and tropical regions by Juarez [50]. The study discussed that thermal mass was effective in temperate climates. In a tropical climate, however, light weight design with minimal thermal mass is preferred. Thermal mass is

beneficial if the building's free running temperature response is considered in the comfort limits; otherwise, it increases energy demand. Therefore, it can be conclude that this type of passive cooling strategy is not effective in tropical climate.

2.3 The third method is based on heat dissipation by transferring excess heat from a building to a lower-temperature environmental sink, and it is significantly influenced by environmental factors. If heat transfer is aided by mechanical devices, the process is known as hybrid cooling. The most applicable techniques for heat dissipation include ventilation cooling and radiative cooling [12].

a. Radiant cooling: Radiant cooling is a method of cooling a floor or ceiling by absorbing the heat emitted from the rest of the space. Radiant floor cooling refers to the cooling of the floor; radiant ceiling cooling refers to the cooling of the ceiling in homes with radiant panels and pipes. The majority of radiant cooling residential applications use aluminium panels hanging from the ceiling to circulate chilled water. The panels must be kept at a temperature extremely close to the dew point within the house to be functional, and the house must be kept dehumidified. Simply opening a door in a humid climate may bring enough humidity into the residence to cause condensation [62]. Figure (8) shows radiant ceiling cooling.



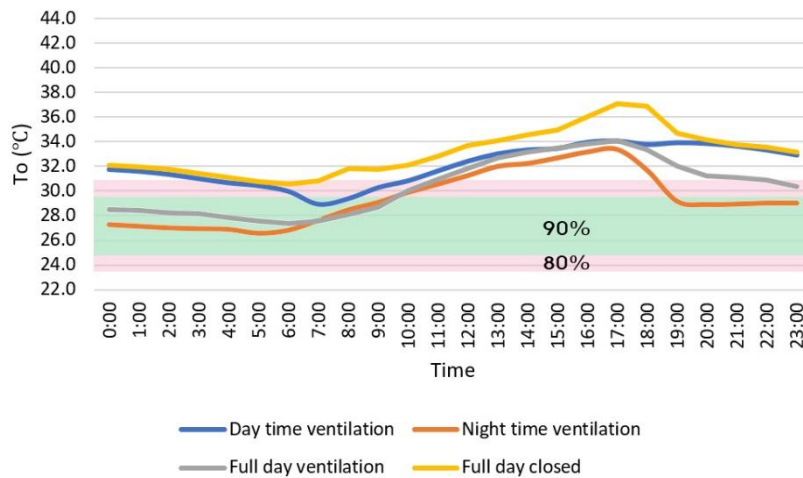
Figure(8): Radiant ceiling cooling.

Source: [63]

b. Natural ventilation: Several studies mentioned that one of the most common and effective strategies for thermal comfort in tropical climate is the use of natural ventilation [22, 25, 29, 30, 39, 47, 51, 53, 64-69]. Doors, blinds and curtains, fans, central cooling, and air blowers are the most common controls available for the occupants in natural-ventilated structures; nonetheless, windows are the most significant controls of the indoor environment [57]. If the occupants are dissatisfied with the thermal environment, they will seek to reclaim their comfort. Usually, they use building controls to increase their comfort in different ways. In every building, the first action that occupants normally do to correct their comfort is opening the windows, particularly when the outdoor temperature is acceptable [70]. It is not only valuable for lowering energy usage during the hot season, but also provides an efficient interaction between the indoor and outdoor environments [71].

In addition, Jamaludin et al. [53] examined natural ventilation technique in low-rise multi-residential building in Malaysia and found that night-time ventilation was the best method, followed by daytime ventilation, full-day ventilation, and no ventilation. This result was

supported by another study which examined different types of ventilation to find the best ventilation that can achieve thermal comfort in the hot-humid climate of Malaysia. The results showed that applying night ventilation by opening the windows and the internal doors during the night -to permit the cool nocturnal air to inter the building- and closing them during the daytime -to prevent the hot diurnal from interrering the building- can eliminate the diurnal indoor air temperature and keep the indoor space within the comfortable temperature [68]. Figure (9) shows the effect of nigh ventilation on indoor operative temperature.



Figure(9): The effect of nigh ventilation on indoor operative temperature.
Source: [68]

Another study conducted by Daghih et al. [69] concluded that the office that have a combination of windows-door opening performed better in terms of air exchange rate, age of the air and air efficiency than the opening the windows and closing the doors of the office.

From the previous studies, it can be concluded that radiant cooling is possibly effective in arid settings, while it is problematic in the hot-humid climes. Additionally, applying natural ventilation is very effective to improve indoor thermal comfort in the hot-humid climate.

c. Combination of different strategies: Some studies combined various passive cooling strategies to identify the most effective solution for achieving interior thermal comfort. The green roof area in Taleb's study [34] was roughly 220 m². Sprinklers were added to the green roof to enable evaporative cooling to ensure that the temperature of the roof remained cool even in the peak hours. The study proved that about 23.6% of the annual building's energy consumption was reduced when passive cooling strategies was used.

Furthermore, the use of natural ventilation for achieving indoor thermal comfort in Singaporean residential buildings has been examined by Liping and Hien [47]. The study found that by combining natural ventilation with intelligent facades [appropriate façade designs with efficient construction materials and shading devices] in residential buildings, thermal comfort can be improved while also conserving energy and ensuring sustainability. The predicted annual energy savings percentages were 73-77%, which is within the acceptable thermal comfort zone of 80% that is suggested by ASHRAE Standard 55. During the hours outside comfort zone, the study suggested using mechanical fan if needed to improve thermal comfort.

The study of Del Rio et al. [66] have employed a variety of different sorts of passive cooling approaches to improve the internal thermal comfort of a residential building in Japan during the hot-humid summer season. The approaches utilised in the study included an evaporative cooling louvre that was developed previously by Hirayama et al. [72] and reducing solar radiation by utilising vegetation and sunscreen to create a semi-outdoor space outside two windows of the house. The ideal ventilation settings to induce the cool air through the windows were then assessed. Figure [10] shows the evaporative cooling louvers that used in

Del Rio et al. [66] study. Table (1) summarised the studies that was conducted in the hot-humid climate and their conclusions.



Figure(10): Evaporative cooling louver

Source: [66]

Table(1): The studies that was conducted in the hot-humid climate and their conclusions.

Study	Climate	Methodology of the study	Conclusion
Mirrahimi et al. 2016 [31]	Tropical climate (Malaysia)	Review study	There is strong effect of different building components and reducing the energy that used for cooling
Bhikhoo et al., 2017 [32]	Tropical climate (Thailand)	Simulation study	Indoor overheating can be reduced when proper building design principles are used (roof materials and presence of balcony)
Husen and Mohamed, 2021 [21]	Tropical climate (Malaysia)	Review study and site observations	
Yusoff, 2020 [22]	Tropical climate (Malaysia)	Field measurement and numerical simulation.	Providing a confined area at the inlet may enhance indoor air velocity (the Venturi effect), thus enhancing the natural cross-ventilation in low-rise buildings located at the area where the wind speed is low.
Oleiwi & Mohamed, 2021 [23]	Tropical climate (Malaysia)	Simulation study	Protecting the building envelope by extending the overhang by 50% of its length enhanced indoor thermal

			comfort compared to other selected strategies.
Mohamed, 2020 [24]	Tropical climate (Malaysia)	Literature review and site observation	In traditional Malaysian mosques and Malay houses, there are at least 26 sustainable approaches which can be used as a starting point or guideline when designing new modern buildings in Malaysia, particularly those with passive design strategies.
Gamero-Salinas et al., 2021 [25]	Tropical climate (Tegucigalpa and San Pedro Sula in Honduras)	Simulation study	Natural ventilation, wall absorptance, the solar heat gain coefficient, and semi-outdoor spaces had the ultimate impact on overheating reduction
Al-Tamimi & Fadzil, 2011 [26]	Tropical climate (Malaysia)	Simulation study	Shading devices to minimise solar heat gain through building design.
Sulaiman, 2017 [27]	Tropical climate (Malaysia)	Experimental study	Using green façades can decrease air temperature inside the buildings.
Dahlan, 2011 [28]	Tropical climate (Malaysia)	Field measurement	The occupants perceived the thermal conditions in rooms that were shaded with a projected balcony (shading ratio of 0.9), a long roof overhang (shading ratio of 1.6) and an operable window-to-wall ratio of 0.3 to be thermally comfortable.
Nguyen, 2012 [29]	Tropical climate (Vietnam)	Simulation study	Natural ventilation strategies for windows opening is very effective cooling strategy. - Using bright colour for the exterior building envelope can improve indoor thermal comfort
Agung Murti Nugroho, 2007 [30]	Tropical climate (Malaysia)	Field measurement and CFD (Computational fluid dynamics) simulation software	Solar chimney can increase indoor thermal comfort and minimise energy consumption in single store terraced houses, while natural ventilation was not effective for this type of housing.
Tong et al., 2021 [33]	Tropical climate (Singapore)	Parametric study	Reducing façade's window-to-wall ratio also proved to have a

			good impact on decreasing indoor air temperature
Taleb, 2014 [34]	Dubai (hot-humid summer)	Simulation study	Energy saving can be achieved by using passive cooling strategies namely shading devices, double glazing, green roofs and using insulation.
Oleiwi & Mohamed, 2022 [35]	Tropical climate (Malaysia)	Simulation study	Protecting the windows from solar radiation by adding shading devices and closing the curtains resulted in good temperature reduction.
Lohia & Dixit, 2015 [37]	Scorching summers (India)	Field measurement	Double glazing is effective at reducing heat transmission inside buildings
Xamán et al., 2014 [38]	Hot- humid summer (Mexico)	Numerical study	Solar control film in a double glazed window can lower energy consumption
Al-Tamimi and Qahtan, 2016 [39]	Tropical climate (Malaysia)	Simulation study	Reflective double glazing can reduce indoor air temperature throughout the day, regardless of ventilation, with an optimal improvement of up to 107% and 14% in unventilated and ventilated rooms, respectively, when compared to single clear glazing.
Shen et al., 2011 [41]	Hot climate (China)	Experimental study	depending on location, season, and orientation, different coatings can reduce exterior and interior surface temperatures, and as a result, can reduce indoor mean radiant temperatures and energy consumption.
Wang et al., 2022 [42]	Hot climate (China)	Experimental study	Using Retro-reflective coatings can give better cooling potential than the Highly-reflective coatings in the high-density areas.
Cheikh and Bouchair, 2008 [43]	Hot climate (Algeria)	Experimental study	protecting roofs from solar radiation is necessary to avoid indoor overheating
Jaffal et al., 2012 [44]	Hot Summer (France)	Simulation study	With the addition of a green roof, the summer indoor air temperature was reduced by 2

			degrees Celsius, and the annual energy demand was reduced by 6%.
Dutta et al., 2017 [49]	Tropical climate (India)	Simulation study	In a tropical climate of the northern hemisphere, heat gain through south-facing windows is the greatest, followed by east, west, and north-facing windows
Mathew et al., 2022 [48]	Tropical climate (India)	Experimental study	Combining Polymer Dispersed Liquid Crystal (PDLC) glazing with southern and the northern windows' orientation for the tropical climate, energy consumption was the less
Sadafi et al., 2012 [51]	Tropical climate (Malaysia)	Case study	<ul style="list-style-type: none"> - Natural ventilation has achieved indoor thermal comfort for about 15 hours during the day for a terrace house. - Increasing air velocity by adding ceiling fan and reducing the absorption of radiant heat by adding shading devices can improve thermal comfort.
Kolokotroni et al., 2018 [54]	Tropical climate (Jamaica, Northeast Brazil and Ghana)	Experimental study	The usage of cool materials is most efficient in places with strong sun radiation and outside high air temperature.
Aldawi et al., 2013 [55]	Tropical climate (Australia)	Case study	Suggested new design wall systems that can increase indoor thermal comfort.
Latha et al., 2013 [58]	Tropical climate	Review study	using certain materials in the building envelope can improve thermal comfort, such as vacuum insulation panels (VIPs), phase change materials (PCMs), autoclaved cellular concrete (ACC), polymer skin, light-coloured external surfaces, reflecting paints, window treatments, and roof gardens.
Juarez, 2014 [50]	Tropical climate & Temperate climate	Simulation study	Thermal mass is effective in temperate climates, however, in a tropical climate, light weight design with minimal thermal mass is preferred.

Del Rio et al., 2019 [66]	Tropical climate (Japan)	Field measurement	Indoor cross ventilation can improve the internal thermal comfort.
Al-Tamimi, 2015 [67]	Tropical climate (Malaysia)	Field measurement	Natural ventilation can improves indoor environmental performance by 80% and 50% during the day and night, respectively.
Oleiwi, 2020 [68]	Tropical climate (Malaysia)	Simulation study	Applying night ventilation can keep the indoor space within the comfortable temperature
Daghih et al., 2012 [69]	Tropical climate (Malaysia)	Field measurement	The office that have a combination of windows-door opening performed better in terms of air exchange rate, age of the air and air efficiency than the opening closed office
Jamaludin et al., 2014 [53]	Tropical climate (Malaysia)	Field measurement	Night ventilation is the best method, followed by daytime ventilation, and then, full-day ventilation.
Liping and Hien, 2007 [47]	Tropical climate (Singapore)	Model	Combining natural ventilation with intelligent facades can improve thermal comfort can and reduce energy consumption.

3. Conclusion

As a part of the movement toward green sustainable building, passive cooling solutions have earned high attention as an alternative method of cooling and ventilating indoor spaces. This paper reviewed different types of passive cooling solutions that can be adopted in the hot-humid climates as means of preventing overheating, decreasing indoor temperature and reducing energy usage by dividing them into three main categories. The first category depends on protecting the building from solar radiation such as using shading devices. The second category of passive cooling depends on controlling thermal storage capacity of building structure such as using high thermal mass materials. The third category depends on heat dissipation such as applying natural ventilation and using radiative cooling.

Many researches have been conducted to emphasise the importance of employing passive cooling solutions to improve thermal comfort inside buildings. This research leads the way for choosing the optimum passive cooling approaches for achieving indoor thermal comfort and energy savings in hot and humid climate. The study concluded that protecting the buildings from direct solar radiation, such as using shading devices, doubling the glazing and applying solar reflective film for the windows, closing the curtains, coating the building with light colour and high reflective materials, using different types of vegetation, installing the appropriate sort of insulation, selecting the best orientation for the building and its openings and using proper construction materials are effective in the hot-humid climate. In addition, applying natural night ventilation by opening the windows during the night was proved as an effective strategy in this climate region. However, using high thermal mass or radiant cooling is not recommended for the hot-humid climate. The study emphasised the need of considering the appropriate passive cooling strategies for the hot- humid climate to reduce energy consumption in this region. It is recommended to study other types of passive cooling strategies in different types of climates to highlight the most preferable passive cooling strategies for each type of climate.

List of abbreviations.

List of abbreviations	
ACC	Autoclaved Cellular Concrete
CFD	Computational Fluid Dynamics
ASHRAE	American Society of Heating, Refrigerating and Air Conditioning Engineers
HR	Highly-reflective
IES-VE	Integrated Environmental Solutions-Virtual Environment
PCMs	Phase Change Materials
PDLC	Polymer Dispersed Liquid Crystal
RR	Retro-Reflective
VIPs	Vacuum Insulation Panels

References

1. M.A. Mujeebu, O.S. Alshamrani, "Prospects of energy conservation and management in buildings–The Saudi Arabian scenario versus global trends", *Renewable and Sustainable Energy Reviews*, 58 [2016] 1647-1663.
2. M. Shafique, R. Kim, "Application of green blue roof to mitigate heat island phenomena and resilient to climate change in urban areas: A case study from Seoul, Korea", *Journal of Water and Land Development*, 33 [2017] 165.
3. H.M. Imran, J. Kala, A. Ng, S. Muthukumaran, "Effectiveness of green and cool roofs in mitigating urban heat island effects during a heatwave event in the city of Melbourne in southeast Australia", *Journal of Cleaner Production*, 197 [2018] 393-405.
4. SEforALL, "Chilling Prospects: Tracking Sustainable Cooling for All" Vienna, [2020].
5. P. Lotfabadi, "Analyzing passive solar strategies in the case of high-rise building", *Renewable and Sustainable Energy Reviews*, 52 [2015] 1340-1353.
6. M. Santamouris, "Cooling the buildings – past, present and future", *Energy and Buildings*, 128 [2016] 617-638.
7. F. Frontini, M. Manfren, L.C. Tagliabue, "A case study of solar technologies adoption: criteria for BIPV integration in sensitive built environment", *Energy Procedia*, 30 [2012] 1006-1015.
8. M. Yeganeh, "Conceptual and theoretical model of integrity between buildings and city", *Sustainable Cities and Society*, 59 [2020] 102-205.
9. M. Norouzi, M. Yeganeh, T. Yusaf, "Landscape framework for the exploitation of renewable energy resources and potentials in urban scale [case study: Iran]", *Renewable Energy*, 163 [2021] 300-319.
10. M. Yeganeh, M. Kamalizadeh, "Territorial behaviors and integration between buildings and city in urban public spaces of Iran' s metropolises" *Frontiers of Architectural Research*, 7 [2018] 588-599.
11. N. Kannan, D. Vakeesan, "Solar energy for future world: A review" *Renewable and Sustainable Energy Reviews*, 62 [2016] 1092-1105.
12. M. Santamouris, D. Asimakopoulos, "Passive cooling of buildings", *Earthscan*, [1996].
13. B. Givoni, "Passive low energy cooling of buildings", *John Wiley & Sons*, [1994].
14. B. Ashraf, M.A. Radwan, M. Sadek, H.A. Elazab, "Preparation and characterization of decorative and heat insulating floor tiles for buildings roofs", *International Journal of Engineering & Technology*, 7 [2018] 1295-1298.
15. A.L. Pisello, "State of the art on the development of cool coatings for buildings and cities", *Solar Energy*, 144 [2017] 660-680.
16. S. Jeong, D. Millstein, R. Levinson, "Modeling potential air temperature reductions yielded by cool roofs and urban irrigation in the Kansas City Metropolitan Area", *Urban Climate*, 37 [2021] 100833.
17. H.L. Macintyre, C. Heaviside, X. Cai, R. Phalkey, "Comparing temperature-related mortality impacts of cool roofs in winter and summer in a highly urbanized European region for present and future climate", *Environment International*, 154 [2021] 106606.
18. J. Testa, M. Krarti, "A review of benefits and limitations of static and switchable cool roof systems", *Renewable and Sustainable Energy Reviews*, 77 [2017] 451-60.
19. J. Hu, X.B. Yu, "Adaptive thermochromic roof system: Assessment of performance under different climates", *Energy and Buildings*, 2019;192:1-14.

20. M. Rawat, R. Singh, "A study on the comparative review of cool roof thermal performance in various regions", *Energy and Built Environment*, [2021] 327-347.
21. N.A. Husen, M.F. Mohamed, "Comparison of Green Design Strategies in Five Traditional Malay Houses", *Jurnal Kejuruteraan*, 33 [2021] 47-53.
22. W.F.M. Yusoff, "The effects of various opening sizes and configurations to air flow dispersion and velocity in cross-ventilated building", *Jurnal Teknologi*, 82 [2020] 17-28.
23. M.Q. Oleiwi, M.F. Mohamed, "An Investigation on Indoor Temperature of Modern Double Storey House with Adapted Common Passive Design Strategies of Malay Traditional House", *Pertanika Journal of Science and Technology*, 29 [2021] 1135 - 1157.
24. M.F. Mohamed, "Sustainable Design Approaches in Malaysia's Traditional Mosques and Houses", *InProceeding International Conference on Engineering*, 1[2020] 13-21.
25. J. Gamero-Salinas, A. Monge-Barrio, N. Kishnani, J. López-Fidalgo, A. Sánchez-Ostiz, "Passive cooling design strategies as adaptation measures for lowering the indoor overheating risk in tropical climates", *Energy and Buildings*, 252 [2021] 111417.
26. N.A. Al-Tamimi, S.F.S. Fadzil, "The potential of shading devices for temperature reduction in high-rise residential buildings in the tropics", *Procedia Engineering*, 21 [2011] 273-282.
27. M.K.A.M. Sulaiman, "Cooling effect performance of indirect green facade on building in tropical climate of Malaysia", [Doctor of philosophy], *Universiti Kebangsaan Malaysia [UKM]*, [2017].
28. N.D. Dahlan, P. Jones, D.K. Alexander, "Operative temperature and thermal sensation assessments in non-air-conditioned multi-storey hostels in Malaysia", *Building and Environment*, 46 [2011] 457-67.
29. A.T. Nguyen, S. Reiter, "An investigation on thermal performance of a low cost apartment in hot humid climate of Danang", *Energy and Buildings*, 47 [2012] 237-46.
30. A.M. Nugroho, M.H. Ahmad, D.R. Ossen, "A preliminary study of thermal comfort in Malaysia's single storey terraced houses", *Journal of Asian Architecture and Building Engineering*, 6 [2007] 175-182.
31. S. Mirrahimi, M. F. Mohamed, L. C. Haw, N. L. N. Ibrahim, W. F. M. Yusoff, A. Aflaki, "The effect of building envelope on the thermal comfort and energy saving for high-rise buildings in hot-humid climate", *Renewable and Sustainable Energy Reviews*, 53 [2016] 1508-1519.
32. N. Bhikhoo, A. Hashemi, H. Cruickshank, "Improving thermal comfort of low-income housing in Thailand through passive design strategies", *Sustainability*, 9 [2017] 1440.
33. S. Tong, J. Wen, N.H. Wong, E. Tan, "Impact of façade design on indoor air temperatures and cooling loads in residential buildings in the tropical climate", *Energy and Buildings*, 243 [2021] 110972.
34. H.M. Taleb, "Using passive cooling strategies to improve thermal performance and reduce energy consumption of residential buildings in UAE buildings", *Frontiers of Architectural Research*, 3 [2014] 154-165.
35. M.Q. Oleiwi, M.F. Mohamed, "The Impacts of Passive Design Strategies on Building Indoor Temperature in Tropical Climate", *Pertanika Journal of Science and Technology*, 31 [2022] 83 - 108.
36. M. Mandalaki, K. Zervas, T. Tsoutsos, A. Vazakas, "Assessment of fixed shading devices with integrated PV for efficient energy use", *Solar Energy*, 86 [2012] 2561-2575.

37. S. Lohia, S. Dixit, "Energy Conservation using Window Glazing in India", *Energy Conservation*, 4 [2015] 8645-8654.
38. J. Xamán, C. Pérez-Nucamendi, J. Arce, J. Hinojosa, G. Álvarez, I. Zavala-Guillén, "Thermal analysis for a double pane window with a solar control film for using in cold and warm climates", *Energy and Buildings*, 76 [2014] 429-439.
39. N. Al-Tamimi, A. Qahtan, "Influence of glazing types on the indoor thermal performance of tropical high-rise residential buildings", *Key Engineering Materials, Trans Tech Publications Ltd.*, 692 [2016] 27-37.
40. Tintgard, "Windows film and solar protection", [2021], [Available from: <https://www.tintgard.ca/solar-film-residential/>]. Accessed on 12 August 2022.
41. H. Shen, H. Tan, A. Tzempelikos, "The effect of reflective coatings on building surface temperatures, indoor environment and energy consumption—An experimental study", *Energy and Buildings*, 43 [2011] 573-580.
42. J. Wang, S. Liu, Z. Liu, X. Meng, C. Xu, W. Gao, "An experimental comparison on regional thermal environment of the high-density enclosed building groups with retro-reflective and high-reflective coatings", *Energy and Buildings*, 259 [2022] 111864.
43. H.B. Cheikh, A. Bouchair, "Experimental studies of a passive cooling roof in hot arid areas", *The Open Fuels & Energy Science Journal*, 1 [2008] 1-6.
44. I. Jaffal, S.E. Ouldboukhitine, R. Belarbi, "A comprehensive study of the impact of green roofs on building energy performance", *Renewable Energy*, 43 [2012] 157-164.
45. S. Pradhan, S.G. Al-Ghamdi, H.R. Mackey, "Greywater recycling in buildings using living walls and green roofs: a review of the applicability and challenges", *Science of The Total Environment*, 652 [2019] 330-344.
46. I. Teotónio, C.M. Silva, C.O. Cruz, "Economics of green roofs and green walls: A literature review", *Sustainable Cities and Society*, 69 [2021] 102781.
47. W. Liping, W.N. Hien, "Applying natural ventilation for thermal comfort in residential buildings in Singapore", *Architectural Science Review*, 50 [2007] 224-233.
48. V. Mathew, C.P. Kurian, N. Augustine, "Spectral, visual, thermal, energy and circadian assessment of PDLC glazing in warm and humid climate", *Solar Energy*, 241 [2022] 576-583.
49. A. Dutta, A. Samanta, S. Neogi, "Influence of orientation and the impact of external window shading on building thermal performance in tropical climate", *Energy and Buildings*, 139 [2017] 680-689.
50. C.E. Mora Juarez, "Impact of Thermal Mass on Energy and Comfort-A parametric study in a temperate and a tropical climate", *Chalmers University of Technology, Göteborg, Sweden*, [2014].
51. N. Sadafi, E. Salleh, L.C. Haw, M.F.Z. Jaafar, "Potential design parameters for enhancing thermal comfort in tropical Terrace House: A case study in Kuala Lumpur", *ALAM CIPTA Journal*, 3 [2012] 15-24.
52. S. Ahmad, "Thermal comfort and building performance of naturally ventilated apartment building in the Kelang valley: A simulation study", *Proceedings of the Energy in buildings [sustainable symbiosis] Seminar*, [2005] 115-132.
53. A.A. Jamaludin, H. Hussein, A.R.M. Ariffin, N. Keumala, "A study on different natural ventilation approaches at a residential college building with the internal courtyard arrangement", *Energy and Buildings*, 72 [2014] 340-352.
54. M. Kolokotroni, E. Shittu, T. Santos, L. Ramowski, A. Mollard, K. Rowe, E. Wilson, J. P.B. Filho, D. Novieto, "Cool roofs: High tech low cost solution for energy efficiency and

thermal comfort in low rise low income houses in high solar radiation countries”, *Energy and Buildings*, 176 [2018] 58-70.

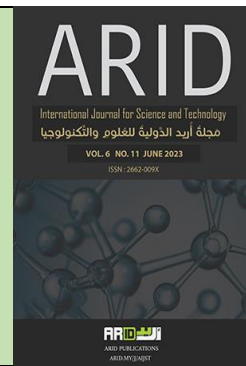
55. F. Aldawi, F. Alam, I. Khan, M. Alghamdi, “Effect of climates and building materials on house wall thermal performance”, *Procedia Engineering*, 56 [2013] 661-666.
56. F. Aldawi, F. Alam, A. Date, A. Kumar, M. Rasul, “Thermal performance modelling of residential house wall systems”, *Procedia engineering*, 49 [2012] 161-168.
57. I.A. Raja, J.F. Nicol, K.J. McCartney, M.A. Humphreys, “Thermal comfort: use of controls in naturally ventilated buildings”, *Energy and Buildings*, 33 [2001] 235-244.
58. P. Latha, Y. Darshana, V. Venugopal, “Role of building material in thermal comfort in tropical climates—A review”, *Journal of Building Engineering*, 3 [2015] 104-113.
59. A. Brambilla, J. Bonvin, F. Flourentzou, T. Jusselme, “On the influence of thermal mass and natural ventilation on overheating risk in offices”, *Buildings*, 8 [2018] 47.
60. Simone, “How Can Thermal Mass Help In Winter or Summer to Regulate Room Temperature?”, *Sustainable Design*, [2017] [Available from: <https://gruenecodesign.com.au/how-can-thermal-mass-help-in-winter-or-summer-to-regulate-room-temperature/#:~:text=In%20winter%2C%20thermal%20mass%20works,reduces%20the%20need%20for%20heating>. Accessed on 14 August 2022.
61. F. Sharaf, “The impact of thermal mass on building energy consumption: A case study in Al Mafrqa city in Jordan”, *Cogent Engineering*, 7 [2020] 1804092.
62. E. Saver “Radiant Cooling: Office of Energy Efficiency & Renewable Energy”, [2022] [Available from: <https://www.energy.gov/energysaver/radiant-cooling#:~:text=Radiant%20cooling%20cools%20a%20floor,in%20homes%20with%20radiant%20panels>. Accessed on 10 August 2022.
63. D-I. Bogatu, O.B. Kazanci, B.W. Olesen, “An experimental study of the active cooling performance of a novel radiant ceiling panel containing phase change material [PCM]”, *Energy and Buildings*, 243 [2021] 110981.
64. A. Zain-Ahmed, A. Sayigh, P. Surendran, M. Othman, “The bioclimatic design approach to low-energy buildings in the Klang Valley, Malaysia”, *Renewable Energy*, 15 [1998] 437-440.
65. A. Nugroho, “Passive cooling performance on Indonesia contemporary tropical facade in producing the present comfortable space”, *IOP Conference Series: Earth and Environmental Science*, IOP Publishing, [2022] 012005.
66. M.A. Del Rio, T. Asawa, Y. Hirayama, R. Sato, I. Ohta, “Evaluation of passive cooling methods to improve microclimate for natural ventilation of a house during summer”, *Building and Environment*, 149 [2019] 275–287.
67. N.A. Al-Tamimi, “Toward sustainable building design: Improving thermal performance by applying natural ventilation in hot–humid climate”, *Indian Journal of Science and Technology*, 8 [2015] 1-8.
68. M.Q. Oleiwi, “Thermal Comfort of Residential Buildings Using Industrialised Building System Through Natural Ventilation in Hot and Humid Climate of Malaysia”, [Doctor of philosophy], Malaysia: National University of Malaysia [UKM]. 2020. Retrieved from: https://www.researchgate.net/publication/363337645_Thermal_Comfort_of_Residential_Buildings_Using_Industrialised_Building_System_Through_Natural_Ventilation_in_Hot_and_Humid_Climate_of_Malaysia.

69. R. Daghih, N.M. Adam, B. Sahari, B. Yousef, M. Ali, "Tracer decay method for determining ventilation characteristics of naturally ventilated office", *International Journal of Engineering Research and Development*, 4 [2012] 69-76.
70. G.V. Fracastoro, G. Mutani, M. Perino, "Experimental and theoretical analysis of natural ventilation by windows opening", *Energy and Buildings*, 34 [2002] 817-827.
71. H.B. Rijal, P. Tuohy, M.A. Humphreys, J.F. Nicol, A. Samuel, J. Clarke, "Using results from field surveys to predict the effect of open windows on thermal comfort and energy use in buildings", *Energy and Buildings*, 39 [2007] 823-836.
72. Y. Hirayama, M. Ohta, A. Hoyano, T. Asawa, "Thermal performance of a passive cooling louver system to form cool microclimate in urban residential outdoor spaces", *Proceedings of the 30th International PLEA Conference, CEPT University, Ahmedabad, India*, [2014] 16-18.



ARID Journals

**ARID International Journal for Science and
Technology (AIJST)**
ISSN: 2662-009X

Journal home page: <http://arid.my/j/aijst>

مَجَلَّةُ أُرَيْدُ الدَّوْلِيَّةُ لِلْعُلُومِ وَالتَّكْنُولُوجِيَا

المجلد 6 ، العدد 11 ، حزيران 2023 م

Investigation of the Effect of Disorder on the Tauc Edge of Hydrogenated Amorphous Silicon Using Dunstan's Bandgap Fluctuations Model

Abdullah Al-Numan ¹, Salwan K. J. Al-Ani ²¹ Physics Department, College of Science for Women, University of Baghdad, Baghdad, Iraq² Department of Physics, College of Science, Al-Mustansirya University, Baghdad, Iraq

استقصاء تأثير اللانظام على حافة تاوس للسليكون العشوائي المهدرج باستخدام نموذج دونستان لفجوة الطاقة المتعاقبة

عبدالله النعمان ⁽¹⁾ سلوان كمال جميل العاني ⁽²⁾

1 قسم الفيزياء، كلية العلوم للبنات، جامعة بغداد، العراق
2 قسم الفيزياء، كلية العلوم، الجامعة المستنصرية، بغداد، العراق

salwan_kamal@yahoo.comArid.my/0001-1999<https://doi.org/10.36772/arid.aijst.2023.6116>

ARTICLE INFO

Article history:

Received 15/04/2023

Received in revised form 01/05/2023

Accepted 10/05/2023

Available online 15/06/2023

<https://doi.org/10.36772/arid.ajst.2023.6116>

ABSTRACT

The optical absorption edge in both Urbach and Tauc regions are analyzed for hydrogenated amorphous silicon optical data of Cody et al and Viturro and Weiser. Dunstan's model, introduces disorder into the band-band absorption through a linear exponential distribution of local energy gaps. This model has a simple mathematical form and has a clear physical meaning in comparison to the somewhat similar models of O'Leary and Guerra, yet Dunstan's model is unjustly neglected in literature.

The most important physical parameter of the model is the energy gap parameter- E_o , which represents the separation between the valence and conduction band edges, it can be considered as the mobility gap of the material. Dunstan's model is found successful in capturing the optical data of Cody et al and, Viturro and Weiser. A plot of the energy parameters of the Dunstan and Cody models, E_o against E_{opt} respectively, was proposed here to separate the masking contribution of tail-related absorption from the real change of the band gap, and was found fruitful for this purpose. This is because E_o is a function only of the separation between valence and conduction band edges, while the meaning of the optical energy E_{opt} is ambiguous because it is also a function of absorption due to tail-related absorption that results from disorder. This simple plot of E_o vs. E_{opt} , through the slope $\Delta E_o / \Delta E_{opt}$ of the fitting straight line, was capable of distinguishing the different relative contributions of disorder between Cody et al and Viturro and Weiser optical data, E_o value was found less sensitive to hydrogen content variation for Viturro and Weiser data which is interpreted due to their better control of the thin film deposition process.

Keywords: optical energy gap, absorption coefficient, amorphous semiconductor, mobility gap.

الملخص

تم تحليل منطقتي اورباخ وتاوس للبيانات البصرية للسليكون العشوائي المهدرج لكودي وجماعته وفيتوررو وفايزر. نموذج دونستان يستقدم اللانتظام إلى الامتصاص بين الحزم من خلال توزيع أسّي خطّي لفجوات الطاقة الموضعية. هذا النموذج يمتلك صيغة رياضية بسيطة ومعنى فيزيائي أوضح بالمقابلة مع نماذج أخرى قريبة لاوليري وكويررا، لكن نموذج دونستان تم إهماله في الأدبيات بشكل غير منصف. أهم معلم فيزيائي لهذا النموذج هو معلم فجوة الطاقة E_0 الذي يمثل الفسحة بين حافتي حزمة التكافؤ والتوصيل، ويمكن اعتباره يمثل فجوة التحركية للمادة. وجد نموذج دونستان ناجحاً في موائمة البيانات البصرية لكودي وجماعته وفيتوررو وفايزر. تم اقتراح رسماً بيانياً بين معلم الطاقة لنموذجي دونستان وكودي، E_0 مقابل E_{opt} وذلك لفصل الإضافة الحاجبة للامتصاص المتعلق بالذيول عن التغير الحقيقي في فجوة الطاقة. وقد وجد هذا الأمر مثمراً لهذا الغرض وذلك بسبب كون E_0 هي دالة للفسحة بين حافتي حزمة التكافؤ والتوصيل فقط، بينما معنى فجوة الطاقة البصرية E_{opt} هو ملتبس لأنها دالة للامتصاص المتعلق بالذيول الناتج عن اللانتظام أيضاً. هذا الرسم البياني بين E_0 و E_{opt} من خلال الميل $\Delta E_{opt}/\Delta E_0$ الناتج عن موائمة الخط المستقيم يتمكن من تمييز المساهمات النسبية للانتظام بين البيانات البصرية لكودي وجماعته وفيتوررو وفايزر، ووجد أن قيمة E_0 هي أقل حساسية لتغير منسوب الهيدروجين لبيانات فيتوررو وفايزر الأمر الذي عزى إلى السيطرة الأفضل على عملية ترسيب الأغشية.

الكلمات المفتاحية: فجوة الطاقة البصرية، معامل الامتصاص، شبه الموصل العشوائي، فجوة التحركية.

1. Introduction:

One of the most important parameters that can be deduced from the analysis of the experimental absorption spectrum of a semiconductor is the optical energy gap E_{opt} . It is for example, a crucial physical parameter for the modeling of optoelectronic semiconductor devices especially solar cells. Its physical meaning is well established in crystalline semiconductors because they have a real and definite energy gap between their conduction band (CB) and valence band (VB) band edges.

In amorphous semiconductors, disorder obscures the physical meaning of the experimental optical gap because there is no real energy gap in their density of states (DOS) diagram due the encroachment of the VB and CB states towards the pseudo-gap region in the form of localized states [1].

Due to the ambiguities in the interpretation of the Tauc edge of semiconductors and especially amorphous semiconductors (mainly because of the complex nature of their density of states), some researchers, including one of the authors of this article, suggested alternative methods to analyze optical absorption data in the Tauc region such as the inverse logarithmic derivative method to obtain E_{opt} and the optical transition matrix element index [2,3]; yet another method was suggested by Zanatta [4], he used a unified formalism based on the Sigmoid (Boltzmann) model that he found appropriate to fit optical absorption edge data and to obtain the energy gap parameter of semiconductors including amorphous ones.

Still, the usual Tauc plot by virtue of its simplicity in defining an effective optical gap is predominately used in amorphous semiconductor literature [5]. However, one main deficiency of the Tauc model is in its neglect of the absorption due to band tail related optical transitions, it is basically a model of optical transitions between valence band extended states and conduction

band extended states. Therefore, it neglects the effect of disorder on the high absorption edge region ($\alpha \geq 10^4 \text{ cm}^{-1}$, where α is the absorption coefficient) [6]. Disorder effect is usually considered to appear mainly in the Urbach tail of amorphous semiconductors, just below the Tauc edge, this Urbach region of the optical absorption edge is most frequently attributed to tail states related optical transitions [7,8,9].

One of the early attempts by us to include the disorder contribution to the Tauc edge of amorphous semiconductors was by employing the full Davis-Mott model formulation which includes the width of localized states ΔE in the optical absorption formula of the Tauc region [10], yet the parameter ΔE is not available experimentally, usually the available parameter is the Urbach energy E_u which is an important marker of disorder [7].

Realistic optical absorption data in the Tauc region of the absorption edge, is not due only to extended to extended state optical transitions, but is also due to optical transitions from valence band localized (extended) states to conduction band extended (localized) states to a lesser extent. The neglect of tail related transitions in the Tauc region impedes us from a more correct interpretation of optical absorption data especially from attaining a reasonable physical meaning for the optical energy gap E_{opt} obtained from optical absorption experimental data [6].Therefore there is an ambiguity in interpreting the variation of optical band gap E_{opt} with deposition parameters whether it is due to is a real change in the mobility gap E_μ or it is due to an indirect effect of disorder [11].

Thus, further development of the Tauc model is needed to take into account the effect of the tail-related transitions in addition to extended-extended transitions. This was achieved by a small number of researchers in a long time span beginning with Dunstan 1982 [12] and Frova et al 1985 [11], through O`Leary and various collaborators [13,14,15,16] and finally the task was

undertaken by Guerra and collaborators [17,18,19]. As tail-related transitions are due to the influence of disorder, these models combine the Urbach region with the Tauc region in one theoretical model, thus the Urbach parameter E_u which is a marker of disorder should also contribute to the Tauc region, as was found in these models.

These models were successful in fitting both the Urbach and Tauc regions of the optical absorption edge and gave new insight to the optical gap interpretation, yet the older model due to Dunstan [12,20] which accounted for disorder through the Urbach edge is the simplest one whether in its mathematical form or its direct physical interpretation compared to the more detailed O'Leary model [14,15] and the polylogarithm model of Guerra [18]. Dunstan claimed and showed that his model accounted successfully for most amorphous semiconductor optical data he analyzed [12]. However, this simple and successful Dunstan model was unjustly neglected in literature with the exception of the analogous Frova et al model [11], and it is also mentioned by Ley and Guerra et al [21, 18].

In a previous joint work by one of the authors [6], Dunstan's model was used to analyze and model optical data of a-Si:H due to Jackson et al [22] and Maurer et al [23] in both the Urbach and Tauc regions, and this model excellently fitted those data. The Cody constant dipole matrix element approximation [24] was employed which is more suitable for a-Si:H thin films than the constant momentum matrix element approximation of the Tauc model as was validated by Jackson et al experimental work [22]. The most important fitting parameter of the Dunstan model is E_o , which is the energy gap parameter of this model, is a marker of the separation between the valence band and conduction band edges thus it avoids the above mentioned ambiguities of the interpretation of the conventional Tauc optical gap E_{opt} .

This paper is organized in the following manner. In section 2, the 3-parameter Dunstan model is presented, then its importance and physical implications are given in section 3, describing the two contributions of extended states absorption and tail-related absorption to the Tauc region, an application of the Dunstan model to Jackson et al [22] optical data of a-Si:H is included, and a density of states diagram is presented to clarify the meaning of some important energy gap parameters. Section 4, is the results and discussion section, Dunstan's model is used to fit the important Cody et al [25] and Viturro and Weiser [26] a-Si:H optical data sets which cover both the Urbach and Tauc regions, this gives us the opportunity to analyze these data in order to investigate the effect of disorder especially on the Tauc edge by taking advantage of the different physical interpretations of the Dunstan energy gap E_0 and the conventional optical gap parameter E_{opt} , through a suggested plot between these the two parameters. Finally, the conclusions are given in section 5.

2. The Description of Dunstan's Model:

Dunstan built his model on the band-gap fluctuations model of Skettrup (1972) [27] originally proposed as an alternative interpretation of the Urbach edge of crystalline semiconductors [28]. In the Skettrup model, a band gap is defined locally within small cells about the size of phonon coherence length. This local band gap is reduced in proportion to the number of thermal phonons present, thus this local band gap fluctuates spatially and temporally with a linear exponential distribution of values. Disorder in Skettrup's model is due to the thermal disorder caused by phonon excitations. Dunstan extended this model to the amorphous case, he considered the static (time-independent) disorder in the amorphous semiconductor as a fictive phonon disorder i.e. structural disorder is considered due to frozen-in phonons, a proposal introduced earlier by Cody et al [25]. Dunstan assumed that the absorption above the gap is given in the general form [20]:

$$\alpha(E) = f(E - E_{oG}) \dots\dots\dots (1)$$

where E_{oG} is the local fluctuating band gap that is assumed to take a distribution of values

$E_o - \varepsilon$, ε has a linear exponential probability distribution $P(\varepsilon)$ with a slope β :

$$P(\varepsilon) = \beta e^{-\beta\varepsilon} \quad \text{for } \varepsilon \geq 0 \dots\dots\dots (2)$$

The absorption spectrum is obtained by integrating the band-to-band absorption eq. (1) of overall values of E_{oG} :

$$\alpha(E) = \int_0^{\infty} P(\varepsilon) f(E - E_o + \varepsilon) d\varepsilon \dots\dots\dots (3)$$

The solution of eq. (3) depends on the mathematical form of the function $f(E)$.

Fortunately, for the special case in which $f(E-E_o)$ obeys a Tauc-law form, the integration eq. (3) can be solved analytically to give the following simple form formulas [20]:

$$\alpha(E) = \frac{2\alpha_o}{E\beta^2} e^{-\beta(E_o - E)} \quad E \leq E_o \dots\dots\dots (4-a)$$

$$\alpha(E) = \frac{\alpha_o}{E} \left\{ (E - E_o)^2 + \frac{2}{\beta}(E - E_o) + \frac{2}{\beta^2} \right\} \quad E \geq E_o \dots\dots (4-b)$$

Dunstan considered the parameter β to be the inverse of the Urbach energy, i.e., $\beta=1/E_u$, E_u is the Urbach energy parameter.

Dunstan claimed that his model described accurately the absorption spectrum in every amorphous semiconductor he tested, it did give an exponential tail and gave the correct strength of absorption in the Urbach tail and the correct form of the spectrum at the transition (around) E_o from the tail to the intrinsic (Tauc-region) absorption. Dunstan assumed that E_o in the absence of any chemical modification is a constant of the material which can be interpreted

as the energy gap in the absence of disorder. The only researchers on optical data using Dunstan mathematical expressions are Frova & Selloni 1985 [11], they neglected conduction band exponential tails because it is well known that in a-Si:H related films, the dominant contribution to the Urbach tail is due to transitions from valence band tail states to conduction band extended states. They assumed an exponential broadening of the valence band extended states into localized states which results from disorder (the γ parameter in Dunstan model), they applied the model to a-Si:H and a-SiC:H optical data with reasonable success.

3. The importance and physical implications of Dunstan's model:

In Tauc or Cody models, the so-called optical energy gap E_{opt} is obtained from the optical absorption data through the Tauc or Cody plots. In the Tauc plot $(\alpha E)^{1/2}$ (or $(E^2 \epsilon_2)^{1/2}$, ϵ_2 is the imaginary part of the dielectric function $\epsilon(\omega)$) is plotted versus photon energy E , whereas in the Cody plot $(\alpha/E)^{1/2}$ (or $\epsilon_2^{1/2}$) is plotted against photon energy E [5,24]. In Tauc theoretical model, E_{opt} is interpreted as an extrapolation of the parabolic valence band and conduction band extended states to the zero of the density of states in the pseudo-gap [29].

Tauc and Cody models consider only the optical transitions between parabolic extended band states, transitions due to localized states are not considered. This makes the extrapolated E_{opt} value obtained from, the Tauc plot equation:

$$(\alpha E)^{1/2} = B_{Tauc} (E - E_{opt}^{Tauc}) \dots\dots\dots(5)$$

Or from the Cody plot equation:

$$(\alpha/E)^{1/2} = C_{Cody} (E - E_{opt}^{Cody}) \dots\dots\dots(6)$$

lower than the theoretical optical energy gap proposed by these models [30]. In fact, with increasing structural or/and thermal disorder this discrepancy between theory and experiment

should increase due to the larger contribution from tail related optical transitions to the Tauc region of the absorption edge [11]. Therefore, more realistically, optical transitions that contribute to the Tauc region of the absorption edge ($\alpha \gtrsim 10^4 \text{ cm}^{-1}$) are not only extended-extended transitions, but also localized (extended) - extended (localized) transitions [14,15] .

Here comes the necessity for such models as Dunstan's model and similar models like O'Leary's and Guerra's models [15, 18] These models take into account exponential tail states related transitions, and thus it is expected to obtain from them a more realistic value of the energy gap of an amorphous semiconductor. In this case, both the Urbach and Tauc regions data must be available from experiment. As the Urbach energy is a measure of disorder, a more explicit and physically meaningful explanation of the role of disorder on the absorption edge of amorphous semiconductors can be obtained.

Dunstan's equation in the Tauc region(eq.4-b) can be re-written in the following more informative form:

$$\alpha(E) = f(E) + \Delta(E) \quad E > E_o \dots\dots\dots(7-a)$$

Where:

$$f(E) = \frac{\alpha_o}{E} (E - E_o)^2 \dots\dots\dots(7-b)$$

gives exclusively the contribution of extended band to band transitions to the Tauc edge.

and,

$$\Delta(E) = \frac{\alpha_o}{E} [2E_u(E - E_o) + 2E_u^2] \dots\dots\dots(7-c)$$

is the contribution of localized-extended transitions to the Tauc edge.

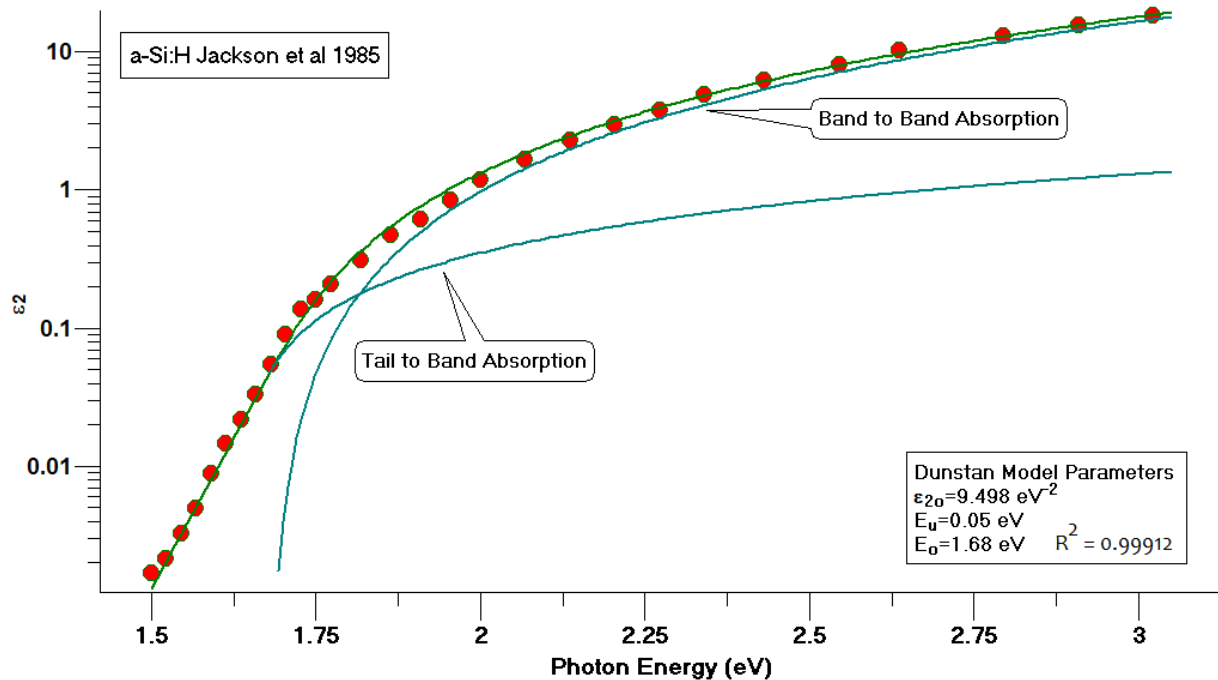
Notice that the Urbach edge parameter E_u is already included in the expression eq. (7-c) indicating the effect of disorder on the Tauc edge. Notice also that with increasing disorder through increasing Urbach edge parameter the $\Delta(E)$ contribution increases, and thus increasingly lowering the obtained value of the experimental Tauc optical gap [11]. The Urbach edge contribution to the Dunstan model (eq.4-a) can be re-written in terms of E_u as:

$$\alpha(E) = 2\alpha_0 E_u^2 \exp \frac{E - E_0}{E_u} \dots\dots\dots(8)$$

Notice from inspecting eqs. (7) & (8) that, $\alpha(E)$ and its first derivative $d\alpha/dE$ are continuous at the threshold energy E_0 .

To show how the simple Dunstan model fits well the optical data in a wide photon energy range, and gives the relative contributions of tail-related and band-related absorption, Fig.1 shows Jackson et al [22] $\epsilon_2(E)$ vs. photon energy a-Si:H data, fitted in a previous work [6] to Dunstan's model; a good fit was obtained for the parameter values, $E_u=0.05\text{eV}$, $E_0=1.68\text{ eV}$ and $\epsilon_{20}=9.498\text{ eV}^{-2}$ (where ϵ_{20} is the counterpart of α_0 in terms of the imaginary part of the dielectric function ϵ_2) in the very wide energy range (1.5 - 3 eV) covering both the Urbach and the Tauc regions of the absorption edge; the constant dipole transition matrix element approximation was used. These results compare very well with O'Leary's model analysis [14]. The relative contributions of tail-related transitions and band-related transitions are depicted in the figure, notice how the relative contributions of $f(E)$ (band to band absorption) and $\Delta(E)$ (tail to band absorption) vary with photon energy, the band-related absorption starts at the threshold energy $E_0=1.68\text{ eV}$, then beyond the intersection point at $E\sim 1.82\text{ eV}$, band-related absorption starts to gradually dominate over tail-related absorption. It is important to mention

that the optical energy gap of these samples as fitted to the Cody plot in the wide photon energy range (1.7 - 3 eV) is ~ 1.63 eV, is lower ~ 0.05 eV than E_0 value for these Jackson et al high-quality a-Si:H samples.



Figure(1): Dunstan's model fitting to Jackson et al a-Si:H data in the photon energy range (1.5-3)eV [6].

In fig. (2), an appropriate density of states diagram is shown to explain the main energy gap parameters relevant to the absorption edge of an amorphous semiconductor [6].

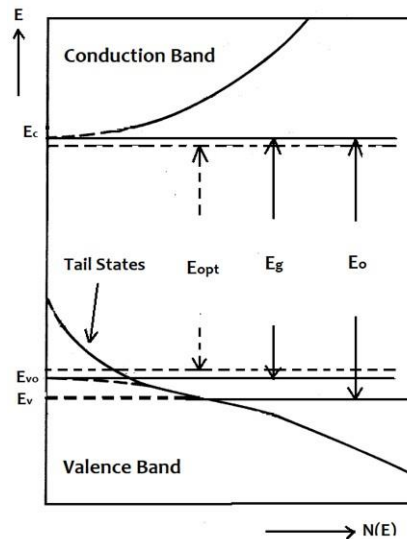


Figure (2): Amorphous density of states diagram that depict the main energy gap parameters, E_{opt} , E_g and E_o .

In this figure, conduction band tails are neglected, this assumption is suitable for a-Si:H and related films, where the valence band tail region is significantly broader than the conduction band tails [11]. E_g in the figure is the extrapolated band gap to the zero density of states; in the limit that the effect of disorder can be neglected $E_g \approx E_{opt}$ as predicted by the Tauc or Cody theoretical models. It is also the important energy gap parameter of the O’Leary model before the introduction of disorder [14]. Due to the contribution of localized states related transitions, E_{opt} determined experimentally is smaller than E_g , and it is in fact a fictitious band gap in the pseudo-gap as depicted in the figure, the difference between E_g and E_{opt} increases with increasing disorder i.e. with increasing Urbach energy E_u . E_o , which is the energy gap of both Dunstan and Guerra models [18,20] and the threshold energy of the O’Leary model, is the energy gap between the band edges ($E_o = E_c - E_v$), only if E_v is the critical energy separation between valence band extended states and the valence band localized tail states, then E_o can be considered to be the mobility gap E_μ of the material, which is a parameter very difficult to extract experimentally [31]. An important point should be

mentioned here about the significance of E_o compared to E_{opt} . E_{opt} physical meaning is ambiguous because it is a function of both the masking contribution of disorder through tail-related absorption, in addition to the separation between the valence band and conduction band edges which is equal to E_o and is more of chemical origin. E_o is very important energy parameter because it signifies the energy separation between the valence band and conduction band, band edges, then its variation with preparation conditions of the sample should be due to a real change in the separation between the band edges, hopefully it could be equal to the mobility gap [32].

4. Results and Discussion:

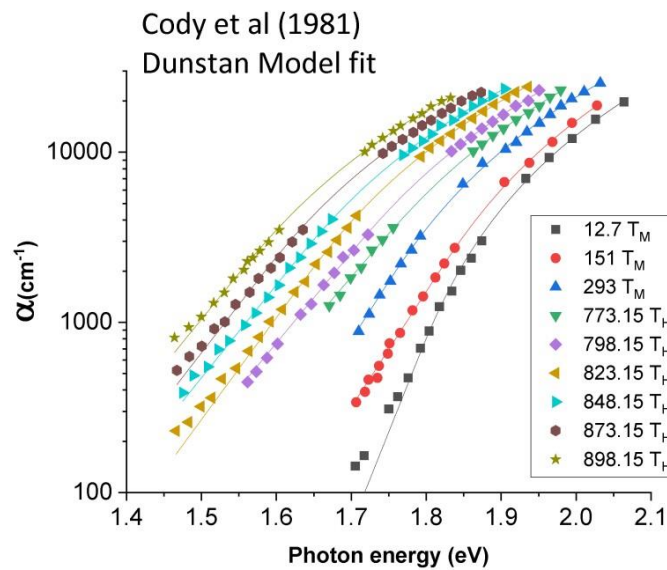
We analyzed optical data sets of a-Si:H thin films due to Cody et al [25] and Viturro and Weiser [26]. These optical data was fitted to Dunstan's model using nonlinear Levenberg-Marquardt fitting algorithm [33].

4.a- Cody et al (1981) [25] optical data analysis:

Cody et al a-Si:H samples were prepared by PECVD onto anodic substrates held at elevated temperatures. They performed an important study of the effects of both thermal and static disorder on the optical absorption edge of a-Si:H. They investigated the relationship between the Tauc optical gap and the Urbach energy, they introduced structural disorder through thermal evolution of hydrogen. They found that their results are compatible with the idea of additive thermal and structural disorder. They suggested that relaxed network disorder rather than hydrogen content is responsible for the dependence of optical energy gap of a-Si:H on hydrogen content. Their results indicated an inverse linear relationship between Tauc optical gap and Urbach energy.

Fig. (3) shows Dunstan's model nonlinear fits to Cody et al a-Si:H data. $T_M=12.7\text{K}$, 151K and 293K are different measurement temperatures for an as-prepared film of composition

a-Si:H_{0.13}, T_H is the isochronal heating temperature of the $T_M=293\text{K}$ film at 25°C intervals from 500°C (773K) to 625°C (898K). This heating procedure was intended to induce varying out-diffusion of hydrogen from the films. The fitting parameters; of the Cody plot (E_{Cody} and B_{Cody} in the Cody model linearized equation, $\varepsilon_2 = B_{\text{Cody}} (E - E_{\text{Cody}})$ and, of Dunstan's model $E_u=1/\beta$, α_o , and E_o in eqs.4-a and 4-b) are given in table (1).



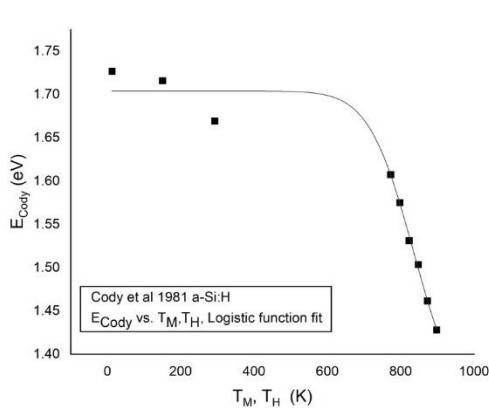
Figure(3): Nonlinear fitting plots of Cody et al data to Dunstan's model, fitting parameters are listed in table1.

It is easily noted from table 1, the inverse proportion between both E_{Cody} and E_o , and the Urbach energy E_u , which means that increasing disorder through increasing E_u decreases both energy gap parameters E_{Cody} and E_o . The behavior of E_{Cody} versus E_u was already accounted for by Cody et al through the well-known Cody model of disorder [25]. However, the

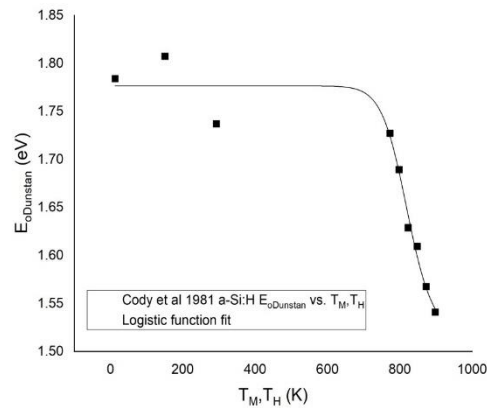
decrease of E_o with increasing disorder through increasing E_u seems to mean that disorder really affects the mobility gap.

Table (1): Cody and Dunstan model fitting parameters for Cody et al a-Si:H data.

Temperature	E_u (eV)	E_{Cody} (eV)	B_{Cody} ($cm^{-1}eV^{-2}$)	E_o (eV)	α_o ($cm^{-1}eV^{-2}$)
12.7 K	0.0402	1.727	84701.2322	1.7839	93353.78
151 K	0.0664	1.716	94403.256	1.8074	106900.60
293 K	0.0659	1.669	96734.957	1.7369	93757.64
773.15 K	0.0892	1.607	83100.4843	1.7273	92796.62
798.15 K	0.0859	1.575	81919.4709	1.6894	90691.59
823.15 K	0.0761	1.531	77566.7904	1.6281	83136.63
848.15 K	0.0838	1.503	77523.765	1.6095	82779.405
873.15 K	0.0806	1.46156	71,854.6808	1.5676	78549.68
898.15 K	0.085	1.42805	70769.4856	1.541	77931.203



(a)



(b)

Figure (4): (a) E_{Cody} vs. T_M, T_H plot for Cody et al a-Si:H samples (b) $E_{oDunstan}$ vs. T_M, T_H plot for Cody et al a-Si:H samples; both data are fitted to a logistic function.

Fig.(4-a) shows E_{Cody} vs. T_M, T_H plot for Cody et al a-Si:H samples. Here a logistic function fit $[y = a / \{1 + \exp(b - cx)\}]$ a, b and, c are constants] is performed as it is found capable to capture the main trend of the data variation. It is seen that E_{Cody} does not change appreciably with T_M , but decreases systematically with increasing T_H which means that hydrogen evolution affects the optical energy gap as already known in literature. The variation of E_o Dunstan with T_M, T_H shows similar behavior to the variation of E_{Cody} with T_M, T_H ,

this is shown in figure (4-b). This means that the evolution of hydrogen changes the band to band gap significantly, i.e. this seems to imply that hydrogen evolution from the films changes the mobility gap appreciably. We expect then that for Cody et al a-Si:H samples, the contribution of tail to band optical transitions which is accounted for by Dunstan's model is relatively insignificant compared to the real change in the mobility gap, i.e. the band to band threshold energy E_o . To check for this in a more quantitative way, $E_{o\text{ Dunstan}}$ in figure (5) is plotted against E_{Cody} for Cody et al a-Si:H samples. A least squares straight line fitting gives a slope value of 0.863 which is closer significantly to 1 than zero, thus Dunstan's model accounts only ~15% for the apparent change of the optical gap, while ~85% is a real change in the separation between the valence band and conduction band band edges. We consider here that a zero slope ($\Delta E_{o\text{ Dunstan}}/\Delta E_{\text{Cody}}=0$) means that $E_{o\text{ Dunstan}}$ is independent of E_{Cody} , while a unity slope means a perfect correspondence between $E_{o\text{ Dunstan}}$ and E_{Cody} .

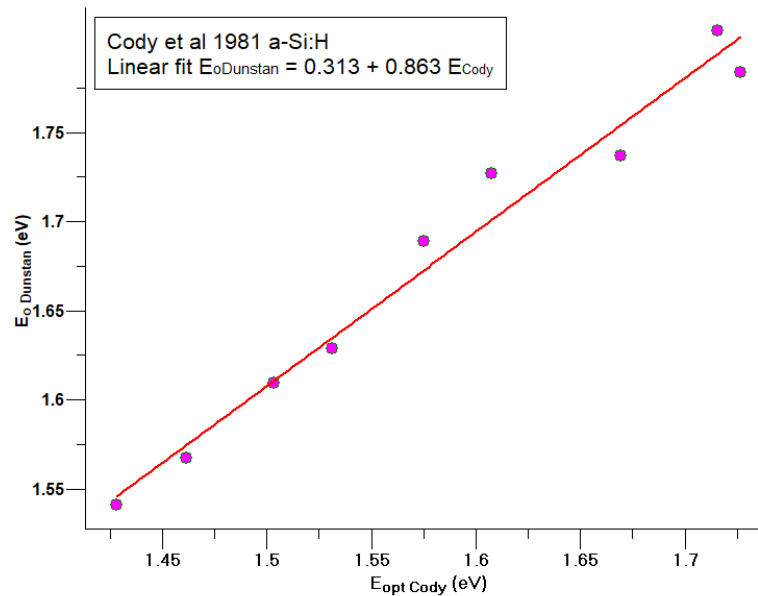


Figure (5): $E_{o\text{ Dunstan}}$ vs. E_{optCody} , plot for Cody et al a-Si:H samples. Each pair of $E_{o\text{ Dunstan}}$ and E_{optCody} values is taken at a definite T_M or T_H value in table 1.

Thus, for Cody et al a-Si:H optical data set, the main contributor to the change of the optical gap E_{Cody} is a real change in the mobility gap. What is the reason for this change? This is a longstanding controversial problem, and opinions were mainly divided between two well-known ones, the shift of the valence band edge or the indirect effect of disorder on the a-Si:H network [34]. Cody et al [25] adopted the second view in that hydrogenation is the primary reason for E_{opt} variation through its indirect network relaxing effect of the random network, and not through the recession of the valence band edge. We see here through Dunstan's model analysis and the inspection of Table I, that although E_o is always larger than E_{opt} because of the subtraction of the masking effect of tail-related absorption, it also changes with hydrogen evolution (Note however, Cody et al did not give measurements results for the hydrogen content of their samples after isochronal heating). This means that there a real shift in the band edges separation, but the source of this change still cannot be decided here whether it is chemical or through disorder or due to both causes . According to theoretical work of Teate and Hadler, the mobility gap of a-Si:H decreases with increasing disorder according to localization theory [35], thus in view of the above-mentioned work, disorder not only creates band tails but can also shifts the mobility edges. It is also necessary to mention here a recent result by Steffens et al [36] that E_{opt} of a-Si:H correlates well with monohydride bond density of a-Si:H rather than either hydrogen concentration or structural disorder, which is an important result that needs to be further exploited. Another point to be mentioned is that E_o is not the same as the Urbach focus energy E_F concept, this issue is well discussed by Guerra in relation to his band-fluctuations model [19], E_F is the energy gap in the absence of any disorder whether thermal or structural disorder or even due to zero-point energy, i.e., for an ideal random network at zero Kelvin. However, $E_{o\text{Dunstan}}$ is the band gap between valence and

conduction band edges at ambient conditions similar to E_o of Guerra's model [18] and the threshold energy gap of O'Leary's model [15] and not an extrapolated gap to the ideal case of the absence of any kind of disorder, that is the Urbach focus of Cody's model of disorder [25]. The most important point that should be clarified here, is that Dunstan's gap $E_{oDunstan}$ (the band edges separation) is masked by the contribution of tail-related absorption to the Tauc edge, therefore only by subtracting this contribution, E_o , the real threshold energy to the onset of the band to band optical transitions, can be determined by any appropriate model such as Dunstan, O'Leary or Guerra models , Dunstan's model is the simplest one beyond the Tauc model.

4-b Viturro and Weiser(1986) [26] Optical Data Analysis:

Vitturo and Weiser [26] used a direct synthesis method for producing a-Si:H in which atomic hydrogen and silicon react on a substrate at ultrahigh vacuum to produce material with good properties. They argued that Cody et al [25] employed hydrogen evolution to produce static disorder, but they claimed that Cody et al procedure might cause other changes in the material in addition to the loss of hydrogen. Thus Vitturo and Weiser varied the hydrogen concentration systematically at the same deposition conditions, in order to reach more decisive results concerning the relation between the optical gap E_{opt} , the Urbach energy E_u , and hydrogen concentration $C_H\%$.

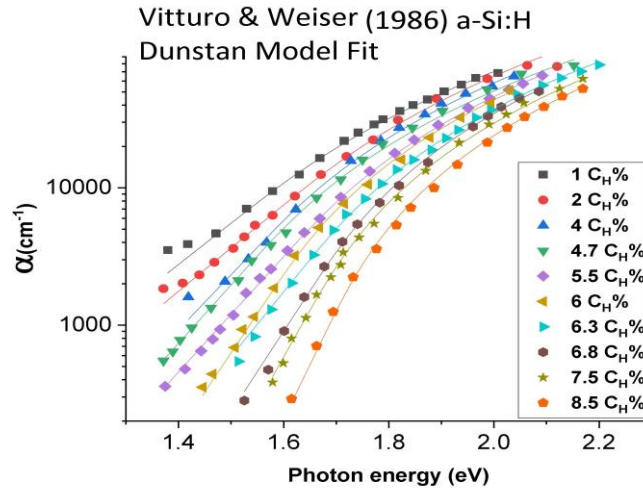


Figure (6): Dunstan model nonlinear fitting plots for Vitturo and Weiser a-Si:H data, fitting parameters are listed in Table 2.

Fig.(6) shows Dunstan's model nonlinear fits to Vitturo and Weiser a-Si:H optical data set for various percentage hydrogen concentrations $C_H\%$ from 1% to 8.5%. These nonlinear fitting results successfully capture Vitturo and Weiser data, confirming the capability of Dunstan model to explain optical data covering Urbach and Tauc regions of the optical absorption edge. All the fitting parameters are given in Table 2.

Table (2): Cody and Dunstan models fitting parameters for Vitturo and Weiser a-Si:H data.

$C_H\%$	E_u (eV)	E_{Cody} (eV)	B_{Cody} ($cm^{-1}eV^{-2}$)	E_s (eV)	α_s ($cm^{-1}eV^{-2}$)
1	0.1606	1.341882	67992.455	1.52	80766.83
2	0.152	1.421464	75742.1910	1.593	96850.9
4	0.117	1.422799	67395.596	1.55	86830.33
4.7	0.11	1.463586	81123.4114	1.535	74147.23
5.5	0.111	1.501475	77677.329	1.6105	87806.23
6	0.08	1.54260	85774.3172	1.575	83469.8
6.3	0.098	1.55189	76535.5267	1.64	85297.12
6.8	0.0776	1.590196	88912.1728	1.654	93777.83
7.5	0.0666	1.60931	83544.18159	1.645	81137.97
8.5	0.0571	1.658137	86524.26294	1.682	83534.25

It can easily be seen from Table (2) that increasing the hydrogen concentration $C_{H\%}$ (1% - 8.5% range) of Viturro and Weiser samples decreases the disorder through decreasing the Urbach parameter E_u .

To show the effect of varying $C_{H\%}$ on the energy gap parameters E_{Cody} and $E_{oDunstan}$, figure. (7) is a combined plot of E_{Cody} and $E_{oDunstan}$ vs. $C_{H\%}$. Both E_{Cody} and $E_{oDunstan}$ increase with hydrogen concentration, but it is observed that E_o increase is significantly slower than E_{Cody} increase, as seen from the magnitudes of the slopes of the fitting straight lines ; 0.477×10^{-1} for E_{Cody} vs. $C_{H\%}$ and 0.187×10^{-1} for $E_{oDunstan}$ vs. $C_{H\%}$. The ratio between the slope of $E_{oDunstan}$ vs. $C_{H\%}$ and the slope of E_{Cody} vs. $C_{H\%}$ ~ 0.4 or 40%. This means that $\sim 60\%$ of the variation of the optical energy gap is explained by Dunstan's model while the remaining variation $\sim 40\%$ is due to a real change in the band edge to band energy gap.

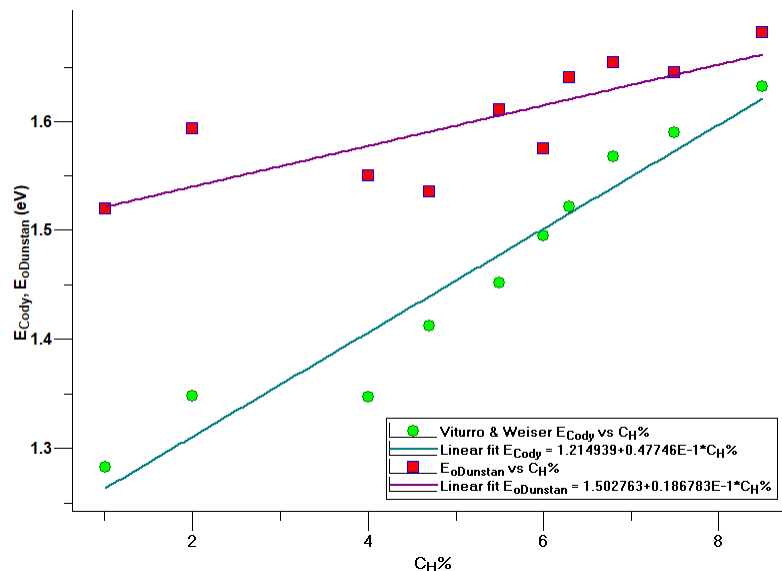


Figure (7): Comparative plots for $E_{oDunstan}$ and E_{Cody} vs. $C_{H\%}$ for Viturro and Weiser a-Si:H samples.

This behavior can be shown also from figure. (8) which depicts a plot of $E_{oDunstan}$ vs. E_{Cody} for Vitturo and Weiser a-Si:H samples. The slope of the fitting straight line $\Delta E_{oDunstan}/\Delta E_{Cody}$ is 0.417, this means that hydrogen causes a real variation in the mobility gap about 40% of the change of E_{opt} with hydrogen, while the other 60% is the due enhanced masking effect of absorption in the Tauc region due to tail related transitions. Thus, in contrast to the results of the analysis of Cody et al a-Si:H optical absorption data through the Dunstan's model which showed a dominating behavior due to mobility gap variation, Vitturo and Weiser a-Si:H data analysis shows a significantly slower mobility gap behavior. This obviously reveals that the more systematic control of hydrogen incorporation in a-Si:H films in Vitturo and Weiser work as compared to Cody et al work was fruitful through lowering the effect of disorder on the mobility gap. This kind of conclusion cannot be reached from the Tauc plot analysis alone. The subtraction of tail-related contribution to the Tauc edge through Dunstan's model is found here necessary to extract more useful physical information that explains the change of E_{opt} with deposition variables, i.e. only 40% of the change in E_{opt} is due to a real change in the separation between the valence and conduction band edges for Vitturo and Weiser a-Si:H samples, the other 60% change is not due to a real band gap change, but due to the masking effect of the tail-related optical transitions contribution to the Tauc edge. Here, one of the important ambiguities in the interpretation of E_{opt} as deduced from the Cody (or Tauc) plot is explicitly revealed, which demands a model that accounts for the effect of disorder on the Tauc edge such as Dunstan's model, but of course, the Urbach region data should also be available to the experimenter to reach such conclusions that are beyond the Tauc model.

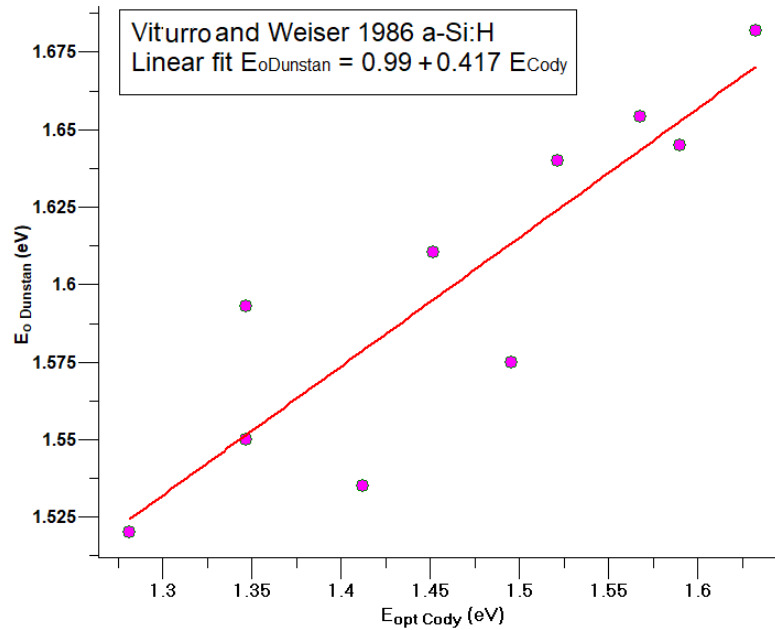


Figure (8): $E_{oDunstan}$ vs. $E_{optCody}$ plot for Viturro and Weiser a-Si:H samples. Each pair of $E_{oDunstan}$ and $E_{optCody}$ values is at a definite $C_H\%$ value in Table 2.

5. Conclusion:

In conclusion, Dunstan's model was found successful in capturing the optical absorption data covering both Urbach and Tauc regions for Cody et al and Viturro and Weiser a-Si:H optical data sets. Aside from this success, this work concentrates on what kind of new physical information can be extracted from the simple Dunstan model beyond the conventional Tauc model through the comparison between the main energy gap parameters of these model; E_{opt} , the optical energy gap and, E_o , the energy gap between the valence and conduction band edges its value is masked by the contribution of the tail-related absorption to the Tauc edge. It was found that the different behavior trends of E_o and E_{opt} are fruitful in differentiating between the masking effect of disorder through tail-related absorption in the Tauc region, and the real change in the band gap of a-Si:H samples. This differentiation was made apparent by adopting the slope ($\Delta E_o / \Delta E_{opt}$) of the straight line fit to the relation between E_o and E_{opt} , assuming

that it as an indicator of the effect of disorder on the Tauc edge of a-Si:H, which is a simple approach not attempted before in previous literature according to our knowledge. Using this approach, we found that there is a larger relative change in $E_{ODunstan}$ of Cody et al a-Si:H samples compared to Viturro and Weiser samples due to varying hydrogen content, and this is attributed to the better control of hydrogen incorporation process of Viturro and Weiser samples, which caused a lower shift in the band edges. Dunstan's model with its simple analytic formulas can easily be implemented in any suitable software such as Origin or Mathematica. It should also be mentioned that Dunstan's original convolution integral (eq.3) can also be applied to crystalline semiconductors and nano- materials optical data by inserting the appropriate form of the function $f(E - E_{oG})$ of eq.1 inside the integral and solving it numerically.

References:

- [1] J. Mullerova, and P. Sutta, "On some ambiguities of the absorption edge and optical band gaps of amorphous and polycrystalline semiconductors", *Commun Lett Univ ilina*, 19(3) (2017) 9–15.
- [2] S. K. J. Al-Ani, "Determination of the optical gap of amorphous materials", *Int. J. Electronics*. 75(6) (1993) 1153-1163.
- [3] Ł. Jarosiński, J. Pawlak, S.K'J. Al-Ani, "Inverse logarithmic derivative method for determining the energy gap and the type of electron transitions as an alternative to the Tauc method", *Opt Mater (Amst)*, 88() (2019) 667–73.
- [4] A.R. Zanatta. "Revisiting the optical bandgap of semiconductors and the proposal of a unified methodology to its determination", *Sci Rep.*, 9(1) (2019) 1–12.
- [5] J. Tauc, R. Grigorovici, A. Vancu, "Optical properties and electronic structure of amorphous germanium", *Phys status solidi*, 15(2) (1966) 627–37.
- [6] L. F. Sahal and A. Al-Numan, "A Study of a-Si:H Absorption Edge Using Dunstan's Model", *Baghdad Sci J.*, 20(2022) 466-472.
- [7] F. Urbach, "The long-wavelength edge of photographic sensitivity and of the electronic Absorption of Solids". *Phys. Rev.*, 92(5) (1953) 324.
- [8] I. Studenyak, M. Kranjčec, M. Kurik, "Urbach rule in solid state physics", *Int. J. Opt Appl.*, 4(3) (2014) 76–83.
- [9] S. K. J. Al-Ani, C. A. Hogarth, and D. N. Waters, "The Effect of Temperature on the Optical Absorption Edge of Amorphous Thin Films of Silicon Monoxide", *phys. stat. sol.(b)* (123) (1984) 653.
- [10] A. Ibrahim and S. K. J. Al-Ani, "Models of optical absorption in amorphous semiconductors at the absorption edge - A review and re-evaluation" *Czechoslov. J.Phys.*, 44(8) (1994) 785–797.
- [11] A. Frova, and A. Selloni, "The Optical Threshold of Hydrogenated Amorphous Silicon". In: *Tetrahedrally-Bonded Amorphous Semiconductors*. Springer; (1985) 271–85.
- [12] D.J. Dunstan, "Evidence for a common origin of the Urbach tails in amorphous and crystalline semiconductors". *J Phys C Solid State Phys*. 15(13) (1982) L419.
- [13] S.K. O'Leary, S.R. Johnson, P.K' Lim, "The relationship between the distribution of electronic states and the optical absorption spectrum of an amorphous semiconductor: An empirical analysis". *J Appl Phys*. 82(7) (1997) 3334–40.
- [14] S. K. O'Leary and S. M. Malik, "A simplified joint density of states analysis of hydrogenated amorphous silicon". *J. Appl Phys*. 92(8) (2002) 4276–82.
- [15] S. K. O'Leary, "An analytical density of states and joint density of states analysis of amorphous semiconductors". *J. Appl Phys*. 96(7) (2004) 3680–6.
- [16] J. J. Thevaril and S. K. O'Leary, "A universal feature in the optical absorption spectrum associated with hydrogenated amorphous silicon: A dimensionless joint density of states analysis". *J. Appl Phys*. 120(13) (2016) 135706.
- [17] J. A. Guerra, A. Tejada, L. Korte, L. Kegelmann, J.A. Töfflinger, S. Albrecht, "Determination of the complex refractive index and optical bandgap of CH₃NH₃PbI₃ thin films". *J. Appl Phys*. 121(17) (2017) 173104.
- [18] J. A. Guerra. "Optical characterization and thermal activation of Tb doped amorphous SiC, AlN and SiN thin films" Ph.D dissertation, Pontificia Universidad Catolica Del Peru, Peru (2017).

- [19] J. A. Guerra, A. Tejada, J. A. Töfflinger, R. Grieseler, L. Korte “Band-fluctuations model for the fundamental absorption of crystalline and amorphous semiconductors : a dimensionless joint density of states analysis”. *J. Phys D Appl Phys.* 52(10) (2019) 105303.
- [20] D. J. Dunstan, “New evidence for a fluctuating band-gap in amorphous semiconductors”. *J. Phys C Solid State Phys.* 16(17) (1983) L567.
- [21] L. Ley, Photoemission and Optical properties “The Physics of Hydrogenated Amorphous Silicon II”, J.D. Joannopouloa and G. Luckovsky eds. Springer-Verlag (1984) pp.61-168
- [22] W. B. Jackson, S. M. Kelso, C. C. Tsai, J.W. Allen, S-J. Oh, “Energy dependence of the optical matrix element in hydrogenated amorphous and crystalline silicon”. *Phys Rev B.* 31(8) (1985) 5187.
- [23] C. Maurer, W. Beyer, M. Hülsbeck, U. Breuer, U. Rau, S. Haas, “Impact of Laser Treatment on Hydrogenated Amorphous Silicon Properties”. *Adv. Eng Mater.* .1901437(2020) (6)22
- [24] G.D. Cody, B. G. Brooks, B. Abeles, “Optical absorption above the optical gap of amorphous silicon hydride”. *Sol Energy Mater.* 8(1–3) (1982) 231–40.
- [25] G. D. Cody, T. Tiedje, B. Abeles, B. Brooks, Y. Goldstein “Disorder and the optical-absorption edge of hydrogenated amorphous silicon”. *Phys Rev Lett.* 47(20) (1981)1480.
- [26] R. E. Viturro and K.Weiser “Some properties of hydrogenated amorphous silicon produced by direct reaction of silicon and hydrogen atoms”. *Philos Mag B Phys Condens Matter; Stat Mech Electron Opt Magn Prop.* 53(2) (1986) 93–103.
- [27] T. Skettrup, “Urbach’s rule derived from thermal fluctuations in the band-gap energy”. *Phys. Rev. B.* 18(6) (1978) 2622.
- [28] J.D. Dow, D. Redfield, Theory of Exponential Absorption Edges in Ionic and Covalent Solids, *Phys. Rev. Lett.*, 26 (1971), 762.
- [29] J. Tauc “Optical Properties of Amorphous Semiconductors” in “Amorphous and Liquid Semiconductors” Plenum Publishing Company (1974), 159 - 220.
- [30] Z. Li ,S. H. Lin, G. M. Qiu,J.Y. Wang, Y. P.Yu “A method for determining band parameters from the optical absorption edge of amorphous semiconductor: Application to a-Si: H”. *J Appl Phys.* 124(2) (2018) 25702.
- [31] S. Chen and C. R. Wronski “Internal photoemission on a-Si: H Schottky barrier structures revisited”. *J. Non Cryst Solids.* 190(1–2) (1995) 58–66.
- [32] F. Orapunt and S. K.O’Leary “Spectral variations in the optical transition matrix element and their impact on the optical properties associated with hydrogenated amorphous silicon”. *Solid State Commun.* 151(5) (2011) 411–4.
- [33] K. Madsen, N.B. Nielsen, O.Tingleff , "Methods for Nonlinear Least Squares Problems "Technical Report, Informatics and Mathematical Modeling". Technical University of Denmark (2004).
- [34] R.A. Street, "Hydrogenated Amorphous Silicon", Cambridge University Press (1991).
- [35] A. A. Teate and N. C. Halder “Band Tailings and Deep Defects in Semiconductors: Self-Consistent Theory”. *Defect Diffus Forum.* 133 (1996) 48–56.
- [36] J. Steffens , J. Rinder, G. Hahn, B. Terheiden , “Correlation between the optical bandgap and the monohydride bond density of hydrogenated amorphous silicon”. *J Non-Crystalline Solids X.* 5 (2020)100044.